2006-07-05

Electric Field Gradient Focusing-UV Detection for Protein Analysis

Shu-Ling Lin
Brigham Young University - Provo

ELECTRIC FIELD GRADIENT FOCUSING-UV DETECTION FOR PROTEIN ANALYSIS

by

Shu-Ling Lin

A dissertation submitted to the faculty of

Brigham Young University

in partial fulfillment of the requirements for the degree of

Doctor of Philosophy

Department of Chemistry and Biochemistry

Brigham Young University

August 2006

BRIGHAM YOUNG NUIVERSITY

GRADUATE COMMITTEE APPROVAL

of a dissertation submitted by

Shu-Ling Lin

This dissertation has been read by each member of the following graduate committee and by majority vote has been found to be satisfactory.

Date	Milton L. Lee, Chair
Date	Steven W. Graves
Date	Aaron R. Hawkins
Date	H. Dennis Tolley
Date	Adam T. Woolley

BRIGHAM YOUNG UNIVERSITY

As chair of the candidate's graduate committee, I have read the dissertation of Shu-Ling Lin in its final form and have found that (1) its format, citation, and bibliographical style are consistent and acceptable and fulfill university and department style requirements; (2) its illustrated materials including figures, tables, and charts are in place; and (3) the final manuscript is satisfactory to the graduate committee and is ready for submission to the university library.

Date

Milton L. Lee
Chair, Graduate Committee

Accepted for the Department

David V. Dearden
Graduate Coordinator

Accepted for the College

Thomas W. Sederberg
Associate Dean, College of Physical and Mathematical Sciences

ABSTRACT

ELECTRIC FIELD GRADIENT FOCUSING-UV DETECTION

FOR PROTEIN ANALYSIS

Shu-Ling Lin

Department of Chemistry and Biochemistry

Doctor of Philosophy

Electric field gradient focusing (EFGF) utilizes a hydrodynamic flow and an electric field gradient to focus and concentrate charged analytes and order them in a separation channel according to electrophoretic mobility. Elution can be achieved by decreasing the applied voltage or increasing the hydrodynamic flow. EFGF has the advantages of concentrating a large volume (100 μL) of target proteins without significant band broadening and simultaneously removing unwanted components from the sample. Two types of EFGF devices have been investigated to concentrate and separate proteins: a fiber-based EFGF device and a hydrogel-based EFGF device.

Using fiber-based EFGF with UV detection, a concentration factor as high as 15,000 and a concentration limit of detection as low as 30 pM were achieved using

bovine serum albumin as a model protein. I also demonstrated the potential of using fiber-based EFGF for quantitative protein analysis. Simultaneous desalting and protein concentration as well as online concentration of ferritin and simultaneous removal of albumin from a sample matrix were also performed using this fiber-based EFGF system.

In the approach of utilizing hydrogel-based EFGF, online concentration of amyloglucosidase indicated a concentration limit of detection of approximately 20 ng/mL (200 pM) from a sample volume of 100 μL. Both voltage-controlled and flow-controlled elution methods were demonstrated using a 3-component protein mixture. Concentration of human α_1-acid glycoprotein with simultaneous removal of human serum albumin was also described.

A tandem EFGF system, which integrates fiber-based and hydrogel-based EFGF sections, was also investigated to selectively concentrate and separate proteins in a mixture. By carefully controlling the voltages applied to both sections, charged analytes with high mobilities were trapped in the fiber-based section, analytes with intermediate mobilities in the hydrogel-based section, and analytes with low mobilities not at all. A 3-way switching valve was incorporated in the system to purge the analytes with high mobilities periodically. Selective concentration and separation of myoglobin from a mixture were performed using the tandem EFGF system.

Based on the experimental results described in this dissertation, EFGF shows potential for selective isolation, concentration, and quantitation of trace analytes such as proteins in biomedical samples.

ACKNOWLEDGEMENTS

First, I would like to present my sincerest thanks to Dr. Milton L. Lee, my advisor, for providing me with the opportunity to work in his research group. Through his guidance, encouragement, and support, I have earned many invaluable learning experiences and memories during my entire graduate studies.

I must extend my appreciation to my graduate committee members, Dr. Graves, Dr. Hawkins, Dr. Tolley, and Dr. Woolley for their instruction and valuable suggestions regarding my research. I also want to thank Dr. Karl Warnick for his help on mathematical treatment for peak profiling of EFGF and Dr. Paul Farnsworth for his helpful opinions on the EFGF project. Dr. Paul Humble and Dr. Qinggang Wang, who are former postdoctoral researchers working on the EFGF project, offered many priceless discussions that led to the completion of this dissertation. I am very grateful to Susan Tachka for her friendship and encouragement throughout my studies at Brigham Young University. Much of my success can be attributed to the support of fellow members in Dr. Lee's group: Jikun Liu, Yansheng Liu, Li Zhou, Binghe Gu, Jenny Armenta, Xuefei Sun, Yuanyuan Li, Yun Li, and Yan Fang. Thank you all for the friendship and support during the past several years.

I would like to give special thanks to my mother, my brother and his wife, my sisters, as well as my other family members in Taiwan for their understanding, persistent support, and encouragement. Without their unconditional love, I would not have gone this far.

Finally, I would like to acknowledge the Department of Chemistry and Biochemistry at Brigham Young University for providing me such a great opportunity, a pleasant environment, and the financial support to pursue my Ph.D. degree. Life at BYU was always enjoyable and will be memorable forever.

TABLE OF CONTENTS

LIST OF TABLES

LIST OF FIGURES

1 INTRODUCTION

1.1 Protein Analysis

Proteomic research includes identifying the proteins present in a biological sample or proteins that are differentially expressed between different samples, discovering protein functions in a biological system, and determining the tertiary structure of proteins [1]. In addition, most drug targets are proteins; therefore, methods to efficiently analyze proteins should directly contribute to drug development. The protein abundances in the body are highly dependent on age, disease stage, and environmental conditions. In some cases, protein expression changes during the progression of a disease. For example, cancer cells exhibit an altered gene expression profile that results in the production of proteins, which are either specific to, or over-expressed in, these cells [2]. Some marker proteins have been found to be associated with particular cancers such as ubiquinol cytochrome reductase, which was found to be expressed in normal kidney tissue but absent in renal cell carcinoma [3]. The ability to detect slight changes in proteins levels associated with abnormal cell propagation would help in early diagnosis and treatment of cancer in clinical practice. In many cases, the target analytes are usually in trace amounts; therefore, an analytical technique that can concentrate and quantitatively determine the target analytes becomes an important tool for diagnosis of cancers. Due to the complexity of protein content and dynamic protein levels in biological samples [4-6], techniques used for protein analysis must have the ability to analyze complex proteins and trace analytes in various sample matrices. The

development of such techniques becomes an important task for protein analysis in proteomic research.

1.1.1 Protein Separation

Frequently, a series of separation processes are necessary for obtaining information on protein structure and function in a biological system. A powerful separation technique is also required for clinical assays of proteins, which include both qualitative and quantitative analysis of body fluids, such as blood and urine, as well as other biopsy materials. Several commonly used techniques for protein separation are discussed in the following sections.

Electrophoresis. Electrophoresis is a common method used for protein separation and analysis in biochemistry. The separation is based on the differences in electrophoretic mobilities of charged analytes in a conductive medium under the influence of an electric field. Several gel media such as starch, agarose, and polyacrylamide have been used for electrophoretic separations [7,8]. Although two-dimensional gel electrophoresis (2D-GE) is more powerful for resolving complex protein mixtures [9-11], one dimensional gel electrophoresis techniques such as SDS-PAGE (sodium dodecylsulfate-polyacrylamide gel electrophoresis) are still widely used for identification and separation of proteins [12,13]. For example, Seigneurin-Berny et al. used classical SDS-PAGE to separate hydrophobic membrane proteins from chloroplast envelopes [14]. However, gel electrophoresis techniques are usually time-consuming, labor intensive, and only relatively low voltages such as 100-200 V can be applied for separation.

Capillary electrophoresis (CE), an analytical technique that can apply a voltage as high as 30 kV and offers the advantages of high speed, automation, and quantification, has been widely used for analyzing peptide and protein samples in the past decade [15-18]. In addition to protein and peptide separations, Menon and Zydney utilized CE for measurement of protein charge and ion binding at different environments on surface-modified capillaries to reduce protein adsorption [19]. A CE-based immunoassay for prion protein was also established by Schmerr and coworkers [20]. Although CE provides high separation efficiency, it is limited by small injection volume. Therefore, on-line pre-concentration or concentrated samples are necessary for dealing with trace analytes.

Isoelectric focusing (IEF), a separation technique that provides high resolving power, can be described as electrophoresis in a pH gradient where the cathode is at a higher pH value than the anode. Recent studies using IEF in pH gradient gels for protein analysis include detection of recombinant human erythropoietin in urine [21] and the use of serial immobilized pH gradient gels to improve protein separation in proteomic analysis [22]. IEF is not restricted to protein analysis, as the size distribution of gold nanoparticles was also analyzed using a polyacrylamide pH gradient gel [23]. Complex protein mixtures from lysates of microorganisms have also been analyzed using capillary IEF in coated capillaries [24]. In addition, capillary IEF was used to separate human cerebrospinal fluid (CSF) proteins [25] as well as for the separation of extremely acidic and basic proteins, for which pI values are below 3 or higher than 10, such as for lysozyme, cytochrome C, and pepsin [26]. Although capillary IEF provides the advantage

of on-line focusing, either mobilization of the focused proteins or whole-column imaging is necessary for detection.

Two-dimensional electrophoresis of serum proteins was achieved in 1956 using free-solution electrophoresis on filter paper followed by starch-gel electrophoretic separation [27]. Currently, the most effective method for protein separation is two-dimensional polyacrylamide gel electrophoresis (2-D PAGE), which was developed and published by O'Farrell in 1975 [28]. This 2-D PAGE format, which utilized IEF as the first dimension, followed by SDS-PAGE in the second dimension, could resolve more than 1000 proteins in one slab-gel. However, this technique is very time-consuming and labor intensive. Other 2-D electrophoretic separation methods including CIEF-CGE [29], 2-D gel IEF [30], online coupling of micellar electrokinetic chromatography (MEKC) and CIEF [31], and IEF-CE in a microchip [32] were also developed for protein analysis. These techniques can be costly in terms of time and money, or labeled proteins may be necessary for detection.

Chromatography. Size-exclusion chromatography (SEC) or gel filtration is a simple chromatographic method, which is based on differences in molecular size for purifying proteins. Although SEC does not offer high resolving power for separation, it does play roles in fractionation [33], desalting [34], removing contaminants [35], studying protein-protein interactions [36], determining enzyme activity [37], etc. Ion-exchange chromatography separates analytes according to their surface charge density. Because of its high capacity and relatively low cost, ion-exchange chromatography is an ideal tool for initial fractionation of proteins from a complex source. For example, ion-

exchange chromatography was used for protein fractionation from different biological sources such as blood plasma [38] and hen egg white [39]. However, the obtained fractions usually included high concentrations of salts. Desalting was necessary before further purification.

Reversed-phase high performance liquid chromatography (RP HPLC) is a frequently used analytical technique to separate various analytes including small molecules [40], DNA [41], and proteins [42]. However, HPLC has relatively low efficiency and poor sensitivity, which makes HPLC unsuitable for analyzing trace analytes. Capillary liquid chromatography (CLC) or micro liquid chromatography (μ-LC) offers the advantage of high-speed analysis. A number of papers have been published using CLC for protein analysis. Ramström et al. used packed CLC coupled with Fourier transform ion cyclotron resonance mass spectrometry to identify proteins in cerebrospinal fluid [43]. Protein analysis of nasal lavage fluids collected from subjects with sinusitis was conducted by Casado and coworkers [44] using CLC/ESI-Q-TOF-MS (electrospray ionization-quadrupole time of flight mass spectrometry). Although capillary LC provides much higher efficiency, it is limited by small injection volume, usually in the low nL range. Therefore, concentrated samples or on-line preconcentration are required for the analysis of trace analytes.

Electric field gradient focusing (EFGF). An alternative technique, electric field gradient focusing, has been developed to overcome some of the drawbacks listed above. EFGF utilizes a hydrodynamic flow and an electric field gradient to focus and concentrate charged analytes and order them in the separation channel according to

electrophoretic mobility. Elution can be achieved by decreasing the applied voltage or increasing the hydrodynamic flow. EFGF offers the following unique advantages over other separation techniques [45-47]: (1) no obvious band broadening will be caused by large injection volumes or slow injections; (2) analytes can be concentrated and retained in the separation channel until sufficient material is present for detection, especially for trace analysis; (3) analytes can be simultaneously concentrated during the separation process; and (4) separation can be achieved by carefully controlling the voltage drop or the hydrodynamic flow rate in the separation channel.

1.1.2 Protein Concentration

Commonly used techniques for concentrating protein samples include precipitation, ultrafiltration, freeze-drying, and immunoaffinity methods [48-52]. Precipitation is achieved by decreasing the solubility of target proteins by adding salts or organic solvents, or by changing the pH or temperature of the sample solution. In the early days, precipitation was used to separate one protein from another [48,49]. Currently, precipitation is only used as a tool for fractionation during early purification steps, and it is usually followed by chromatographic separation for further purification. Precipitation is also used for concentrating proteins prior to purification or characterization.

Ultrafiltration is a commonly used technique for protein concentration. The molecular weight cut-off of commercial ultrafiltration membranes ranges from 1,000 Da to 300,000 Da. Water and other smaller components are driven through the semi-permeable membrane by centrifugation or high pressure [50]. For proteins and/or peptides of low molecular weight, which cannot be retained by ultrafiltration membranes,

freeze-drying or lyophilization is a technique for concentrating and drying them as powders [50]. Ultrafiltration is usually a gentle and fast process compared to freeze-drying. Ultrafiltration can also be used to remove salts from the initial solution. Techniques including precipitation, ultrafiltation, and freeze-drying are usually performed offline and can result in considerable loss of protein sample.

Another typical approach for purifying proteins is accomplished by immunoaffinity [51,52], in which antibodies are used as ligands to interact with target proteins and separate them from other components in the sample. The purified and concentrated proteins are then recovered from the antibodies by a change in pH or ionic strength, adding a high concentration of substrate, or adding other ligands with higher affinity than the immobilized antibodies. However, the preparation of antibodies is usually expensive and time-consuming, and the proteins are often recovered in a solution with high concentration of salts or eluting agents. Therefore, the removal of salts and eluting agents becomes desirable before further purification and final characterization.

Other recently developed concentration techniques for CE include online electrophoretic concentration with a semi-permeable hollow fiber [53], IEF sample injection (concentration) [54], and online concentration and separation of proteins using polymer solutions [55]. However, these methods can only work with small sample volumes and they are not suitable for large volume injections.

1.1.3 Protein Quantitative Analysis

In addition to qualitative analysis, quantitative analysis is also important for studies of changes in protein content in sample solutions. One popular technique to

quantify proteins in PAGE after electrophoretic separation and staining is the comparison of protein spot intensities using image analyzing software tools [56,57]. With these software tools, many manual procedures such as spot matching and defining spot boundaries become automated. However, difficulties in correctly defining weak spot boundaries consequently result in increased loss of reproducibility in quantitative protein analysis.

Other approaches have also been investigated for quantitative protein analysis. Werner and coworkers quantified immobilized proteins by amino acid analysis using HPLC [58]. Nakamura et al. used affinity chromatography for the quantitative analysis of IgA1 binding protein prepared from human serum [59]. Mass spectrometric detection was recently developed for quantification of a large range of biomolecules, including small molecules, peptides, and proteins [60]. For example, CIEF coupled with MS was applied for the quantitative analysis of peptides and proteins using angiotensin II and human tetrasialo-transferrin as model samples [61]. However, mass spectrometry is usually costly and requires a delicate instrumental setup.

EFGF has also been investigated for quantitative analysis of proteins. For example, the use of EFGF for quantitative analysis was explored by generating a calibration curve of BSA concentration versus peak area with UV detection [46]. In addition, a calibration curve of enhanced green fluorescent protein (GFP) was used to determine the degree of preconcentration using EFGF with laser-induced fluorescence (LIF) detection [47].

1.1.4 Desalting and Removal of Albumin

Besides protein concentration, removing salts from the sample matrix is another major concern for protein analysis. In addition to ultrafiltration, dialysis, gel filtration, and reversed phase high performance liquid chromatography (HPLC) are frequently used for removing salts from the protein solution [13,62,63]. Methods such as dialysis and gel filtration are usually utilized for handling samples with larger volumes (tens of μL to mL), while HPLC can handle samples in the low μL range. However, these techniques all result in more dilute protein solutions after desalting. Other techniques based on membrane-containing microchips for on-chip desalting and micropipette-tip solid phase extraction have been developed for the removal of salts prior to protein analysis using mass spectrometry (MS) or other protein characterization techniques [64-66]. Microchip formats can handle only very small volumes of samples (usually a few μL or less) and the fabrication processes can be very complicated and time consuming. As mentioned in Section 1.1.2, EFGF provides the advantages of simultaneous desalting and online protein concentration [46]. EFGF can also handle samples with both small (1 μL) and relatively large volumes (100 μL). These unique advantages make EFGF a potentially powerful tool for the removal of salts and unwanted buffer components in a sample solution [46].

In many cases, the concentrations of proteins of interest, such as cancer marker proteins, are usually low in biological samples. The detection of such low abundance proteins is therefore hindered by the existence of high abundance proteins, such as

albumin. Several approaches have been conducted to remove albumin from biological samples. Commonly, albumin can be removed by methods based on the high affinity of albumin for certain dyes such as Cibacron Blue F3GA [67]. Although dye-based affinity methods have high binding capacity for albumin, they usually lack sufficient specificity. Steel et al. [68] developed an immunoaffinity resin using monoclonal antibodies against human serum albumin (HSA) to specifically remove HSA from human serum. However, this technique is costly in terms of time and money for antibody preparation. Baker and coworkers [69] evaluated centrifugal ultrafiltration to remove albumin and other high molecular weight proteins from human plasma and found that centrifugal ultrafiltration did not adequately remove these proteins. The removal of albumin was also demonstrated under neutral conditions using EFGF, which is relatively low cost and can effectively remove albumin from a target protein such as ferritin [46].

1.1.5 Detection

UV absorption detection. A commonly used detection method for protein analysis is UV absorption. Figure 1.1 shows the setup of the UV detector used for protein analysis in the work described in this dissertation, where a ball lens was utilized for focusing incident UV light. The spot size of the incident light is an important factor that affects the resolution. As seen in Figure 1.2, two separated peaks can be observed if the spot size is smaller than the channel diameter. However, only one broad peak can be seen if the spot size is larger than the channel diameter.

All proteins and peptides strongly absorb UV light around the wavelength of 214 nm, which makes the sensitivity of protein/peptide detection relatively high. For proteins

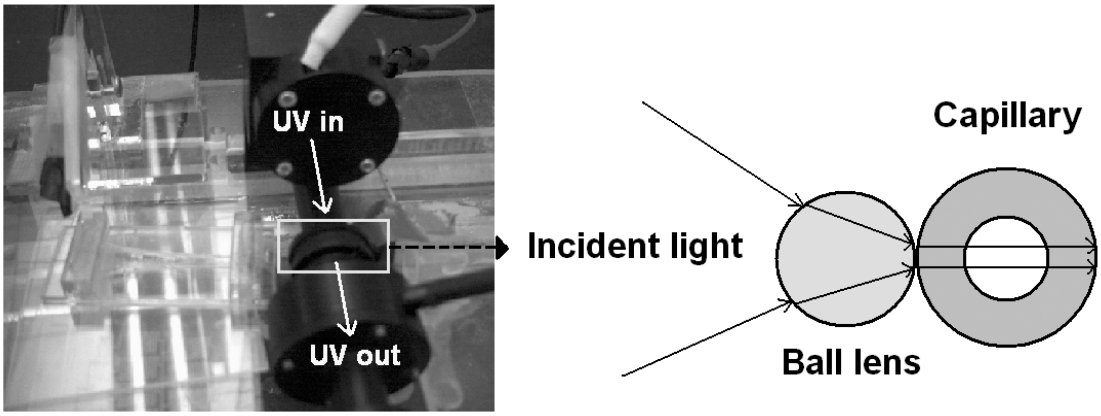

Figure 1.1. Setup of the UV detector and utilization of a ball lens for UV illumination.

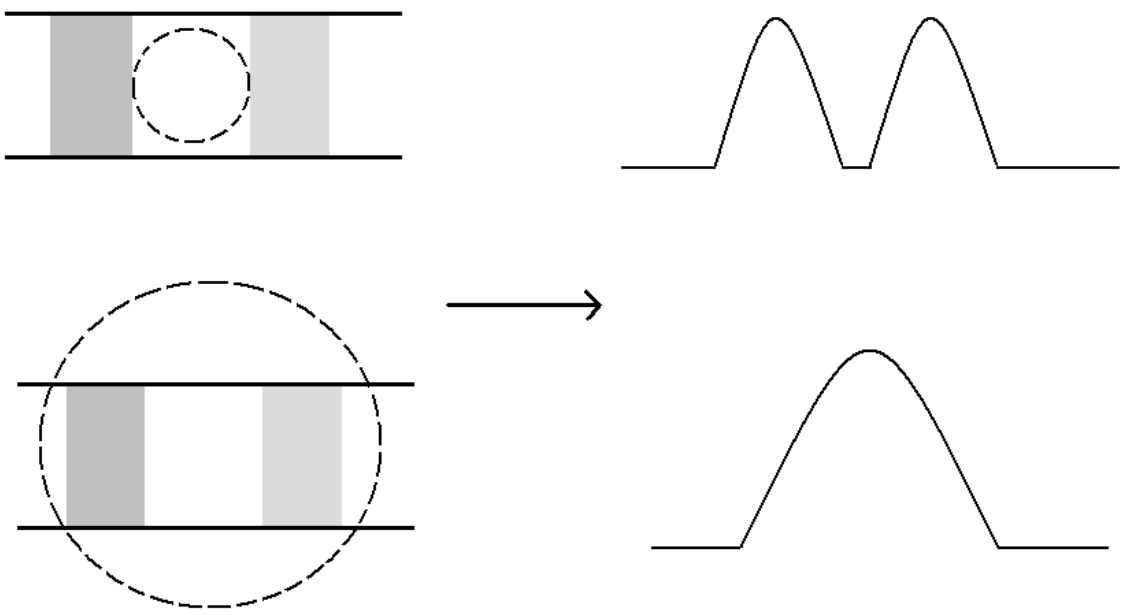

Figure 1.2. Relationship between the spot size of the incident light and resolution.

or peptides containing high content of aromatic amino acids, absorption at 280 nm is another choice for UV detection of proteins and/or peptides. The absorption responses of individual proteins vary due to their distinctive molar absorptivities, which are determined by the amino acid sequences of the analytes. Based on the relatively strong absorption of the peptide bond around 214 nm, UV absorption detection has become a universal detection method for protein analysis. In addition, the ease of application and the relatively low cost for equipment setup make UV detection an attractive method compared to fluorescence. Lee and coworkers utilized UV absorption detection at 214 nm for protein analysis by electric field gradient focusing, also called electromobility focusing [45,46]. Luo et al. performed high-throughput protein analysis by multiplexed SDS-CGE (sodium dodecyl sulfate capillary gel electrophoresis) with UV detection at 214 nm as well [70]. UV detection at 280 nm has also been utilized for high-resolution CIEF of complex protein mixtures from lysates of microorganisms [24] and separation of human cerebrospinal fluid proteins by CIEF [25].

Laser-induced fluorescence. Laser-induced fluorescence (LIF) is a sensitive detection method for capillary and microchip separation techniques. In LIF, analytes are excited to higher electronic energy states by laser absorption and subsequent fluorescence. LIF has been widely used as a detection method for protein and DNA analysis in microanalysis techniques such as capillary electrophoresis [71-73]. Remarkable detection limits have been described for proteins or DNA fragments labeled with fluorescent tags: a concentration detection limit of 3×10^{-13} M for conalbumin using capillary

electrophoresis [72] and detection limits on the order of a few zeptomoles (10^{-21} mol) for DNA restriction fragments using microchip CE [73].

LIF was also used for focusing and online concentration of natively fluorescent proteins by EFGF [47]. In addition to its potential for providing very high detection sensitivity, LIF also provides selective excitation of target analytes to avoid interference. However, the number of natively fluorescent proteins, which contain aromatic amino acid residues such as phenylalanine, tyrosine, and tryptophan in the sequence, is limited. Moreover, the labeling process with fluorescent tags greatly complicates sample preparation and can also critically influence the separation by generating multiple reaction products from a single protein.

Two-photon excitation of fluorescence. Although typical LIF provides high sensitivity protein detection, one-photon excitation of the three aromatic amino acid residues in natively fluorescent proteins usually produces large fluorescence backgrounds. Raman scattering is another significant background radiation, which frequently overlaps fluorescence emission of proteins [74,75]. Figure 1.3 shows a simple diagram of one- and two-photon excitation of fluorescence emission. The wavelengths of one-photon excitation, two-photon excitation, and fluorescence emission are λ, λ_1, and λ_2, respectively [74, 76]. A radiation source such as a YAG laser at 266 nm can be used for one-photon excitation and a laser source at 532 nm can be used for two-photon excitation of phenylalanine, tyrosine, and tryptophan [74,75]. Unlike conventional one-photon excitation for fluorescence detection, two-photon excitation moves the wavelength of

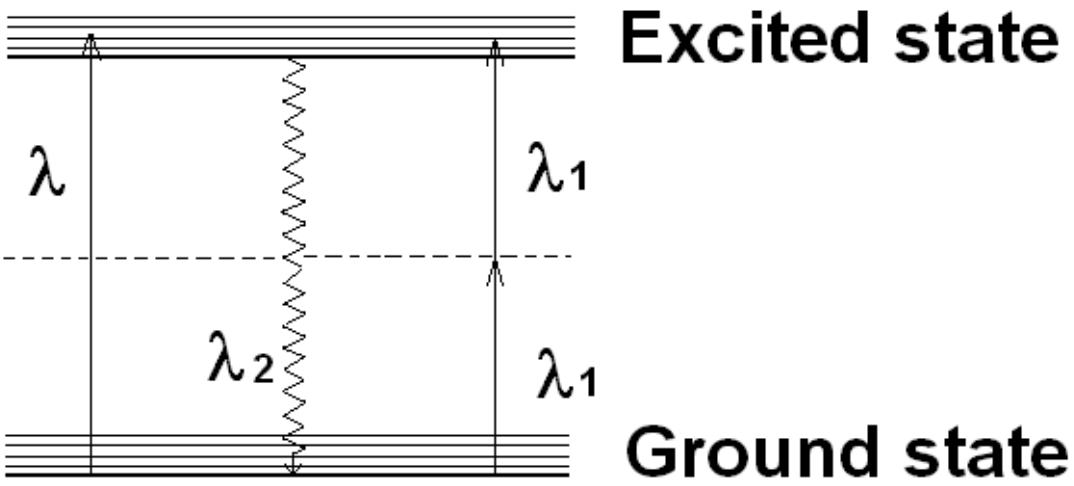

Figure 1.3. Simple diagram of fluorescence emission based on one- and two-photon excitation.

fluorescence emission away from background radiation, such as Raman scattering and reflected excitation radiation, to reduce the background noise [74,75].

Although it is not as popular as one-photon excitation, two-photon excitation has been used for fluorescence detection of natively fluorescent proteins for more than two decades. Xu et al. studied the fluorescence spectra of proteins (including albumin, trypsin, and hemoglobin) using both one-photon excitation at 266 nm and two-photon excitation at 532 nm [74]. In their study, the fluorescence spectra excited at 532 nm had a red shift of about 20 nm compared to spectra excited at 266 nm. More recently, Lippitz et al. reported single-molecule detection of the 24-meric hemocyanin, a respiratory protein containing 148 tryptophan residues [77]. Farnsworth and coworkers reported a detection limit of 130 nM for bovine serum albumin using a compact microchip laser as a source for two-photon excitation at 532 nm [75]. However, the cost of instrumentation is relatively high and proper focusing of the focal point in the channel is critical for detection.

Mass spectrometry. High sensitivity, selectivity, and universality make mass spectrometry (MS) attractive for use as a detection tool in proteomic research [78]. Two sample introduction techniques, electrospray ionization (ESI) and matrix-assisted laser desorption/ionization (MALDI), are widely used with time-of-flight (TOF) mass analyzers for MS detection of proteins and peptides.

ESI is an ionization technique that is carried out under atmospheric pressure and temperature [79]. The ionization principle can be illustrated by a simple diagram shown in Figure 1.4. A sample solution flows through a stainless-steel needle (a few μL/min)

and a voltage difference of several kV between the needle and the walls of the surrounding electrode is applied to disperse the solution into fine charged droplets. During solvent evaporation assisted by a flow of drying gas, the charge density of the droplets becomes greater as the charged droplets become smaller, and finally, desorption of ions into the gas phase occurs. The ions are then transported to a mass analyzer to obtain mass information (mass-to-charge ratio, *m*/*z*) of the analytes. No significant fragmentation of large biomolecules occurs during the electrospray process and the ions formed usually contain multiple charges, which allow detection of high molecular weight proteins by MS. However, ionization is not 100% efficient and it is not suitable for sample solutions containing high concentration of salts.

MALDI utilizes a pulsed laser beam as the energy source for desorption/ionization of analytes [79]. A sample solution is first mixed with an excess of matrix material such as nicotinic acid or benzoic acid derivatives, which can absorb the laser radiation. The mixture is evaporated on a metallic surface for sample introduction. The solid mixture is then exposed to a pulsed laser beam that causes sublimation of the analyte as ions. Finally the resulting ions are drawn toward a mass analyzer such as a TOF for mass analysis. MALDI mass spectra of proteins usually provide signals of singly protonated target molecules and their oligomeric ions (e.g., $[M+H]^+$ and $[2M+H]^+$). This process allows desorption of very large molecules to occur, and turns them into gas phase ions without thermal degradation, which makes MALDI a promising technique for obtaining mass information of large biomolecules. However, the preparation of a MALDI

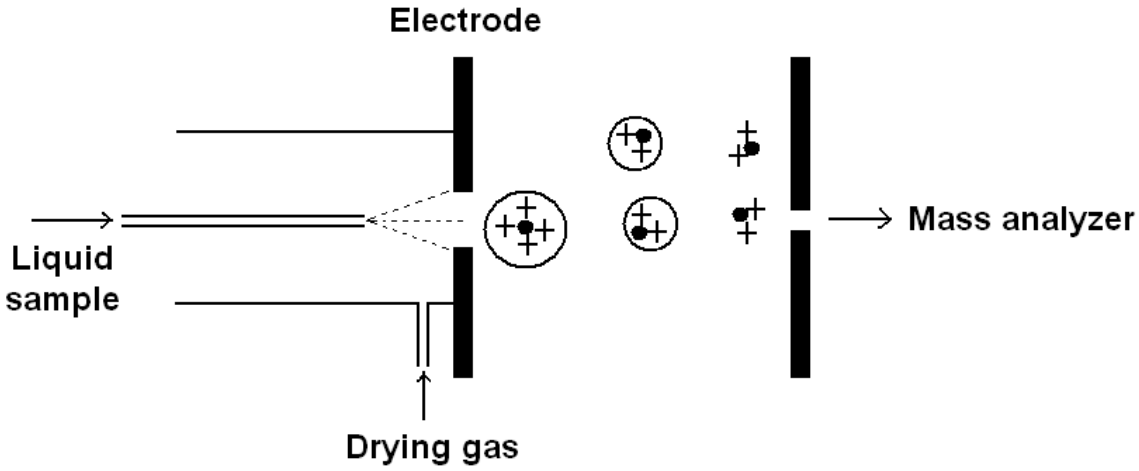

Figure 1.4. Schematic diagram of electrospray ionization.

target, which requires homogeneous sample spots formed at the region that is exposed to the laser beam, is very critical and easily results in inhomogeneous target preparation [80].

TOF is a simple and widely used mass analyzer for mass spectrometry [79]. In TOF, ions are accelerated after ionization and are separated according to their velocity differences. The lighter ions move faster and arrive at the detector, which is placed at the end of the flight tube, earlier than the heavier ions. A key requirement for using TOF as a mass analyzer is that all ions must enter the flight tube at the same time. An ionization technique such as MALDI is a good match for this requirement. ESI, a continuous ion source, can only be coupled with a TOF analyzer after converting the generated ions into discrete portions. TOF offers several advantages such as simplicity and virtually unlimited mass range. In a TOF analyzer, the time difference for various ions to reach the detector is very short, which limits the mass selectivity of a TOF analyzer and results in relatively poor resolution.

ESI-MS and MALDI-MS have been commonly used for the detection of peptides and proteins. Veuthey and coworkers coupled nanoscale LC and CE with ESI-MS for detecting amyloid-β peptide that is related to Alzheimer's disease [81]. Banks et al. used CE for peptide/protein separations with ESI-TOF MS and reported a detection limit of 8 fmol for leucine enkephalin [82]. Banks also reported protein analysis using packed capillary LC with ESI-TOF MS detection [83]. Walker et al. developed an off-line coupled CE and MALDI-TOF MS system and utilized the system for analyzing a tryptic digest of cytochrome *c* and mixtures of four proteins [84]. A two-dimensional liquid-phase separation (IEF-nonporous RP HPLC) was developed by Lubman and coworkers

for mapping and identifying cellular proteins using MALDI-TOF MS [85]. In addition to qualitative analysis, MS has also been used for quantitative analysis of biological fluids [60]. Although MS provides more molecular information than other detection techniques such as UV detection, the cost of instrumentation is relatively high compared to other detection methods.

1.2 Capillary Electrophoresis

1.2.1 Basic Theory of CE

Starting from the mid-1980s, CE has competed with conventional slab gel electrophoresis for protein/peptide analysis in proteomic research. CE, compared to conventional electrophoresis, offers high-speed and high-resolution separation, small sample volume (0.1 to 10 nL) requirement, and quantitative analysis.

Electroosmotic flow (EOF) occurs when a voltage is applied across a silica capillary containing a buffer solution. As shown in Figure 1.5, EOF is caused by the electrical double layer that develops on the capillary surface. The inside wall of the capillary is negatively charged above pH 3, due to ionization of the silanol groups (Si–OH) on the silica surface. The cations in the buffer then move and gather adjacent to the negative capillary surface to form an electrical double layer. The cations on the outer layer, which are solvated, are attracted toward the cathode (negative electrode) and drag the bulk buffer solution along with them to form EOF in the capillary.

The electroosmotic flow velocity in a capillary is given by

$$v_{eof} = \mu_{eof} E = \mu_{eof} \frac{V}{L} \tag{1.1}$$

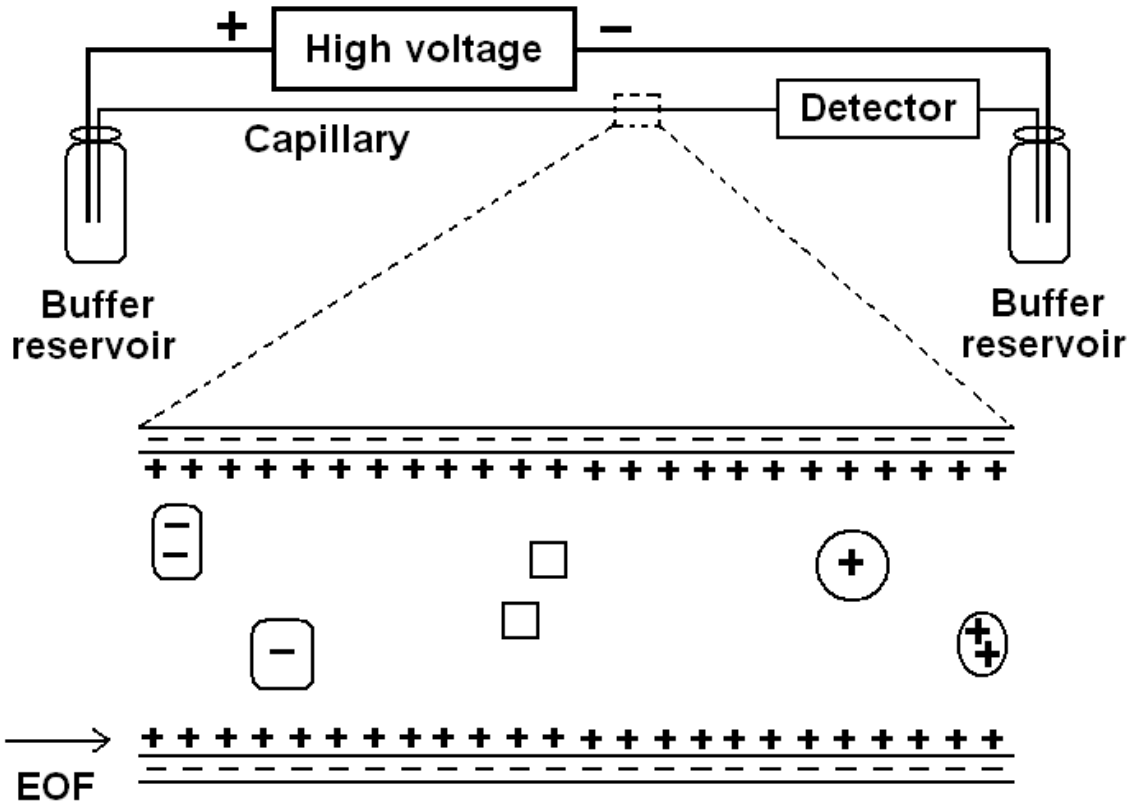

Figure 1.5. Schematic diagram of a basic CE system. (□: neutral analytes)

where ν_{eof} is the electroosmotic flow velocity, μ_{eof} is the electroosmotic mobility, E is the applied electric field in volts/cm, L is the capillary length, and V is the applied voltage. An analyte's migration velocity (ν) is influenced by both the EOF and its electrophoretic velocity, and can be expressed by

$$\nu = \nu_e + \nu_{eof} = (\mu_e + \mu_{eof})E = \mu E \tag{1.2}$$

where ν_e and μ_e are the electrophoretic velocity and the electrophoretic mobility of the analyte, respectively, and μ is the observed electrophoretic mobility of the analyte. In CE, the migration time for an analyte is given by

$$t = \frac{L}{\nu} = \frac{L}{(\mu_e + \mu_{eof})E} = \frac{L^2}{(\mu_e + \mu_{eof})V} \tag{1.3}$$

where t is the migration time. The total number of theoretical plates, N, or the separation efficiency can be expressed by

$$N = \frac{(\mu_e + \mu_{eof})V}{2D} \tag{1.4}$$

where D is the diffusion coefficient of the analyte in cm^2/s. According to equation (1.4), the separation efficiency increases as the applied voltage increases, which indicates that high resolution separations can be achieved by raising the applied voltage. Also, the capillary length does not affect the separation efficiency, but has a great influence on migration time. The resolution of two analytes in CE is given by [86]

$$R_s = 0.177(\mu_1 - \mu_2)\left(\frac{V}{D(\overline{\mu} + \mu_{eof})}\right)^{1/2} \tag{1.5}$$

where R_s is the resolution, μ_1 and μ_2 are the electrophoretic mobilities of two analytes, and $\bar{\mu}$ is the average mobility of the two analytes. Under fixed conditions such as the same applied voltage and the same μ_{eof}, the resolution is determined by the mobility difference between the two analytes.

1.2.2 Electrophoretic Mobility Measurements by CE

Electrophoretic mobility measurements of analytes such as proteins can be performed by capillary electrophoresis using a coated capillary to eliminate electroosmotic flow. The electrophoretic mobility of each protein is then determined using the following equation, assuming the electroosmotic flow is zero:

$$\mu_e = \nu_e / E = (L_D / t_m) / (V / L_T) \tag{1.6}$$

where μ_e is the electrophoretic mobility, ν_e is the electrophoretic velocity, L_D is the distance from the capillary inlet to the detection window, t_m is the migration time for an analyte to travel through the capillary to the detection window under an applied voltage, and L_T is the total capillary length.

In many cases, EOF may not be completely eliminated after coating. Janini et al. used mesityl oxide, a neutral organic compound, to determine the electroosmotic mobility (μ_{eof}) by the following equations [87]:

$$l_{mo} = L_D - \left(\frac{t_p^{'}}{t_p} \right) L_D \tag{1.7}$$

$$\mu_{eof} = \frac{l_{mo} L_T}{t_V V} \tag{1.8}$$

Mesityl oxide was first injected and eluted by applying low pressure to a coated capillary. The time for mesityl oxide to reach the detection window at low pressure was recorded as t_p. A second injection of mesityl oxide was performed with an applied working voltage, V, for a period of time, t_V . The neutral marker, mesityl oxide, moved a distance l_{mo} during this period of time. The applied voltage was then stopped and the marker was moved through the capillary by low pressure and the pressure elution time, $t_p^{'}$, was recorded. The value of l_{mo} was calculated using equation (1.7) and the electroosmotic mobility, μ_{eof}, was obtained from equation (1.8). This value was then used to obtain the electroosmotic mobility of a charged analyte.

The observed electroosmotic mobility, μ, for a charged analyte was first determined based on the equation

$$\mu = \frac{L_D L_T}{Vt} \tag{1.9}$$

The electroosmotic mobility of the analyte was then obtained by

$$\mu_e = \mu - \mu_{eof} \tag{1.10}$$

Therefore, the electrophoretic mobility data for a series of target analytes can be obtained by using either equation (1.6) or (1.10).

1.3 Electric Field Gradient Focusing (EFGF)

1.3.1 Brief History of EFGF

Giddings and Dahlgren [88] first defined an equilibrium gradient method as a method in which a gradient or combination of gradients causes each species to seek an

equilibrium position along the separation path. In practice, two counteracting forces are applied to an analyte, and focusing occurs at the equilibrium point where the net force is equal to zero as shown in Figure 1.6 [89]. An important advantage of equilibrium gradient methods is that on-line focusing and concentration of analytes occur simultaneously during the separation process. Depending on the properties of the analytes, various applied forces/gradients are possible to perform equilibrium gradient focusing. A well-known equilibrium gradient method is IEF, which utilizes a pH gradient along the separation channel.

For electrically charged analytes such as proteins, the idea of using hydrodynamic flow against electrophoretic migration for protein separation was introduced by O'Farrell in 1985 [90]. Using his method, a protein could be focused at the interface between two different gel filtration media packed into the upper and lower halves of an electrochromatography column. However, this method did not satisfy the purpose of separating complex protein mixtures. More recently, Ivory and coworkers introduced a novel equilibrium gradient method, electric field gradient focusing (EFGF), for protein separation that used an electric field gradient and a constant hydrodynamic flow to focus proteins in order of electrophoretic mobility along the separation channel (as shown in Figure 1.7) [91-95].

Ivory and coworkers demonstrated several different types of electrofocusing techniques in their previous studies. The first method involved an electric field gradient formed by spatially varying the current density due to changes in cross-sectional area along the separation channel [91,92]. Although this method offered a continuous electric

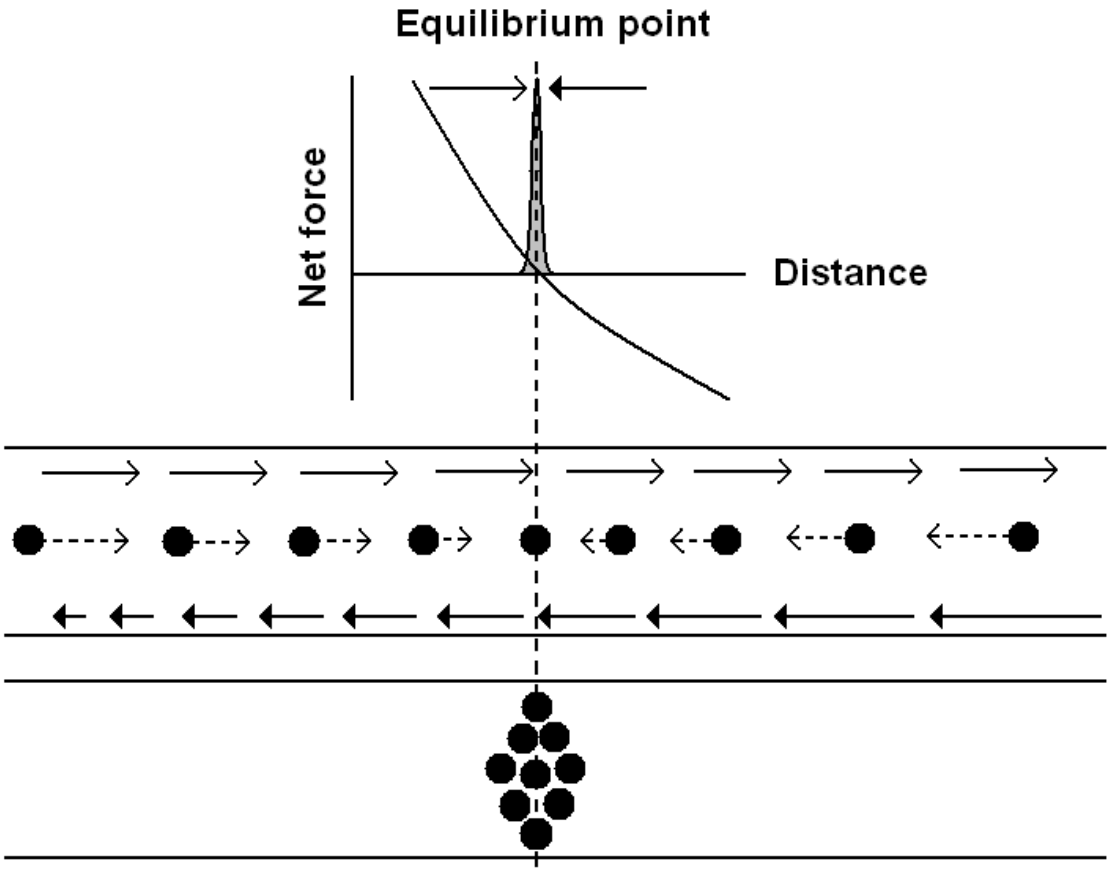

Figure 1.6. Principle of equilibrium gradient focusing. The solid curve and the dashed arrows represent the net force on an analyte, the solid arrows show the direction and the magnitude of two counteracting forces, the dashed line represents the position of the equilibrium point, and the shadowed shape is the profile of the focused band.

field gradient, the configuration could not control the gradient well enough to give satisfactory results. The second method established and maintained the electric field gradient by using a linear array of 50 discrete electrodes. The voltages were then individually monitored and adjusted by a computer-controlled circuit board [93,94]. The advantages of this approach include generating different shapes of electric field gradients such as non-linear profiles and step changes and manipulating the field by computer control to eliminate noise and drift. The third method used a dialysis membrane to form a buffer conductivity gradient along the separation channel [95]. The apparatus was simple to build, however, the gradient profile inside the channel could not be changed without changing the dialysis membrane.

1.3.2 Basic Theory of EFGF

The following assumptions were used to derive the basic theory of EFGF [96]: (1) only low concentrations of analytes are applied; (2) linear flux equations are adequate to represent transport of the analytes; and (3) transport and separation of analytes occur in only one dimension. The basic theory of EFGF can be derived starting with the basic flux equation,

$$J = -D_T \frac{dc(x)}{dx} + (u + \mu E(x))c(x) = 0 \qquad (1.11)$$

where J is the flux density of the target analyte, D_T is the total dispersion, $c(x)$ is the concentration of the analyte at position x, u is the linear velocity of the hydrodynamic flow, μ is the electrophoretic mobility of the analyte, and $E(x)$ is the electric field intensity at position x. When the analyte is focused, the flux intensity is set equal to zero

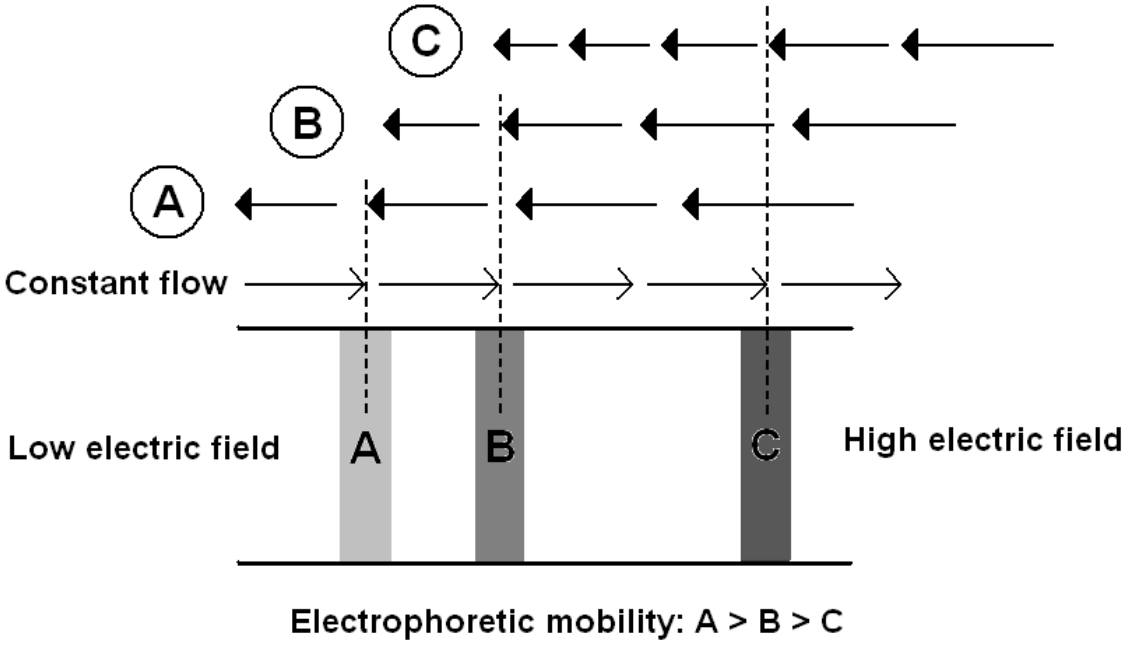

Figure 1.7. Principle of electric field gradient focusing.

to indicate the formation of a steady-state band. Using a Taylor expansion, the electric field intensity profile around the focusing point ($x = x_0$) can be expressed as

$$E(x) = E(x_0) + \left(\frac{dE(x)}{dx}\right)_{x=x_0} \cdot (x - x_0) + \frac{1}{2}\left(\frac{d^2E(x)}{dx^2}\right)_{x=x_0} \cdot (x - x_0)^2 + \cdots\cdots \qquad (1.12)$$

Terms of second and higher orders may be assumed negligible for the narrow band around x_0. Therefore, in this narrow band, $E(x)$ can be described as

$$E(x) \cong E(x_0) + \left(\frac{dE(x)}{dx}\right)_{x=x_0} \cdot (x - x_0) \qquad (1.13)$$

If we let

$$b = -\left(\frac{dE(x)}{dx}\right)_{x=x_0} \qquad (1.14)$$

and consider x_0 to be the equilibrium point,

$$u + \mu E(x_0) = 0 \qquad (1.15)$$

Substituting equations (1.13)-(1.15) into equation (1.11), we obtain

$$D_T \frac{dc(x)}{dx} + b\mu(x - x_0)c(x) = 0 \qquad (1.16)$$

By integrating equation (1.16), we obtain

$$c(x) = c_0 \exp\left(-\frac{b\mu}{2D_T}(x - x_0)^2\right) \qquad (1.17)$$

From this equation, we find that the focused band of analyte is a Gaussian distribution with a standard deviation, σ, of

$$\sigma = \left(\frac{D_T}{b\mu} \right)^{1/2} \tag{1.18}$$

The resolution can be expressed as

$$R_s = \frac{\Delta x}{4\overline{\sigma}} = \frac{|u|}{4} \cdot \left(\frac{\overline{\mu}}{bD_T} \right)^{1/2} \cdot \frac{\Delta \mu}{\overline{\mu}^2} \tag{1.19}$$

and the peak capacity can be expressed as

$$n = \frac{L}{4\overline{\sigma}} = \frac{L}{4} \cdot \overline{\left(\frac{b\mu}{D_T} \right)^{1/2}} \tag{1.20}$$

It can be seen, from equation (1.19), that the resolution is inversely proportional to the square root of the slope of the electric field intensity using a linear electric field gradient. This indicates that resolution would be increased using a shallow gradient, although bands would become broader, which would lead to a decrease in peak capacity for a fixed channel length.

1.3.3 Approaches to Achieve Focusing

An important characteristic in EFGF is the formation of an electric field gradient along the separation channel. Several approaches such as generating a conductivity gradient, changing the cross-sectional area, establishing a temperature gradient, and creating field gradients using a computer-controlled array of electrodes have been investigated by different groups. Once a gradient is established along the separation channel, a voltage is then applied to the system to generate an electric field gradient along the channel. A simplified diagram of a linear electric field gradient is shown in Figure 1.8

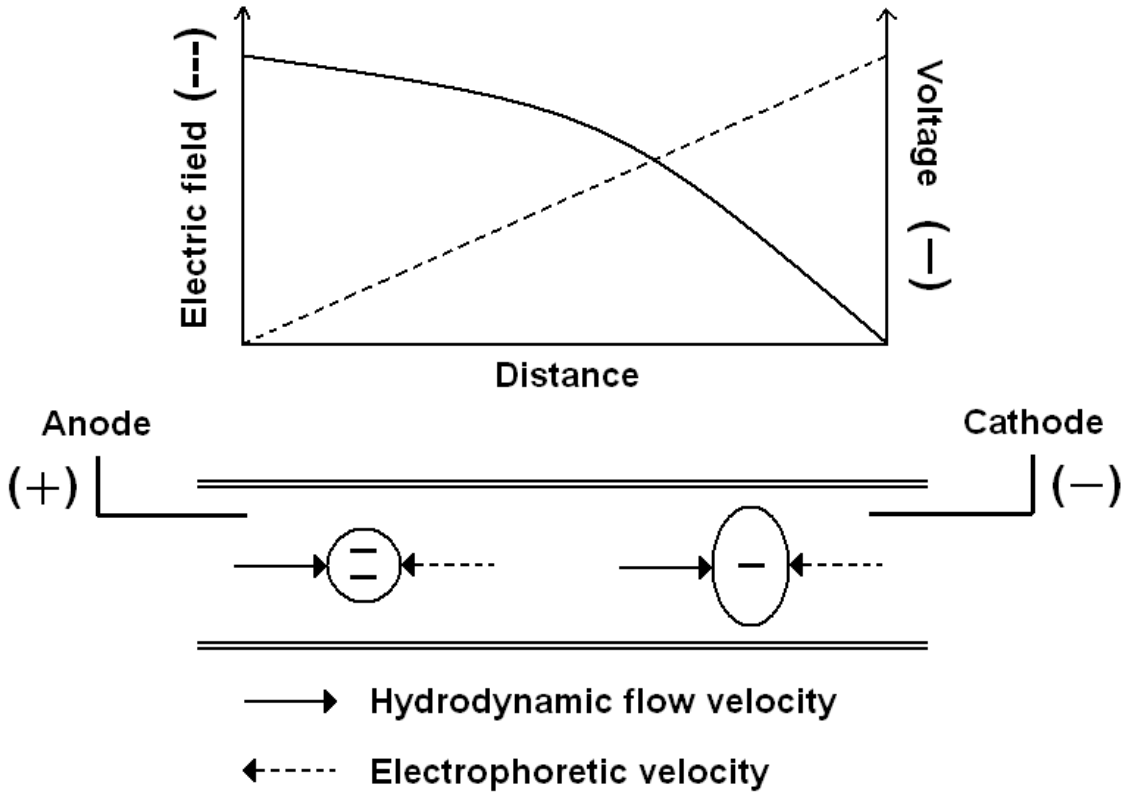

Figure 1.8. Linear electric field gradient to focus charged analytes.

to focus charged analytes along the separation channel according to their electrophoretic mobilities. The different approaches for focusing are discussed in the following sections.

EFGF in a conductivity gradient. A simple approach to establish a conductivity gradient is to generate a concentration gradient of electrolytes as ions diffuse across a porous interface from the high concentration region to the low concentration region. Once the gradient is established, a voltage is applied to form an electric field gradient along the channel.

The first demonstration of EFGF in a conductivity gradient was performed by Ivory's group [95]. The conductivity gradient in the electric field was formed by gradually decreasing electrolyte concentration through a dialysis membrane. The channels (800 μm wide, 500 μm deep, and 10 cm long) were machined into two Plexiglas blocks and separated by a piece of cellulose membrane with a molecular weight cutoff (MWCO) of 6000 Da. Two blocks were bolted together, low concentration (low conductivity) buffer solution and high concentration (high conductivity) buffer flowed through the channels individually to form the conductivity gradient. The electrodes were placed in the purge channel, which allowed electrolysis gases to be removed from the system. The protein samples were injected into the channel with high concentration of buffer for focusing. The purge buffer was also cooled externally to remove Joule heat from the system. When a voltage was applied, the electric field (E) could be determined by [95]

$$E = \frac{I_t}{A\sigma} \tag{1.21}$$

where I_t is the total current, A is the cross-sectional area, and σ is the conductivity.

A mixture of two colored proteins, blue bovine serum albumin (BSA) and bovine hemoglobin, was mainly used to perform protein focusing and separation in the gradient channel (or focusing channel). The experiments were carried out at pH 9.0 using 100 mM Tris-buffer and 10 mM Tris-buffer as the initial gradient buffer and the purge buffer, respectively. At this pH, both proteins were negatively charged. Greenlee et al. [94] reported that protein bands tended to focus adjacent to each other but not overlap in an open channel. The authors proposed an explanation for the adjacent bands in that the electric field might be disturbed by the local electric field created by the concentrated protein bands. In order to eliminate the stacking effect, the concentration of purge buffer was raised to increase the conductivity in the focusing channel, which made a shallower gradient in the channel. Although the proteins were more separated, the focused bands became wider due to the shallower gradient.

To reduce dispersion and increase the resolution of proteins in a conductive gradient EFGF system, 45 μm particles were packed into the focusing channel. With this packed channel, narrower bands of individual proteins and increased resolution of BSA and hemoglobin bands was observed. By increasing the applied voltage and decreasing the hydrodynamic flow, hemoglobin could be focused and resolved into four bands after 2 hours of focusing. The results indicated a great improvement in resolution in the packed channel compared to the resolution obtained in the open channel.

Another approach to form a conductivity gradient was developed in our laboratory, for which a section of 200-μm dialysis fiber served as the separation channel.

Figure 1.9 shows how a concentration gradient forms in a dialysis hollow fiber. High concentration of electrolyte buffer flows through the channel and the electrolyte ions diffuse across the fiber to form a concentration/conductivity gradient along the channel. An electric field gradient is generated when a voltage is applied to the system.

This fiber-based EFGF system had smaller dimensions than the one used in Greenlee's work, which we predicted would produce higher resolution and shorter running time. In addition, the separation channel was surrounded by the purge buffer, which allowed faster and better mixing of electrolyte ions in the separation channel. The EFGF experiments performed in the fiber-based system are discussed later in Chapter 2.

EFGF based on changing cross-sectional area. An electric field gradient can also be generated by changing the cross-sectional area where the current flows, which changes the current density as the cross-sectional area varies. Koegler and Ivory reported the first EFGF device based on changing cross-sectional area in which a dialysis tubing was surrounded by a shaped Plexiglas cylinder [91,92]. The cross-sectional area of the separation channel (dialysis tubing) remained the same so that the hydrodynamic flow rate would be constant. The current density was determined by the shape of the outside Plexiglas cylinder. Once the current crossed the porous interface via the electrolyte ions, an electric field gradient was generated along the separation channel.

At constant electrolyte concentrations, the local electric field could be described as

$$E(x) = \frac{I}{\sigma A(x)} \tag{1.22}$$

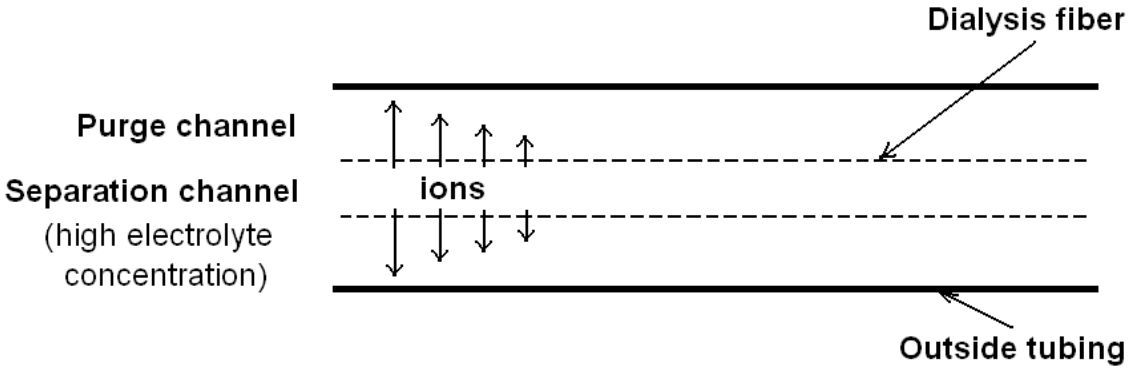

Figure 1.9. Formation of concentration gradient of an electrolyte in a dialysis hollow fiber.

where I is the total current, σ is the conductivity of the buffer, and $A(x)$ is the cross-sectional area of the outside chamber perpendicular to the flow.

The inner dialysis tubing had a diameter of 6.4 mm and was packed with 45 μm size exclusion resin. The dialysis tubing was mounted in the center of the shaped outer Plexiglas chamber. Two electrodes, one on the top and the other on the bottom of the outer chamber, were placed in the ring-shaped space, through which the cooling electrolytes flowed. Bovine hemoglobin was used to demonstrate the focusing of proteins using this type of EFGF system. The experimental results showed a 2- to 3-fold increase in protein concentration after a 7 h focusing time.

This preparative-scale EFGF system only gave mediocre results, it took several hours for focusing, and the fabrication process was complicated [91,92,94]. Smaller channel dimensions should boost the speed for focusing and allow higher voltage to be applied in order to increase the concentration factor. The design and fabrication of the shaped region should be simplified to make the system easier to operate.

A simple design of an EFGF system based on a shaped ionically conductive acrylic polymer (hydrogel) was developed in our laboratory. Humble et al. [47] reported that a miniaturized EFGF device, which utilized a shaped ionically conductive acrylic polymer to establish an electric field gradient, could analyze proteins in low concentrations and concentrate a protein up to 10,000-fold.

The fabrication process for the hydrogel-based EFGF device is shown in Figure 1.10. The shape of the conductive hydrogel could be easily changed to create the

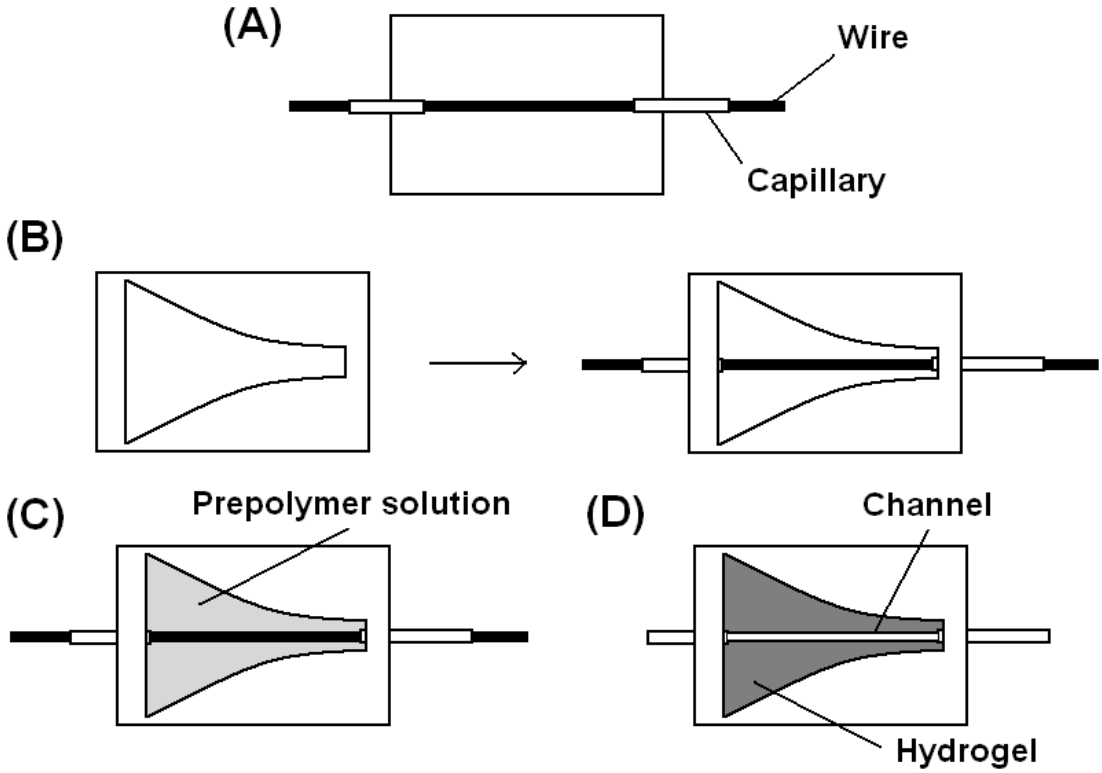

Figure 1.10. Fabrication of the hydrogel-based EFGF device. (A) A Nichrome wire is threaded through two capillaries and placed on the top of a blank PMMA substrate. (B) A shaped PMMA substrate with a cavity, which is used to form the hydrogel, is placed on the blank substrate with the Nichrome wire suspended through the center of the cavity. The two PMMA substrates are then thermally bonded. (C) A prepolymer solution is added to the cavity and the device is placed under a UV lamp to form the polymeric hydrogel. (D) The Nichrome wire is pulled out to leave a separation channel.

desired electric field gradient. The device was easy to fabricate and the dimensions (diameter = 110 μm, length = 4 cm) were smaller than the one developed by Koegler et al. Several fluorescent proteins including natively fluorescent proteins (green fluorescent protein and R-phycoerythrin) and fluorescently labeled proteins (lysozyme labeled with Oregon green and hemoglobin labeled with FITC) were used to demonstrate protein analysis using the hydrogel-based EFGF device.

In the study, proteins could be focused in the separation channel, and varying either the applied voltage or the counteracting hydrodynamic flow could move the focused bands inside the channel. A calibration curve was also created to determine the degree of concentration using the hydrogel-based EFGF device with LIF detection. Green fluorescent protein (GFP) samples of concentrations between 37 nM and 1.5 μM were used to construct a calibration curve of GFP concentration versus signal intensity using a CCD camera with an integration time of 50 ms. A linear relationship was found for GFP concentrations between 150 nM and 1.5 μM. Concentration experiments were then performed by filling the separation channel with 18 pM GFP continuously at a counter-flow rate of 30 nL/min using a syringe pump and applying a voltage of 2 kV to the system. After 40 min, the concentration of the focused GFP band was determined to be 180 nM using the established calibration curve, which reached a concentration factor of 10,000. The concentration factor could be increased by increasing the focusing time with continuous sampling. In addition, the authors demonstrated the separation of a four-protein mixture using the hydrogel-based EFGF system. Oregon green-lysozyme was

baseline separated from the other three proteins (FITC-hemoglobin, R-phycoerythrin, and GFP), which were not completely resolved. The resolution could be improved by applying a shallower electric field gradient, which would move the adjacent protein bands away from each other. Based on theory [96], a shallower field gradient would produce a wider bandwidth for each protein, but higher resolution would be obtained.

The study demonstrated concentration and separation of proteins using the miniaturized hydrogel-based EFGF system. However, natively fluorescent proteins or fluorescently labeled proteins were required for detection. A detection method such as UV detection, which does not require labeling, coupled with the EFGF device should be investigated to allow a wider selection of analytes for protein analysis. The use of hydrogel-based EFGF for protein analysis with UV detection will be discussed in Chapter 3.

Digitally controlled field gradient focusing. Digitally controlled, or dynamic, field gradient focusing was first developed by Huang and Ivory [93] using a computer-controlled array of electrodes to generate and dynamically change an electric field gradient along the focusing chamber for EFGF. The focusing chamber ($8 \times 0.1 \times 0.05$ cm^3) was machined into the front Plexiglas block and packed with 4.5 μm chromatographic packing materials. Fifty controllable electrodes, made from platinum wire (0.25-mm O.D.), and the cooling/recirculating chamber ($6.4 \times 0.3 \times 1.5$ cm^3) were located on the rear Plexiglas block to remove electrolysis gases from the electrodes. Two blocks were then bolted together, and the two chambers were separated by a piece of

dialysis membrane. Each electrode was connected to a controller board for applying and monitoring the voltage by a computer.

This approach offered the advantage of varying the voltages of the individual electrodes to adjust the field profile at any time during a run. Arbitrary shapes of the electric field profiles such as nonlinear profiles and step changes could be established by adjusting the electrode controllers using a computer program.

Several colored proteins were used for demonstrating the focusing and separation of proteins utilizing dynamic field gradient focusing (DFGF). Up to four proteins could be separated in a single run. The resolution between selected species could also be improved by manipulating the applied voltages on individual electrodes to decrease the slope of the field gradient during a run. Concentrating proteins higher than 50 mg/mL was done in a packed-channel format for preparative purposes. The same as in other EFGF approaches, the conductivity in the focusing channel could change considerably when the concentration of a focused protein came close to that of the running buffer.

Myers et al. recently developed a miniaturized system for DFGF of proteins [97]. In their study, protein focusing and separation were demonstrated in a channel filled with a porous polymer monolith using a miniaturized DFGF system. Five discrete gold electrodes were digitally controlled by computer software to generate a variable electric field gradient in the separation channel through a porous glass membrane. Similar to the design developed by Huang and Ivory, two relatively small Plexiglas blocks were used to accommodate the focusing/separation chamber (2.5 cm × 0. 1 mm) and the field gradient chamber. A porous glass membrane was used to separate the two chambers. The

separation channel was packed with a styrene divinylbenzene Poly-Hipe monolith [98] to reduce band broadening. Pre-stained protein samples with a molecular weight range of 6.5−200 kDa were used as model proteins for demonstration, and detection was achieved in the visible range using a digital camera.

A mixture of pre-stained proteins was introduced into the separation channel and the applied voltages on individual electrodes were first set to form an electric field well that would trap the analytes. The voltage profile was then changed to start separating proteins into individual bands. The mixture contained seven proteins, and six of them were separated and identified by computer color matching. The resulting focused bands were narrower than the previous DFGF study reported by Huang and Ivory [93] due to the smaller channel dimensions with packed polymer monolith. The buffer concentration difference in the two channels generated a conductivity gradient along the separation channel. However, this effect was not taken into account in the study. The development of a UV detection system is necessary for viewing unstained proteins.

Temperature gradient focusing. Temperature gradient focusing (TGF), a new type of gradient focusing technique, was first developed by Ross and Locascio [99]. In TGF, there is no need of using membranes or embedded electrodes to establish an electric field gradient. TGF simply utilizes a temperature gradient and a buffer with temperature-dependent ionic strength to generate the electric field gradient for focusing.

In electric field gradient focusing, the electric field (E) in the channel is given by

$$E(x) = \frac{I}{\sigma A} \tag{1.23}$$

where I is the current running through the channel, σ is the conductivity of the buffer, and A is the channel cross-sectional area. Here, the channel cross-section area is a constant and we assume a constant current runs through any given section of the channel. Because the buffer conductivity is temperature-dependent, the electric field is also temperature-dependent. The primary temperature-dependent characteristic of the buffer conductivity is the change in buffer viscosity with temperature, which can be described as

$$\sigma = \frac{\eta(20)\sigma(20)}{\eta(T)f(T)} \tag{1.24}$$

where T is the temperature, $\eta(20)$ and $\sigma(20)$ are the viscosity and the conductivity of the running buffer at T = 20 ºC, respectively, $\eta(T)$ is the temperature-dependent viscosity, and $f(T)$ is a function of any other temperature-dependent factors (e.g., $f(20)$ = 1) such as ionic strength. Using equations (1.23) and (1.24), the temperature-dependent electric field becomes

$$E = \frac{I\eta(T)f(T)}{A\sigma(20)\eta(20)} \equiv E_0 \frac{\eta(T)f(T)}{\eta(20)} \tag{1.25}$$

Since the electrophoretic mobility (μ_e) of an analyte is also temperature-dependent through the viscosity, it can be expressed in a similar way as that used for the conductivity [equation (1.24)]:

$$\mu_e = \frac{\eta(20)\mu_e^0}{\eta(T)f_e(T)} \tag{1.26}$$

where μ_e^0 is the electrophoretic mobility of the analyte at T = 20 ºC and $f_e(T)$ is a function of any other temperature-dependent factors (e.g., $f_e(20)$ = 1). Using equations (1.25) and (1.26), the electrophoretic velocity becomes

$$v_e = \mu_e E = E_0 \mu_e^0 \frac{f(T)}{f_e(T)} \tag{1.27}$$

If $f(T)$ and $f_e(T)$ do not have the same temperature dependence, gradients in the electrophoretic velocity can be established due to the temperature gradient occurring in the channel. Therefore, analytes can be focused and concentrated using TGF. A simplified equipment setup for TGF is shown in Figure 1.11.

Most commonly, a buffer should have a strongly temperature-dependent $f(T)$ and the analytes should have a constant or nearly constant $f_e(T)$ in order to employ TGF for analytical purposes. Ross et al. [98] used a high concentration Tris/boric acid buffer (900 mM Tris, 900 mM boric acid) as the running buffer, which had a non-constant $f(T)$ which decreased as the temperature was raised. The pH of the buffer was also temperature-dependent, which varied from 8.6 at 20 ºC to 7.5 at 70 ºC. The pK_a's of the analytes should be away from this pH range so that $f_e(T)$ could be regarded as a constant.

The authors utilized TGF in both microchip and capillary formats, and demonstrated that TGF could be applied to a wide range of analytes, including fluorescent dyes and green fluorescent protein, as well as fluorescently labeled amino acids and DNA. In the study, the degree of concentration was also investigated. After 100 min of focusing, a 10,000-fold increase in concentration was observed using an 8 nM Oregon Green 488 carboxylic acid as the initial solution.

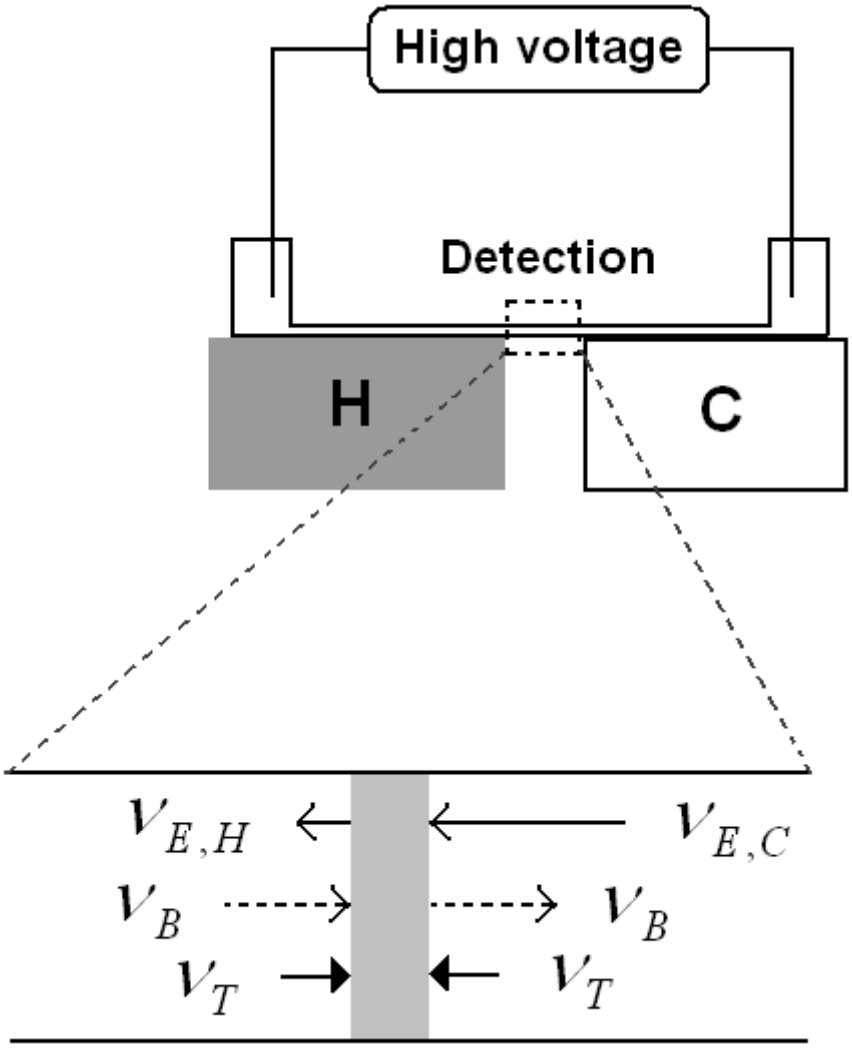

Figure 1.11. Simplified diagram of the equipment setup for TGF. H = heating block, C = cooling block, $v_{E,H}$ = the electrophoretic velocity close to the heating block, $v_{E,C}$ = the electrophoretic velocity close to the cooling block, v_B = the bulk flow velocity, and v_T = the total velocity of the analyte. ($v_T = v_E + v_B$)

Balss et al. have also implemented TGF for DNA hybridization assays [100]. They chose the hybridization of DNA with PNA (peptide nucleic acid) for TGF assays due to the significant difference in electrophoretic mobility between ssDNA (single-stranded DNA) targets and the PNA/DNA hybrid. Therefore, the focused bands of the ssDNA and the PNA/DNA hybrid could be well resolved by TGF. Moreover, the fluorescently labeled PNA was hard to focus by TGF due to its nearly zero electrophoretic mobility, so that the hybridization assays would not be affected by the presence of neutral PNA. Two types of TGF assays were performed in the study: stationary TGF and scanning TGF.

In stationary TGF, the focused bands roughly remained at the same position through the experiment. The assay was carried out in a 10-cm-long capillary with an applied voltage of 3 kV using a temperature gradient of 20–65 ºC across 2 mm. The ssDNA targets were first focused and concentrated at the equilibrium point in the capillary. The fluorescently labeled PNA was then carried into the capillary by bulk flow through the focused band of ssDNA. If hybridization occurred, the PNA/DNA hybrid would focus at different position along the capillary and a second fluorescent band was observed. If the PNA was not matched to the focused ssDNA, no hybridization would occur and the neutral PNA would just pass through and not be retained in the capillary. Therefore, no subsequent fluorescent band would be observed.

In scanning TGF, the bulk flow was carefully controlled to increase gradually during the course of the experiment. The focused bands were therefore moved from the one end to the other end of the temperature gradient. The hybrids of PNA/DNA were first introduced into the capillary, and the bulk flow was adjusted to focus the hybrids at a

point close to the cool end of the temperature gradient. The bulk flow rate was then increased to slowly move the focused PNA/DNA band toward the high-temperature end. When the band reached the melting temperature of the PNA/DNA hybrids, the hybrids started thermally denaturing. Therefore, the melting point of the hybrids could be determined by the decrease in the fluorescence intensity of the band. The authors used the scanning TGF technique to detect SBPMs (single base pair mutations), important indicators for diagnosis of diseases such as cystic fibrosis and cancer, by monitoring the fluorescence intensity of PNA/DNA hybrids as a function of temperature. The SBPM analysis was accomplished within 5 min and 100-fold more dilute analytes could be used for the analysis compared to conventional UV melting measurements.

Ross and coworkers [101] also employed TGF for simultaneous concentration and separation of enantiomers, including amino acids and small pharmaceutical molecules. All analytes were labeled for fluorescence detection. In order to perform chiral separations by TGF, a chiral selector such as cyclodextrin was added into the running buffer to interact with the enantiomeric analytes and then shift their electrophoretic mobilities, which resulted in a change in their focusing points. In the study, a low concentration of dansyl-DL-glutamic acid solution was continuously introduced into the capillary for 30 min (concentration enriched >600-fold), and then the solution in the sample reservoir was replaced with buffer containing cyclodextrin. By tracing the separation with fluorescence video microscopy, splitting of the focused peak into two well-resolved peaks, which corresponded to the D- and L- enantiomers, was observed in less than 30 seconds. For the analysis of biological fluids, the drug, baclofen, was spiked

in a urine sample which was analyzed with chiral TGF. Two enantiomer peaks were well resolved, although decreased resolution (peaks were closer together compared to a similar experiment without urine) was observed due to the presence of urine.

Although TGF could achieve a concentration factor greater than 10,000-fold, the temperature gradient only occurred in a small section (2 mm) of the whole separation channel and the determination of temperature-dependency of running buffer was critical. Control of the temperature gradient across the whole channel should be investigated and a database of temperature-dependency of running buffers needs to be established as well.

1.4 Dissertation Overview

My research solely focused on implementing EFGF for protein analysis. Two approaches were explored to establish the electric field gradient along the separation channel to accomplish EFGF. Unlike other field gradient focusing studies, all analyses in this dissertation were monitored using online UV detection.

Several bioanalytical applications using EFGF in a conductivity gradient with online UV detection are described in Chapter 2. A section of hollow dialysis fiber was used to generate a concentration gradient of electrolytes, which caused an electric field gradient when a voltage was applied to the system. Online focusing and concentration of proteins, simultaneous desalting and protein concentration, protein quantitative analysis, as well as the removal of albumin were demonstrated using this fiber-based EFGF system. Another approach for implementing EFGF is to establish an electric field gradient based on changing cross-sectional area utilizing a shaped ionically conductive polymer (or hydrogel). Protein analysis using the hydrogel-based EFGF system is described in

Chapter 3. Chapter 4 describes a tandem EFGF system, which integrates a section of dialysis fiber in front of the hydrogel device, for isolating and concentrating target proteins. Chapter 5 presents a theoretical treatment to interpret the peak profile of an eluting peak from EFGF. Finally, future directions for utilizing an integrated EFGF system for selective isolation and concentration of target proteins, such as cancer markers, in biological samples are discussed in Chapter 6.

1.5 References

[1] Figeys, D. *Anal. Chem.* **2003**, *75*, 2891-2905.

[2] Seliger, B.; Kellner, R. *Proteomics* **2002**, *2,* 1641-1651.

[3] Alaiya, A. A.; Franzén, B.; Auer, G.; Linder, S. *Electrophoresis* **2000**, *21,* 1210-1217.

[4] Binz, P.-A. et al. *Anal. Chem.* **1999**, *71*, 4981-4988.

[5] Johnson, A. M.; Rohlfs, E. M.; Silverman, L. M. *Tietz Textbook of Clinical Chemistry*, *3rd ed*, edited by Burtis, C. A. and Ashwood, E. R., Saunders, Philadelphia, **1999**, 479-512.

[6] Corthals, G. L.; Wasinger, V. C.; Hochstrasser, D. F.; Sanchez, J.-C. *Electrophoresis*. **2000**, *21,* 1104-1115.

[7] Allen, R. C.; Budowle, B. *Gel Electrophoresis of Proteins and Nucleic Acids: Selected Techniques,* Walter de Gruyter, Berlin, **1994**.

[8] Mikkelsen, S. R.; Cortón, E. *Bioanalytical Chemistry*, John Wiley & Sons, Hoboken, New Jersey, **2004**.

[9] O'Farrell, P. H. *J. Biol. Chem*. **1975**, *250*, 4007-4021.

[10] Görg, A.; Obermaier, C.; Boguth, G.; Harder A.; Scheibe, B.; Wildgruber, R.; Weiss, W. *Electrophoresis* **2000**, *21,* 1037-1053.

[11] Lilley, K. S.; Razzaq, A.; Dupree, P. *Curr. Opin. Chem. Biol.* **2002**, *6,* 46-50.

[12] Harris, E. L. V.; Angal, S. *Protein Purification Applications: a practical approach*, IRL Press, Oxford; New York, **1990**.

[]3] Roy, S. *Protein Purification Techniques, 2nd ed*, Oxford University Press, Oxford; New York, **2001.**

[14] Seigneurin-Berny, D.; Rolland, N; Garin, J.; Joyard, J. *Plant J*. **1999**, *19,* 217-228.

[15] Basha, S. M. *J. Agric. Food Chem.* **1997**, *45*, 400-402.

[16] Zhang, Z.; Krylov, S.; Arriaga, E. A.; Polakowski, R.; Dovichi, N. J. *Anal. Chem.* **2000**, *72*, 318-322.

[17] Hu, S.; Zhang, L.; Newitt, R.; Aebersold, R.; Kraly, J. R.; Jones, M.; Dovichi, N. J. *Anal. Chem.* **2003**, *75*, 3502-3505.

[18] Kato, M.; Sakai-Kato, K.; Jin, H.; Kubota, K.; Miyano, H.; Toyo'oka, T.; Dulay, M. T.; Zare, R. N. *Anal. Chem.* **2004**, *76*, 1896-1902.

[19] Menon, M. K.; Zydney, A. L. *Anal. Chem.* **1998**, *70*, 1581-1584.

[20] Yang, W.-C.; Schmerr, M. J.; Jackman, R.; Bodemer, W.; Yeung, E. S. *Anal. Chem.* **2005**, *77*, 4489-4494.

[21] Breidbach, A.; Catlin, D. H.; Green, G. A.; Tregub, I.; Truong, H.; Gorzek, J. *Clin. Chem.* **2003**, *49*, 901-907.

[22] Poznanovic, S.; Schwall, G.; Zengerling, H.; Cahill, M. A. *Electrophoresis* **2005**, *26,* 3185-3190.

[23] Arnaud, I.; Abid, J.-P.; Roussel, C.; Girault, H. H. *Chem. Commun.* **2005**, *14*, 787-788.

[24] Shen, Y.; Xiang, F.; Veenstra, T. D.; Fung, E. N.; Smith, R. D. *Anal. Chem.* **1999**, *71*, 5348-5353.

[25] Manabe, T.; Miyamoto, H.; Inoue, K.; Nakatsu, M.; Arai, M. *Electrophoresis* **1999**, *20,* 3677-3683.

[26] Yang, C.; Zhang, W.; Zhang, J.; Duan, J.; Zhang, Y. *J. Sep Sci.* **2005**, *28*, 78-86.

[27] Smithies, O.; Poulik, M. D. *Nature* **1956**, *177*, 1033.

[28] O'Farrell, P. H. *J. Biol. Chem*. **1975**, *250*, 4007-4021.

[29] Yang, C.; Liu, H.; Yang, Q.; Zhang, L.; Zhang, W.; Zhang, Y. *Anal. Chem.* **2003**, *75*, 215-218.

[30] Štastná, M.; Šlais, K. *Electrophoresis* **2005**, *26,* 3586-3591.

[31] Sheng, L.; Pawliszyn, J. *Analyst* **2002**, *127,* 1159-1163.

[32] Herr, A. E.; Molho, J. I.; Drouvalakis, K. A.; Mikkelsen, J. C.; Utz, P. J.; Santiago, J. G.; Kenny, T. W. *Anal. Chem.* **2003**, *75*, 1180-1187.

[33] Lee, K. A.; Kim, S.-H. *Food Chem.* **2005**, *90*, 389-393.

[34] George, W. H. S. *Nature* **1962**, *195*, 155-157.

[35] Burnouf, T. *J. Chromatogr. B* **1995**, *664*, 3-15.

[36] Beeckmans, S. *Methods* **1999**, *19*, 278-305.

[37] Niederwanger, A.; Kranebitter, M.; Ritsch, A.; Patsch, J. R.; Pedrini, M. T. *J. Chromatogr. B* **2005**, *820*, 143-145.

[38] Moure, F.; Rendueles, M.; Díaz, M. *Meat Sci.* **2003**, *64*, 391-398.

[39] Guérin-Dubiard, C.; Pasco, M.; Hietanen, A.; Quiros de Bosque, A.; Nau, F.; Croguennec, T. *J. Chromatogr. A* **2005**, *1090*, 58-67.

[40] You, J.; Cui, F.-D.; Li, Q.-P.; Wang, Y.-S.; Han, X.; Yu, Y.-W. *J. Chromatogr. B* **2005**, *823*, 172-176.

[41] Castro, R. M. R.P.S.; Landemberger, M. C.; Walz, R.; Carlotti, C. G., Jr.; Huang, N.; Cunha, D. R.; Moura, R.; Caballero, O. L.; Sakamoto, A. C.; Nitrini, R.; Brentani, R. R.; Martins, V. R. *J. Neuroscience Methods* **2004**, *139*, 263-269.

[42] Paschen, C.; Griese, M. *J. Chromatogr. B* **2005**, *814*, 325-330.

[43] Ramström, M.; Palmblad, M.; Markides, K. E.; Håkansson, P.; Bergquist, J. *Proteomics* **2003**, *3*, 184-190.

[44] Casado, B.; Pannell, L. K.; Viglio, S.; Iadarola, P.; Baraniuk, J. N. *Electrophoresis* **2004**, *25*, 1386-1393.

[45] Wang, Q.; Lin, S.-L.; Warnick, K. F.; Tolley, H. D.; Lee, M. L. *J. Chromatogr. A* **2003**, *985*, 455-462.

[46] Lin, S.-L.; Tolley, H. D.; Lee, M. L. *Chromatoghraphia* **2005**, *62*, 277-281.

[47] Humble, P. H.; Kelly, R. T.; Woolley, A. T.; Tolley, H. D.; Lee, M. L. *Anal. Chem.* **2004**, *76*, 5641-5648.

[48] Johns, E. W. *Biochem. J.* **1964**, *92*, 55-59.

[49] Cohn, E. J.; Strong, L. L.; Hughes, W. L.; Mulford, D. L.; Ashworth, J. N.; Talor, H. L. *J. Am. Chem. Soc.* **1946**, *68,* 459-475.

[50] Harris, E. L. V. *Protein Purification Techniques, 2nd ed,* edited by Roy, S., Oxford University Press, New York, **2001**, pp111-154.

[51] Bhikhabhai, R.; Sjöberg, A.; Hedkvist, L.; Galin, M.; Liljedahl, P.; Frigård, T.; Pettersson, N.; Nilsson, M.; Sigrell-Simon, J. A.; Markeland-Johansson, C. *J. Chromatogr. A* **2005**, *1080*, 83-92.

[52] Link, A. J.; Fleischer, T. C.; Weaver, C. M.; Gerbasi, V. R.; Jennings, J. L. *Methods* **2005**, *35*, 274-290.

[53] Wu, X.-Z.; Hosaka, A.; Hobo, T. *Anal. Chem.* **1998**, *70*, 2081-2084.

[54] Wu, X.-Z.; Zhang, L.-H.; Onoda, K. *Electrophoresis* **2005**, *26*, 563-570.

[55] Tseng, W.-L.; Chang, H.-T. *Anal. Chem.* **2000**, *72*, 4805-4811.

[56] Lilley, K. S.; Razzaq, A.; Dupree, P. *Curr. Opin. Chem. Biol.* **2002**, *6*, 46-50.

[57] Moritz, B.; Meyer, H. E. *Proteomics* **2003**, *3*, 2208-2220.

[58] Salchert, K.; Pompe, T.; Sperling, C.; Werner, C. *J. Chromatogr. A* **2003**, *1005*, 113-122.

[59] Nakamura, I.; Iwase, H.; Ohba, Y.; Hiki, Y.; Katsumata, T.; Kobayashi, Y. *J. Chromatogr. B* **2002**, *776*, 101-106.

[60] Hopfgartner, G.; Varesio, E. *Trends Anal. Chem.* **2005**, *24*, 583-589.

[61] Kuroda, Y.; Yukinaga; H.; Kitano, M.; Noguchi, T.; Nemati, M.; Shibukawa, A.; Nakagawa, T.; Matsuzaki, K. *J. Pharm. Biomed. Anal.* **2005**, *37*, 423-428.

[62] Bagshaw, R. D.; Callahan, J. W.; Mahuran, D. J. *Anal. Biochem*. **2000**, *284*, 432-435.

[63] Cavanagh, J.; Benson, L. M.; Thompson, R.; Naylor, S. *Anal. Chem*. **2003**, *75*, 3281-3286.

[64] Palmblad, M.; Vogel, J. S. *J. Chromatogr. B* **2005**, *814,* 309-313.

[65] Lion, N.; Gellon, J.-O.; Jensen, H.; Girault, H. H. *J. Chromatogr. A* **2003**, *1003*, 11-19.

[66] Pluskal, M. G. *Nat. Biotechnol*. **2000**, *18*, 104-105.

[67] Ahmed, N.; Barker, G.; Oliva, K.; Garfin, D.; Talmadge, K.; Georgiou, H.; Quinn, M.; Rice, G. *Proteomics.* **2003**, *3*, 1980-1987.

[68] Steel, L. F.; Trotter, M. G.; Nakajima, P. B.; Mattu, T. S.; Gonye, G.; Block, T. *Mol. Cell. Proteomics.* **2003**, *2*, 262-270.

[69] Georgiou, H. M.; Rice, G. E.; Baker, M. S. *Proteomics* **2001**, *1*, 1503-1506.

[70] Luo, S.; Feng, J.; Pang, H. M. *J. Chromatogr. A* **2004**, *1051*, 131-134.

[71] Lee, T. T.; Yeung, E. S. *J. Chromatogr.* **1992**, *595,* 319-325.

[72] Lee, I. H.; Pinto, D.; Arriaga, E. A.; Zhang, Z.; Dovichi, N. J. *Anal. Chem.* **1998**, *70,* 4546-4548.

[73] Effenhauser, C. S.; Bruin, G. J. M.; Paulus, A.; Ehrat, M. *Anal. Chem.* **1997**, *69,* 3451-3457.

[74] Xu, Y.-W.; Zhang, J.-R.; Deng, Y.-M.; Hui, L.-K.; Jiang, S.-P.; Lian, S.-H. *J. Photochem. Photobiol. B: Biol.* **1987**, *1*, 223-227.

[75] Paul, U. P.; Li, L.; Lee, M. L.; Farnsworth, P. B. *Anal. Chem.* **2005**, *77,* 3690-3693.

[76] Diaspro, A.; Robello, M. *J. Photochem. Photobiol. B: Biol.* **2000**, *55*, 1-8.

[77] Lippitz, M.; Erker, W.; Decker, H.; van Holde, K. E.; Basché, T. *Proc. Natl. Acad. Sci. USA* **2002**, *99*, 2772-2777.

[78] Tomer, K. B. *Chem. Rev*. **2001**, *101*, 297-328.

[79] Dass, C. *Principles and Practice of Biological Mass Spectrometry*, John Wiley & Sons, New York, **2001**.

[80] Garbis, S.; Lubec, G.; Fountoulakis, M. *J. Chromatogr. A* **2005**, *1077*, 1-18.

[81] Varesio, E.; Rudaz, S.; Krause, K.-H.; Veuthey, J.-L. *J. Chromatogr. A* **2002**, *974*, 135-142.

[82] Banks, J. F.; Dresch, T. *Anal. Chem.* **1996**, *68,* 1480-1485.

[83] Banks, J. F. *J. Chromatogr. A* **1997**, *786*, 67-73.

[84] Walker, K. L.; Chiu, R. W.; Monnig, C. A.; Wilkins, C. L. *Anal. Chem.* **1995**, *67,* 4197-4204.

[85] Wall, D. B.; Kachman, M. T.; Gong, S.; Hinderer, R.; Parus, S.; Misek, D. E.; Hanash, S. M.; Lubman, D. M. *Anal. Chem.* **2000**, *72,* 1099-1111.

[86] Baker, D. R. *Capillary Electrophoresis*, John Wiley & Sons, New York, **1995**.

[87] Janini, G. M.; Metral, C. J.; Issaq, H. J.; Muschik, G. M. *J. Chromatogr. A* **1999**, *848*, 417-433.

[88] Giddings, J. C.; Dahlgren, K. *Sep. Sci*. **1971**, *6*, 345-356.

[89] Wang, Q.; Tolley, H. D.; LeFebre, D. A.; Lee, M. L. *Anal. Bioanal. Chem.* **2002**, *373*, 125-135.

[90] O'Farrell, P. H. *Science* **1985**, *227*, 1586-1589.

[91] Koegler, W. S.; Ivory, C. F. *J. Chromatogr. A* **1996**, *726,*229-236.

[92] Koegler, W. S.; Ivory, C. F. *Biotechnol. Prog.* **1996**, *12*,822-836.

[93] Huang, Z.; Ivory, C. F. *Anal. Chem.* **1999**, *71*,1628-1632.

[94] Ivory, C. F. *Sep. Sci. Technol*. **2000**, *35*, 1777-1793.

[95] Greenlee, R. D.; Ivory, C. F. *Biotechnol. Prog.* **1998**, *14*,300-309.

[96] Tolley, H. D.; Wang, Q.; LeFebre, D. A.; Lee, M. L. *Anal. Chem.* **2002**, *74*, 4456-4463.

[97] Myers, P.; Bartle, K. D. *J. Chromatogr. A* **2004**, *1044*,253-258.

[98] Cameron, N. R.; Sherrington, D. C. *Adv. Polym. Sci*. **1996**, *126*,163-214.

[99] Ross, D.; Locascio, L. E. *Anal. Chem.* **2002**, *74*, 2556-2564.

[100] Balss, K. M.; Ross, D.; Begley, H. C.; Olsen, K. G.; Tarlov, M. J. *J. Am. Chem. Soc.* **2004**, *126*,13474-13479.

[101] Balss, K. M.; Vreeland, W. N.; Phinney, K. W.; Ross, D. *Anal. Chem.* **2004**, *76*, 7243-7249.

2 ELECTRIC FIELD GRADIENT FOCUSING IN A CONDUCTIVITY GRADIENT✳

2.1 Introduction

In this chapter, I investigated the potential of using a fiber-based EFGF device for quantitative protein analysis, simultaneous desalting (separation of a target analyte from a complex cell culture medium with high salt concentration), and protein concentration. In addition, ferritin, an iron storage protein as well as a cancer correlated indicator [1-3], was concentrated with simultaneous removal of albumin.

2.2 Experimental Section

2.2.1 Chemicals and Materials

The dialysis hollow fiber, a modified cellulose fiber with internal diameter (I.D.) of 200 μm and dry wall thickness of 8 μm, was purchased from Membrana (Wuppertal, Germany). This dialysis fiber had a molecular weight cut-off (MWCO) of approximately 10000. Untreated fused-silica capillaries, 250 μm I.D. × 360 μm O.D. and 535 μm I.D. × 693 μm O.D., were obtained from Polymicro Technologies (Phoenix, AZ). Bovine serum albumin (BSA) and ferritin from horse spleen, were purchased from Sigma (St. Louis, MO. Dulbecco's Modified Eagle Medium (DMEM) was purchased from GIBCO BRL Life Technologies (Gaithersburg, MD).

✳ This chapter (except Sections 2.1, 2.3.1, and 2.3.3) is reproduced with permission from *J. Chromatogr. A* **2003**, *985*, 455-462 (Copyright 2003 Elsevier) and *Chromatoghraphia* **2005**, *62*, 277-281 (Copyright 2005 Vieweg Publishing).

2.2.2 Device Setup and Instrumentation

A section of commercial dialysis hollow fiber was connected to a fused silica capillary (250 μm I.D. × 360 μm O.D.) at each end using epoxy. The fiber section was then inserted coaxially inside another fused silica (535 μm I.D. × 693 μm O.D.) capillary and assembled with two low-pressure crosses as shown in Figure 2.1. Two syringe pumps were used to deliver (1) the sample and high concentration buffer solution into the dialysis fiber (separation channel) and (2) low concentration buffer solution through the outside tubing (purge channel), respectively. A high voltage power supply was connected at both ends of the purge channel. The two electrodes were approximately 12 cm apart and the voltage polarity was as shown in Figure 2.1 for negatively charged analytes.

A syringe pump (Model PicoPlus, Harvard Apparatus, Holliston, MA) utilizing a 500-μL gas tight syringe (Hamilton, Reno, NV) was used to deliver high concentration buffer solution and sample into the dialysis fiber. Another syringe pump (Model 11Plus, Harvard Apparatus, Holliston, MA) utilizing a 60-mL plastic syringe (Becton Dickinson, Franklin Lake, NJ) was used to deliver low concentration buffer solution through the outside capillary. Sample injections were performed using an injection valve with a 1-μL or 100-μL sample loop from VICI Valco (Houston, TX). A high voltage power supply from Spellman (Model SL 30, Hauppauge, NY) was used to apply voltage to the EFGF system. A detection window was made at the end of the fiber for online detection with a UV-Vis absorption detector from ThermoQuest (Model Spectra 100, Riviera Beach, FL).

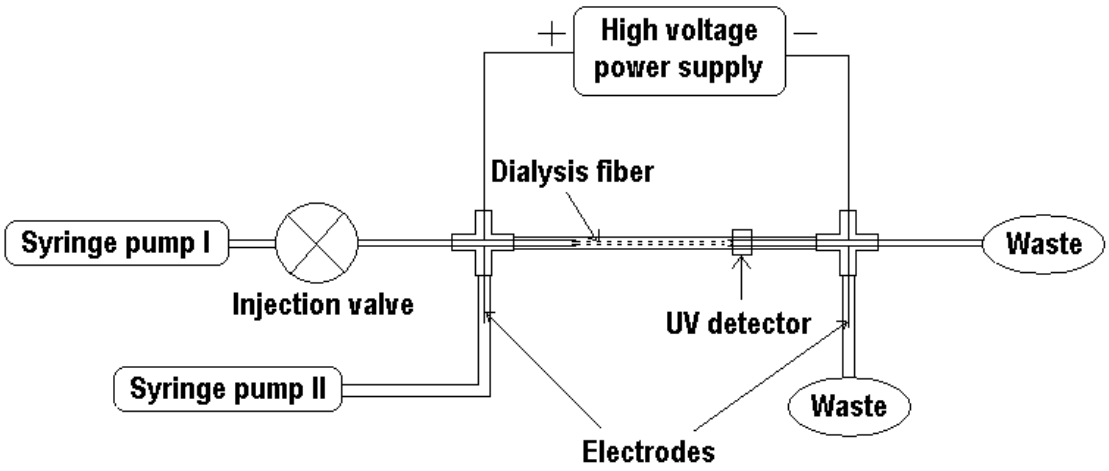

Figure 2.1. Schematic diagram of the hollow dialysis fiber-based EFGF device.

2.2.3 Experimental Conditions

Most experiments were performed at pH 8.7, except for the separation of ferritin from albumin, which was performed at pH 7.0. For operation under basic conditions, the concentration inside the dialysis fiber was 100 mM Tris buffer and the concentration in the outside tubing was 1 mM Tris buffer adjusted to pH 8.7. The flow rate through the hollow fiber was 0.5 μL/min (a linear velocity of 2.65×10^{-2} cm/s) and the outside purge flow rate was 200 μL/min. For pH 7.0 conditions, the concentration inside the dialysis fiber was 100 mM phosphate buffer and the concentration in the outside tubing was 2 mM BisTris buffer adjusted to pH 7.0. The flow rate through the hollow fiber, which served as the separation channel, was 0.3 μL/min (a linear velocity of 1.59×10^{-2}cm/s), and the outside purge flow-rate was 300 μL/min. For experiments carried out under basic conditions, various BSA solutions were prepared in 100 mM Tris buffer at pH 8.7. A voltage of 5 kV was applied across the dialysis fiber for focusing. After various time intervals, depending on the sample size, the voltage was dropped to 3 kV for elution. For the experiments carried out under neutral conditions, a mixture of 1 mg/mL BSA and 0.02 mg/mL ferritin was prepared in 100 mM phosphate buffer at pH 7.0. For focusing, a voltage of 2 kV was applied across the length of the fiber for 120 min for multiple injections or 75 min for a single injection; the voltage was then decreased to 1 kV for elution. UV absorption detection was accomplished at 214 nm.

2.3 Results and Discussion

2.3.1 Protein Focusing

Figure 2.2 shows how a protein can be focused using a dialysis hollow fiber-based EFGF device. Without voltage applied, 1 μL of 0.1 mg/mL BSA (bovine serum albumin) solution was injected and carried through the dialysis hollow fiber by hydrodynamic flow. A broad peak appeared at about 35 min after injection (bottom trace).

Because the protein was negatively charged at pH 8.7, the electrophoretic force drew the protein toward the beginning of the fiber while the hydrodynamic flow drove it toward the end of the fiber when an external voltage was applied. As shown in the top trace of Figure 2.2, when 5 kV was applied and all other conditions were kept the same, the protein was still retained in the fiber after 61 min. In this case, the electrophoretic migration velocity of BSA balanced the hydrodynamic flow velocity; then, the protein was focused inside the fiber. When the voltage was dropped to 3 kV, the electric field deceased and the electrophoretic migration velocity was not able to balance the hydrodynamic flow velocity. Therefore, the protein lost its focusing position and eluted from the fiber.

The eluted BSA peak had a signal-to-noise (S/N) ratio of over 200, which indicates that a protein sample with much lower concentration can be detected after focusing. Although the peak eluted at about 61 min, it did not require such a long time to focus the protein. According to earlier experiments using colored proteins, it took approximately 10-15 min to focus the proteins after they were introduced into the fiber.

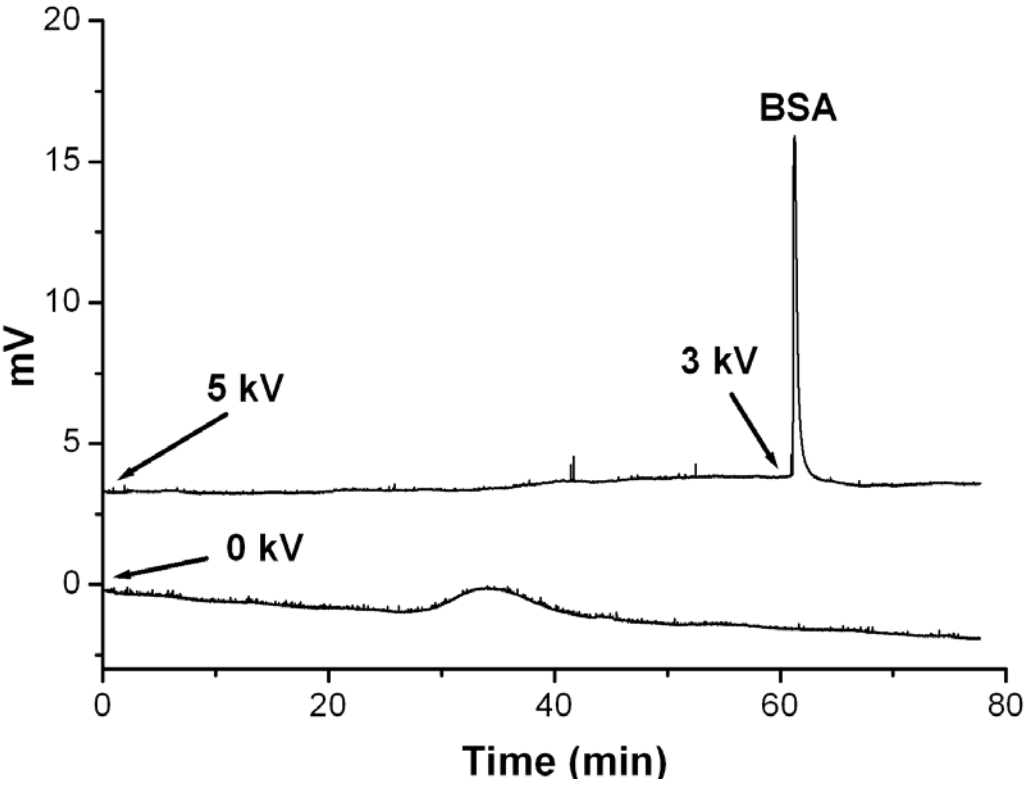

Figure 2.2. Protein focusing using a fiber-based EFGF device. Conditions:1 μL of 0.1 mg/mL BSA was injected and other conditions are listed in Section 2.2.3.

The relatively long focusing time in Figure 2.2 was chosen to show that the analyte could be trapped in the fiber as long as necessary before decreasing the voltage for elution.

2.3.2 Online Protein Concentration

Simultaneous online protein concentration during separation is a great advantage of EFGF. Multiple injections and large volume injections have been accomplished using fiber-based EFGF. The experimental results are shown in Figures 2.3 and 2.4. Simply making 5 consecutive injections using a 1 μL sample loop, Figure 2.3 shows the online concentration power of a dialysis hollow fiber-based EFGF device. The experimental results of large volume injection using a 100 μL sample loop are shown in Figure 2.4.

Both injection methods gave similar peak widths when compared to a single 1 μL injection (Figure 2.3). This indicates that large injection volumes do not result in band broadening using EFGF techniques. It should be mentioned that the time scale shown in Figure 2.4 includes 200 min for sample loading (0.5 μL/min for 100 μL) and 25 min for focusing prior to decreasing voltage for elution. The long running time in Figure 2.4 was chosen to demonstrate that EFGF offered high sample loading capacity and that protein could be retained in the separation channel as long as necessary without significant band broadening. The running time could be reduced by simply increasing the hydrodynamic flow rate and/or the voltage applied to the system.

Figure 2.4 also shows a high concentration factor and low detection limit that can be obtained using this EFGF system. Using colored proteins, the width of a focused protein band was measured to be approximately 0.2 mm. Therefore, the concentration

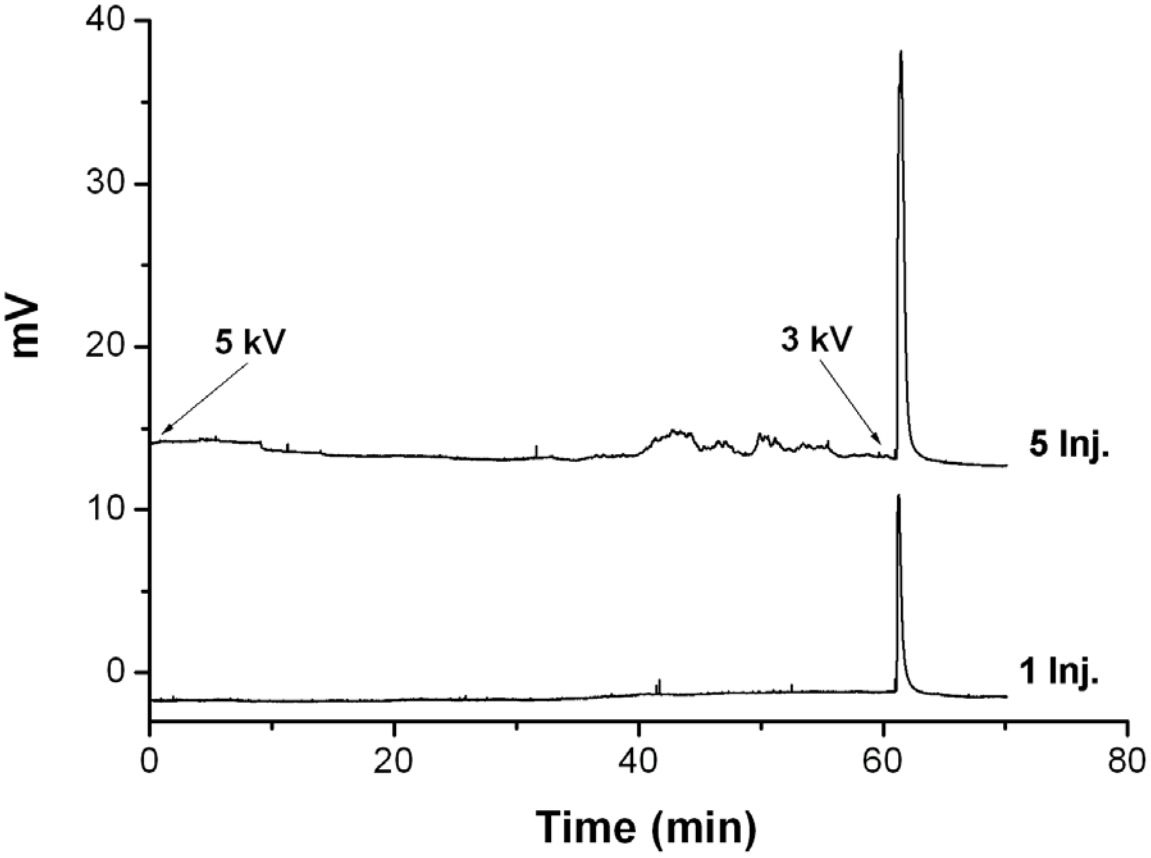

Figure 2.3. Online protein concentration by multiple injections using fiber-base EFGF. A 1 μL volume of 0.1 mg/mL BSA was introduced for one injection and other conditions are listed in Sections 2.2.2 and 2.2.3.

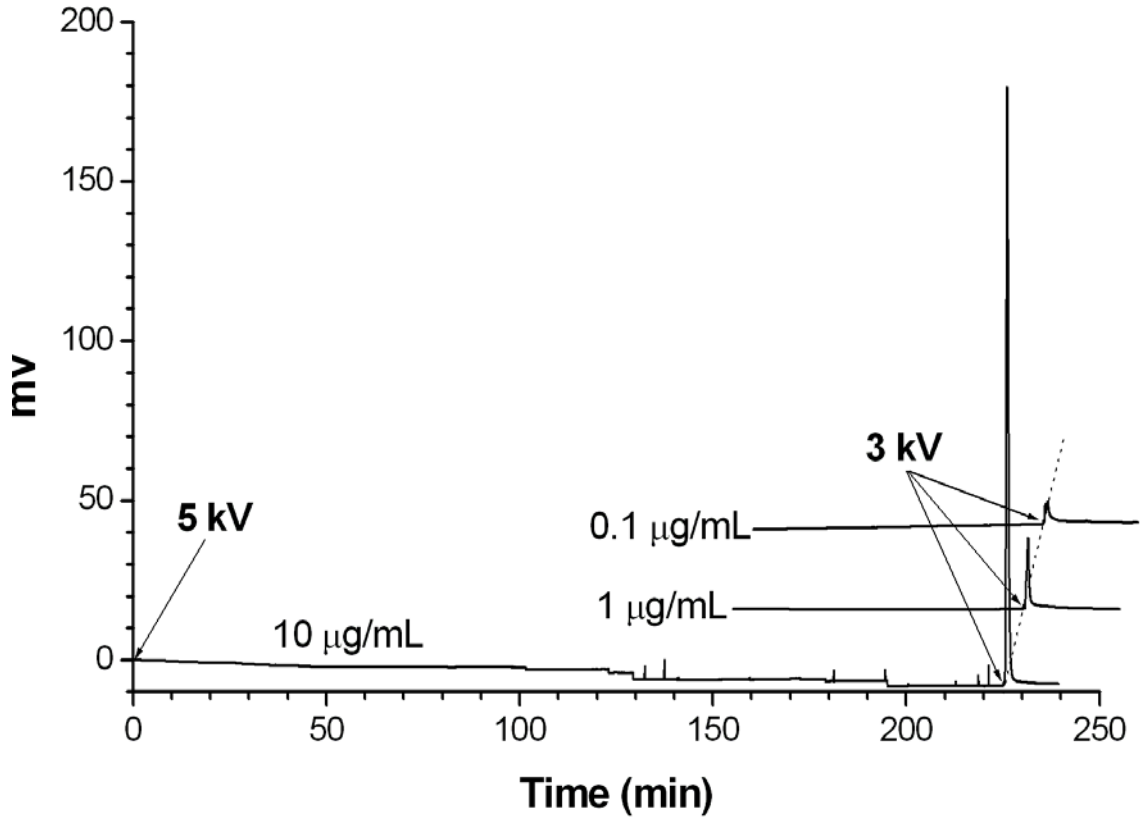

Figure 2.4. Online protein concentration from large volume (100 μL) injection using a hollow dialysis fiber-based EFGF system. The plots of BSA at 0.1 μg/mL and 1 μg/mL were shifted to show the focused peaks. Conditions are described in Section 2.2.3.

factor using a 100 μL sample loop could be determined using the following equation:

$$\text{Concentration Factor} = \frac{V_0}{V_f} \tag{2.1}$$

where V_0 is the injection volume of a sample and V_f is the sample volume after concentration. The results show a concentration factor of over 15,000. The BSA peak in Figure 2.4 for 0.1 μg/mL (about 1.5 nM) had a signal-to-noise ratio of over 100, which indicates a concentration limit of detection of approximately 2 ng/mL (30 pM) for BSA.

2.3.3 Voltage-Controlled Protein Separation

While performing an EFGF experiment for separation, proteins are first focused inside the separation channel in order of their electrophoretic mobilities. Proteins with high mobilities focus at the low electric field (high electrolyte concentration) region and proteins with low mobilities focus at the high field (low electrolyte concentration) region.

After decreasing the total voltage drop along the separation channel, the electric field decreases as well; therefore, the equilibrium is changed. All of the focused proteins move to new equilibrium points, which are closer to the end of the channel. Sequentially, a protein with lowest mobility moves out of the channel for detection, while others move toward the end of the channel and are refocused. If the voltage is kept constant after the first protein elutes, all other proteins stay focused and are retained in the channel. If we keep decreasing the voltage, proteins move out of the channel one by one in order of electrophoretic mobility [4]. Figure 2.5 shows the experimental results of voltage-controlled separation of BSA and Mb (myoglobin).

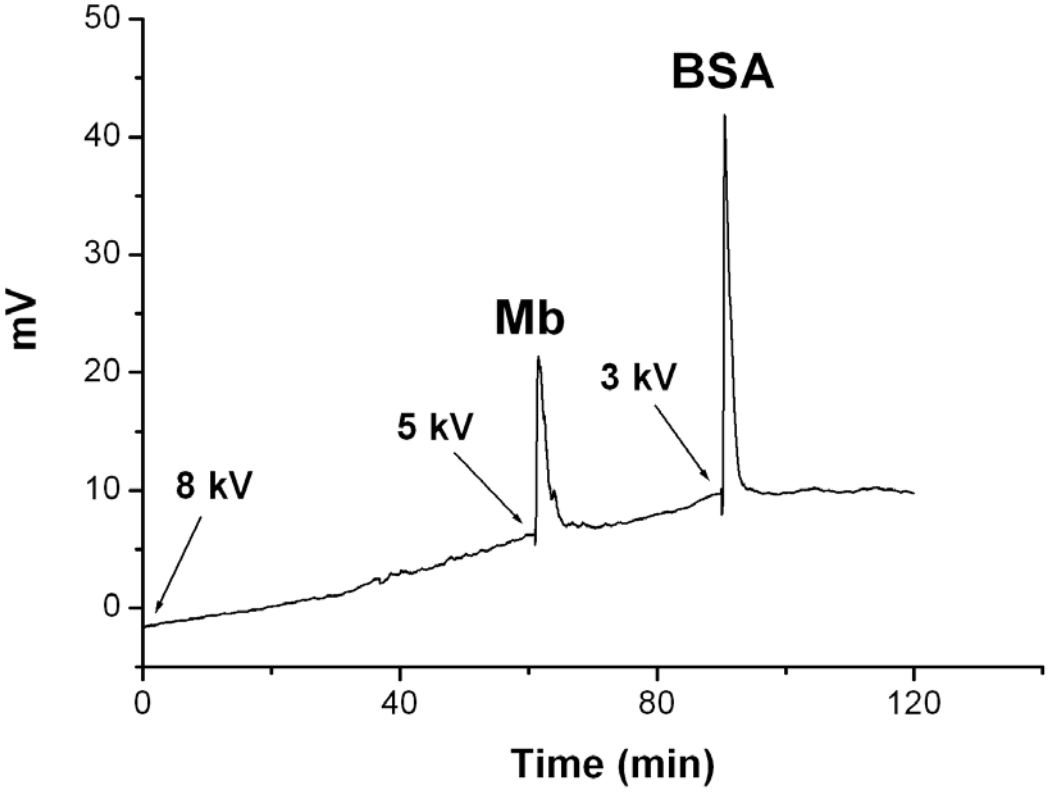

Figure 2.5. Voltage-controlled separation of BSA and Mb by fiber-based EFGF. Conditions: the concencentions of both proteins were 0.5 mg/mL and other conditions are listed in Section 2.2.3.

2.3.4 Quantitative Analysis

In addition to qualitative analysis, I investigated the use of EFGF for quantitative analysis by generating a calibration curve of BSA concentration versus peak area. Four different concentrations of BSA solutions were prepared and six runs of each sample were performed with a 1 μL sample loop. The slope and intercept for the calibration plot were 0.55 and -0.07, respectively. The numerical results of the calibration are summarized in Table 2.1. According to the R^2 value calculated from the calibration, a fairly linear relationship was found between BSA concentration and peak area, which indicates the potential of using fiber-based EFGF for quantitative protein analysis.

Table 2.1. Numerical results of the calibration of BSA concentration versus peak area using a hollow dialysis fiber-based EFGF system. Conditions are described in Section 2.2.3.

	BSA Concentration (μg/mL)			
	50	100	250	500
Average peak area	27.6	62.7	106.4	287.4
Relative standard deviation (RSD, %)	3.85	7.34	8.69	6.96
Regression (R^2)	0.97			
Standard deviation of the slope	0.070			
Standard deviation of the intercept	20.6			

2.3.5 Simultaneous Desalting and Protein Concentration

Protein purity is an important factor in protein research. Desalting and concentrating are two operations that must be accomplished during the purification process. Dulbecco's Modified Eagle Media (DMEM), a commonly used cell culture medium, contains more than 30 components including amino acids, vitamins, inorganic salts, D-glucose, and other substances. Table 2.2 lists some major components in the medium. Two BSA solutions (1 and 10 μg/mL) were prepared in DMEM with 2 M NaCl to demonstrate the ability of EFGF to desalt and concentrate protein samples using a dialysis fiber. Fig. 2.6 shows experimental results of simultaneous desalting and concentrating. BSA in a high salt mixture could be successfully focused and recovered from the complex sample by dropping the voltage.

Table 2.2. Representative major components in DMEM cell medium.

Substance	Concentration
D-glucose	4,500 mg L^{-1} (25 mM)
L-glutamine	584 mg L^{-1} (4 mM)
Sodium pyruvate	110 mg L^{-1} (1 mM)
Pyridoxine HCl	4 mg L^{-1} (20 μM)
Sodium bicarbonate	3.7 g L^{-1} (44 mM)

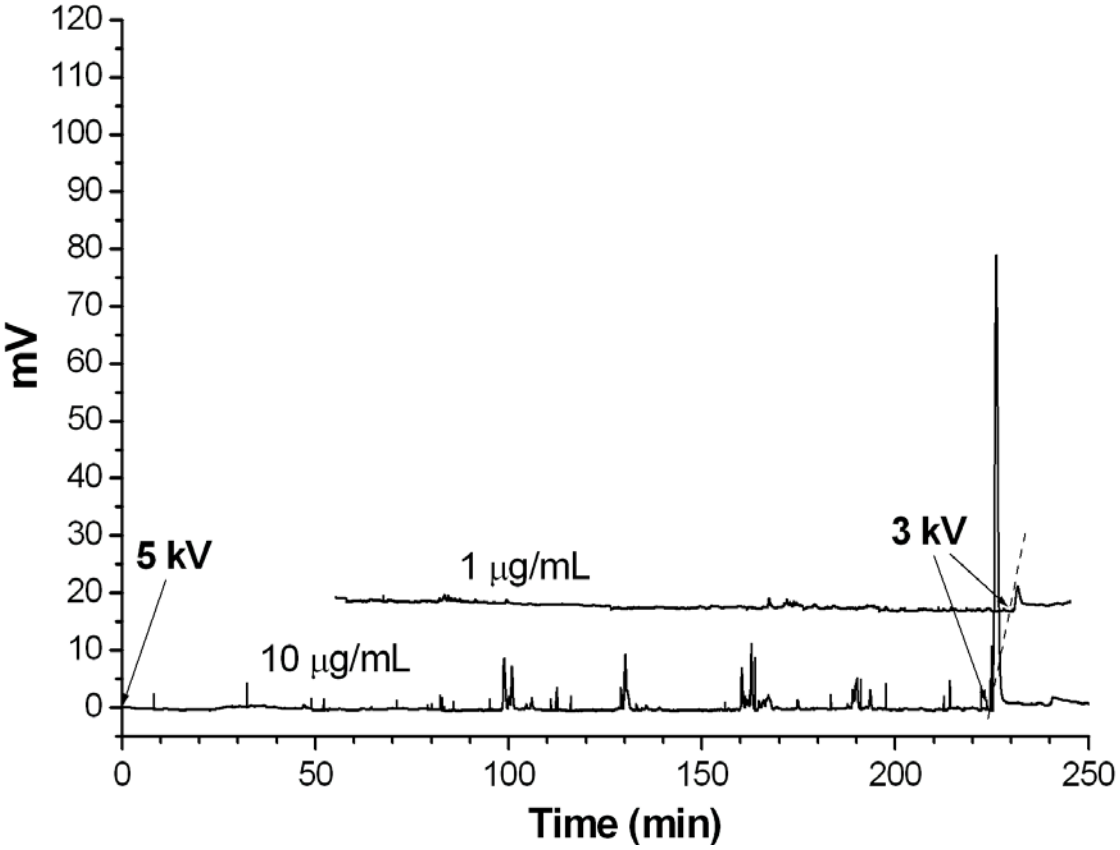

Figure 2.6. Simultaneous sample desalting and protein concentration using a hollow dialysis fiber-based EFGF system. The plot of BSA at 1 μg/mL was shifted to show the focused peak. Conditions are described in Section 2.2.3.

2.3.6 Online Concentration of Ferritin and Simultaneous Removal of Albumin

Ferritin, an iron storage protein, is found in a number of cell types such as liver, spleen, and bone marrow. Ferritin plays a key role in iron metabolism, both iron detoxification and iron storage [1]. Ferritin has been used in the diagnosis of anemia and has been correlated with cancer [2,3]. Serum ferritin is present in relatively low concentration in humans (123 ng/mL in males and 56 ng/mL in females [1]). However, the detection of such a low abundance protein is usually hindered by the existence of high abundance proteins, such as albumin. In addition, the identification of ferritin commonly depends on immunoassays [5-7] such as immunoradiometry and immunodiffusion. It would be useful to have a technique that could detect a specific low abundance protein, and simultaneously, remove albumin from the sample matrix without an expensive and time-consuming radiolabelling process as well as antibody preparation.

My previous results showed that both BSA and ferritin could be focused and eluted separately from the channel at pH 8.7 using voltage-controlled EFGF. However, concentrating proteins under neutral conditions would be more suitable for dealing with biological samples. From preliminary experiments, I found that both BSA and ferritin could be focused in the fiber at pH 7.0 when 5 kV was applied. BSA began to elute from the fiber while ferritin was still retained as the voltage was dropped. Ten consecutive injections of a mixture of BSA and ferritin were made with a 1 μL sample loop to demonstrate the ability of using voltage-controlled fiber-based EFGF for simultaneous online protein concentration and removal of albumin. In order to remove BSA, 2 kV was chosen to focus and concentrate ferritin, while BSA eluted from the channel without

focusing. As shown in Figure 2.7, a voltage of 2 kV was first applied to the system for 2 h to remove most of the BSA from the sample matrix. The complex pattern of BSA was due to multiple injections of the protein mixture without focusing BSA. The concentrated ferritin was eluted from the fiber as the voltage was decreased to 1 kV. The inset shows the results of a single injection to support my claim that simultaneous online protein concentration and removal of albumin are not degraded by the presence of large amounts of albumin resulting from multiple injections.

Many proteins, including albumin and ferritin, become glycated in body fluids. A common glycated form results from the condensation of glucose with an amine group at the N-terminus of a protein to form an unstable Schiff base (aldimine), which then undergoes an Amadori arrangement to form a stable ketoamine. Glycation may also occur at sites other than the N-terminus, such as lysine residues with primary amine groups on the side chains. These glycated forms contribute to the charge heterogeneity of proteins. In this work, the charge heterogeneity of the proteins did not affect the results of separating ferritin from albumin. The separation or purification of these charge heterogeneous species remains a significant challenge using current analytical techniques such as SDS-PAGE.

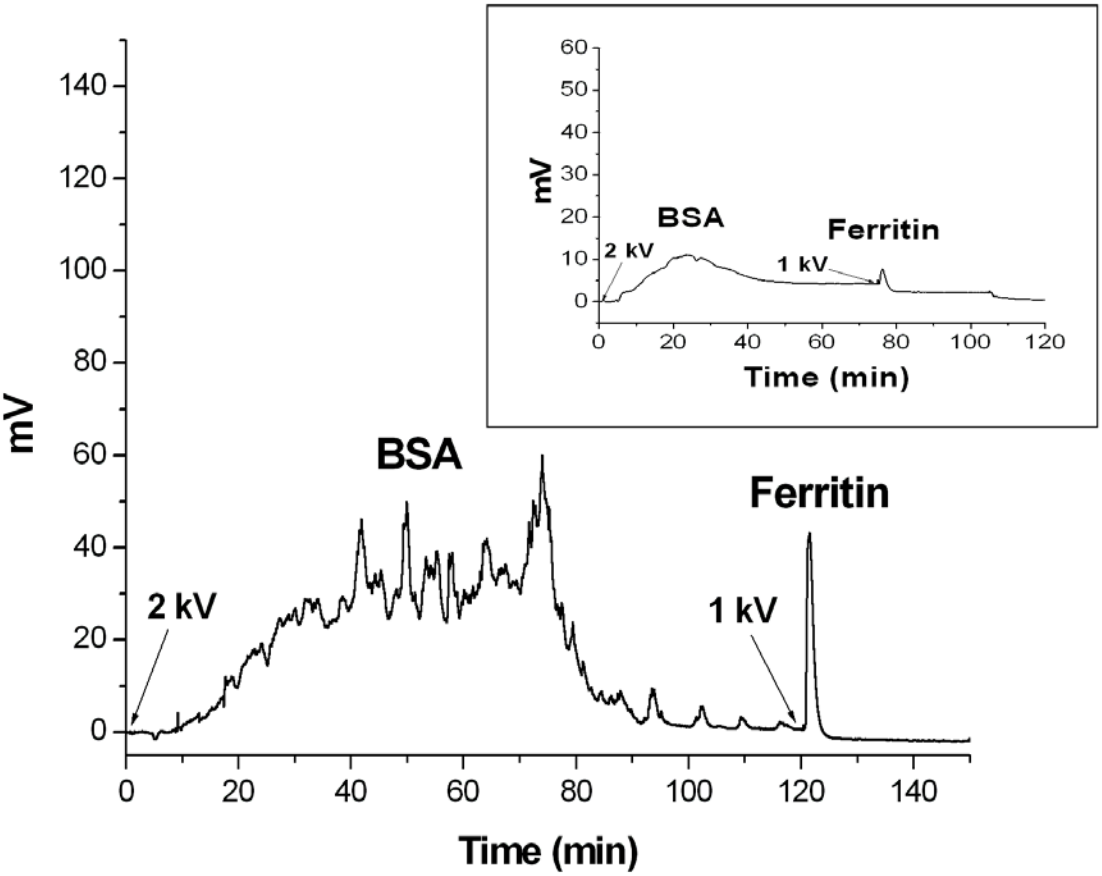

Figure 2.7. Online concentration of ferritin and simultaneous removal of albumin using a hollow dialysis fiber-based EFGF system. Conditions are described in Section 2.2.3.

2.4 Conclusions

EFGF has the ability to selectively retain, concentrate, and separate a trace target protein from a complex medium, and can be used for both qualitative and quantitative protein analysis. In addition, EFGF is able to simultaneously concentrate a low abundance target protein and remove high abundance proteins such as albumin from the sample matrix in a relatively large sample volume without band broadening. The ease of application (including the absence of tedious labeling schemes) and the relatively low cost for equipment setup make UV detection an attractive detection method compared to fluorescence.

The limitations of this technique as described by Wang et al. [4] include a very steep electric field gradient formed in a narrow section at the beginning of the EFGF channel and a very shallow gradient throughout the rest of the dialysis fiber that result in relatively broad peaks due to the large dispersion from hydrodynamic flow as a result of the commercially available modified cellulose fiber. This electric field gradient profile is not suitable for analyzing complex protein mixtures. For a complex mixture such as plasma containing multiple abundant components, a different electric field profile and a multi-step voltage program will be required to sequentially remove unwanted components and concentrate target analytes. On the other hand, this fiber provides high mass transfer which is beneficial for desalting and removing unwanted smaller molecules (molecular weights <10,000) from the sample matrix for purification as well as for simultaneous online concentration of target analytes. This device could be coupled with other techniques such as capillary LC, CE, and mass spectrometry as a pre-concentrator.

2.5 References

[1] Harrison, P. M.; Arosio, P. *Biochim. Biophys. Acta* **1996**, *1275*, 161-203.

[2] Ali, M. A.; Akhmedkhanov, A.; Zeleniuch-Jaquotte, A.; Toniolo, P.; Frenkel, K.; Huang, X. *Cancer Detection & Prevention* **2003**, *27*, 116-121.

[3] Akiba, S.; Neriishi, K.; Blot, W. J.; Kabuto, M.; Stevens, R. G.; Kato, H.; Land, C. E. *Cancer* **1991**, *67*, 1707-1712.

[4] Wang, Q.; Lin, S.-L.; Warnick, K. F.; Tolley, H. D.; Lee, M. L. *J. Chromatogr. A* **2003**, *985*, 455-462.

[5] Campbell, C. H.; Crocker, D.; Gruntmeir, J. J.; Head, M.; Kelly, T.; Langfur, M. I.; Leimer, A. H. *J. Cell Biochem.* **1993**, *53*, 420-432.

[6] Worwood, M.; Dawkins, S.; Wagstaff, M.; Jacobs, A. *Biochem. J.* **1976**, *157*, 97-103.

[7] Suryakala, S.; Deshpande, V. *Vet. Res. Commun.* **1999**, *23*, 165-181.

3 ELECTRIC FIELD GRADIENT FOCUSING BASED ON CHANGING CROSS-SECTIONAL AREA✳

3.1 Introduction

In this chapter, a shaped ionically conductive acrylic polymer (or called hydrogel), similar to the one reported by Humble et al. [1], with a separation channel along its center axis is used to generate an electric field gradient based on changing cross-sectional area. The use of online UV-Vis detection for a conductive hydrogel-based EFGF system is described. Proteins are first focused in the separation channel and then sequentially eluted from the channel for detection by varying either the voltage drop or the hydrodynamic flow rate. Both voltage-controlled and flow-controlled elution methods are described. Removal of human serum albumin and simultaneous concentration of an acute phase plasma protein, α_1-acid glycoprotein, are performed using a multiple injection method.

3.2 Experimental Section

3.2.1 Materials and Sample Preparation

IEF marker proteins including amyloglucosidase, trypsin inhibitor, β-lactoglobulin A, and carbonic anhydrase II were prepared in 10 mM Tris buffer at pH 8.5 for protein analysis and mobility measurements under basic conditions. Human serum albumin (HSA) and α_1-acid glycoprotein (AAG) from human plasma were prepared in 10 mM Bis-Tris buffer adjusted to pH 7.0 for simultaneous protein concentration and

---

✳ This chapter (except Section 3.3.4 and Figure 3.5) is reproduced with permission from *J. Chromatogr. A* **2006**, *in press.* Copyright 2006 Elsevier.

removal of albumin. The following proteins were used as model proteins for mobility measurements under acidic conditions: hemoglobin from bovine blood, ribonuclease A from bovine pancreas, lysozyme from chicken egg white, and four IEF marker proteins (carbonic anhydrase II, myoglobin, lentil lectin, and trypsinogen). These proteins were prepared in 20 mM acetate buffer at pH 4.3. Poly(vinyl alcohol), PVA, was used to coat fused silica capillaries using procedures published previously to reduce electroosmotic flow [2].

For constructing the ionically conductive polymeric hydrogel, the following components were used to make a transparent pre-polymer solution: 33.3 wt% 2-hydroxyethyl methacrylate (HEMA), 23.3 wt% methyl methacrylate (MMA), 20 wt% poly(ethylene glycol) acrylate (PEGA, average molecular weight ~375), 16.7 wt% buffer solution, 6.7 wt% ethylene dimethacrylate (EDMA), and 1 wt% 2,2-dimethoxy-2-phenylacetophenone (DMPA) that served as a photoinitiator. A Nichrom wire with a diameter of 120 μm was used to form a separation channel inside the conductive polymer. All proteins and chemicals mentioned above were purchased from Sigma-Aldrich (St. Louis, MO). Dulbecco's Modified Eagle Medium (DMEM) was purchased from GIBCO BRL Life Technologies (Gaithersburg, MD). Untreated fused-silica capillaries, 150 μm I.D. × 360 μm O.D. (outer diameter) and 75 μm I.D. × 360 μm O.D., were obtained from Polymicro Technologies (Phoenix, AZ).

3.2.2 Device Fabrication and Instrumentation

Construction of the hydrogel-based EFGF device used in this study was described in a previous paper [1] and in Figure 1.8. The shape of the conductive polymer was designed to generate a linear electric field gradient for which the field strength increased by a factor of 6 across the whole separation channel. A simple diagram of the device setup is shown in Figure 3.1. A UV lamp (Model 5000, Dymax, Torrington, CT) was used for photoinitiated polymerization. A programmable syringe pump (PHD2000, Harvard Apparatus, Holliston, MA) with a 500-μL gas tight syringe (Hamilton, Reno, NV) was used to deliver buffer solution and sample into the separation channel. Single and multiple injections were performed using an injection valve with a 1-μL sample loop from VICI Valco (Houston, TX). A high voltage power supply from Spellman (Model SL 30, Hauppauge, NY) was used with polarity as shown in Figure 3.1 for negatively charged analytes. A detection window was made at 2 cm after the end of the separation channel for online detection with a UV-Vis absorption detector from ThermoQuest (Model UV3000, Riviera Beach, FL). A 60 cm PVA-coated fused-silica capillary, 75 μm I.D. × 360 μm O.D., was used for electrophoretic mobility measurements of proteins, and the experiments were performed using a CE 300 system from ATI (Madison, WI) with an online variable wavelength UV/Vis detector from Applied Biosystems (Model 759A, Foster City, CA).

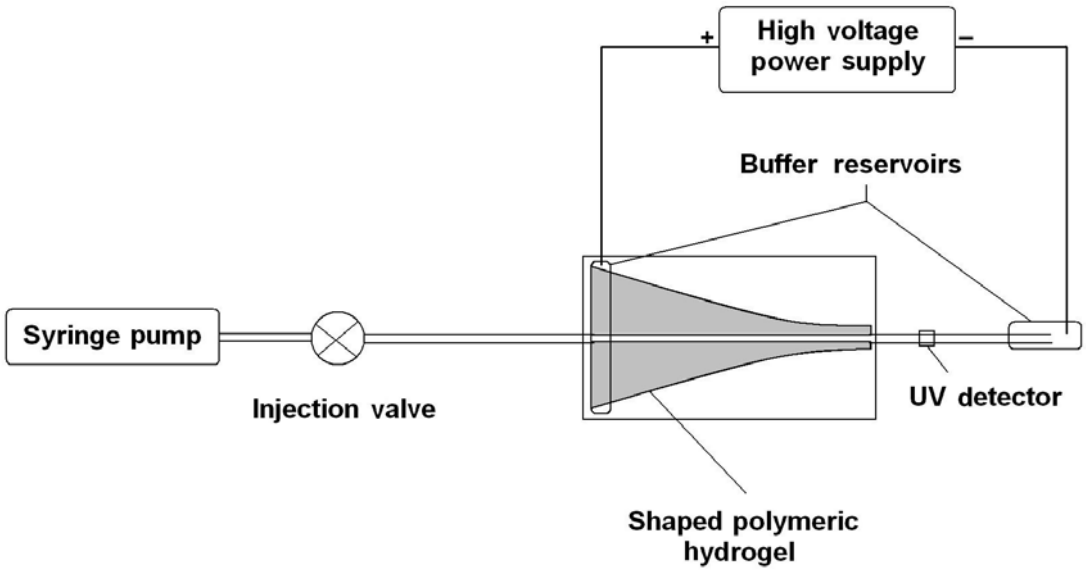

Figure 3.1. Schematic diagram of the ionically conductive polymeric hydrogel-based EFGF device.

3.2.3 Experimental Conditions

Most experiments were conducted at pH 8.5 (10 mM Tris buffer), except for the separation of α_1-acid glycoprotein from albumin, which was performed at pH 7.0 (10 mM Bis-Tris buffer), and the mobility measurements for positively charged proteins were performed at pH 4.3 (20 mM acetate buffer). The flow-rate in the separation channel was set at 0.1 μL/min (linear velocity of 1.75×10^{-2} cm/s) for the experiments carried out under basic conditions and 0.2 μL/min (linear velocity of 3.51×10^{-2} cm/s) for the experiments performed at pH 4.3 and pH 7.0. The initial applied voltage for focusing was 2 kV at all conditions and the focusing time was varied for different experiments. The voltage or flow programs used in the individual experiments are described in either Section 3.3 or in the figure legends. UV absorption detection was accomplished at 214 nm for all experiments.

3.3 Results and Discussion

3.3.1 Online Protein Concentration

Online protein concentration with high loading capacity is a major advantage of EFGF [3]. In order to investigate the use of the hydrogel-based EFGF system for protein concentration from a large sample volume, online concentration of amyloglucosidase was performed using the system shown in Figure 3.1. In addition to demonstrating multiple injections (5 consecutive injections with a 1-μL sample loop), large volume injection was performed with continuous sample loading. The top and bottom traces in Figure 3.2 show the experimental results of protein concentration with 20 μg/mL and 2

μg/mL of amyloglucosidase prepared in 10 mM Tris buffer at pH 8.5, respectively. Both large volume (100 μL) and multiple injections gave similar peak widths when compared to a single 1 μL injection. Compared to the channel volume (<0.4 μL), a sample volume of 100 μL is >250-fold larger. From the results, large sample volumes do not result in significant band broadening, which is a great advantage for online sample concentration of trace analytes. It should be noted that the time scale shown in Figure 3.2 includes 500 min for continuous sample loading (0.2 μL/min for 100 μL) and focusing prior to decreasing the voltage for elution. The long running time in Figure 3.2 was chosen to demonstrate that EFGF offers high sample loading capacity with continuous sampling and that target analytes can be retained in the separation channel as long as necessary without significant band broadening. The running time for online concentration can be reduced by increasing the hydrodynamic flow-rate and/or the voltage applied to the system.

The amyloglucosidase peak in the bottom trace in Figure 3.2 (2 μg/mL, or approximately 20 nM) had a signal-to-noise ratio of over 200, which indicates a concentration limit of detection of approximately 20 ng/mL (200 pM) using this EFGF system. The low concentration limit of detection allows the use of a UV-Vis detector for trace analysis, which usually provides a detection limit in the μM range. The voltage program used in these experiments is an example of voltage-controlled elution; a linear voltage program can also be used for this purpose.

3.3.2 Protein Mobility Measurements and Focusing Experiments

Protein focusing and separation using EFGF are based on the electrophoretic mobilities of the charged proteins under the various operating conditions. In order to explore the mobility range of this hydrogel-based EFGF device for protein analysis, two sets of conditions were used. These operating conditions are summarized in Table 3.1. Focusing experiments were carried out using the hydrogel-based EFGF device shown in Figure 3.1. Electrophoretic mobility measurements of proteins were performed by capillary electrophoresis using a PVA-coated capillary to eliminate electroosmotic flow. The electrophoretic mobility of each protein was then determined using the following equation:

$$\mu_{ep} = \nu_{ep} / E = (L_D / t_m) / (V / L_T) \tag{3.1}$$

where μ_{ep} is the electrophoretic mobility, ν_{ep} is the electrophoretic velocity, E is the applied electric field, L_D (48.6 cm) is the distance from the capillary inlet to the detection window, t_m is the migration time for an analyte to travel through the capillary to the detection window under an applied voltage, L_T (60 cm) is the total capillary length, and V is the applied voltage (30 kV for positively charged analytes and –30 kV for negatively charged analytes). The results of mobility measurements and focusing experiments under basic and acidic conditions are summarized in Table 3.2.

Under basic conditions, four IEF markers were used as model proteins, which were negatively charged at pH 8.5. Table 3.2 shows that carbonic anhydrase II had the lowest electrophoretic mobility, followed by β-lactoglobulin A, trypsin inhibitor, and

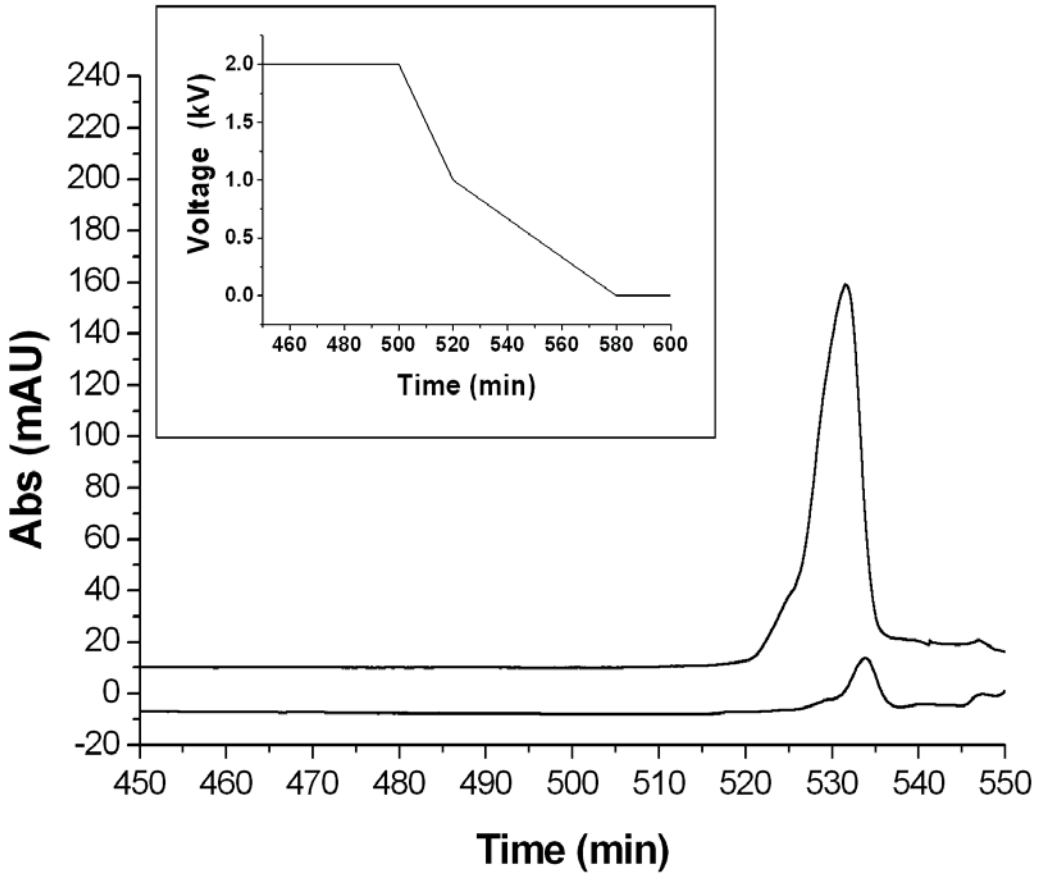

Figure 3.2. Online protein concentration from a large sampling volume (100 μL) using an ionically conductive polymeric hydrogel-based EFGF system. After focusing, the initial voltage, 2 kV, was decreased for elution (voltage program is shown in the inset). Other conditions are described in Section 3.2.3.

Table 3.1. Operating conditions for protein mobility measurements and focusing experiments.

	Basic (10 mM Tris, pH 8.5)	Acidic (20 mM Acetate, pH 4.3)
Channel dimensions (i.d., length)	110 μm, 4 cm	110 μm, 4 cm
Voltage applied	2 kV	2 kV
Flow-rate	0.1 μL/min	0.2 μL/min
Maximum slope of electric field gradient	62.5 V/cm^2	62.5 V/cm^2

amyloglucosidase. According to the results of focusing experiments, I found that carbonic anhydrase II, with an electrophoretic mobility of 0.73×10^{-4} $cm^2/(V\cdot s)$, could not be retained and focused in the separation channel.

In order to further explore the relationship between electrophoretic mobility and protein focusing, mobility measurements and focusing experiments were also performed under acidic conditions, which allowed a wider selection of positively charged proteins at pH 4.3. Table 3.2 shows that carbonic anhydrase II had an electrophoretic mobility of 1.63×10^{-4} $cm^2/(V\cdot s)$ and could not be focused in the separation channel when 2 kV was applied to the system. In this group, the protein with the lowest mobility which could be focused in the separation channel was lentil lectin, which had an average electrophoretic mobility of 1.91×10^{-4} $cm^2/(V\cdot s)$. With more thorough investigations of electrophoretic mobilities of proteins under different conditions, including electric field gradient profile (shape of the conductive polymeric hydrogel), applied voltage, and hydrodynamic flow-rate, I should be able to find specific operating conditions that can selectively focus and concentrate proteins of interest as well as remove unwanted components in a sample solution.

3.3.3 Voltage-Controlled and Flow-Controlled Elution of Proteins

Two major parameters in EFGF that can be manipulated for focusing and separation of charged analytes are the electric field profile that is generated by applying a voltage to the system and hydrodynamic flow velocity in the separation channel. Three IEF marker proteins were chosen for demonstration of protein separation for both

Table 3.2. Protein mobility measurements and the results of focusing experiments under basic and acidic conditions.

	Analyte	Mobility [$cm^2/(V \cdot s)$]	Focusing[a]
Basic conditions	Carbonic anhydrase II	0.73×10^{-4}	N
	β-Lactoglobulin A	2.66×10^{-4}	Y
	Trypsin inhibitor	2.94×10^{-4}	Y
	Amyloglucosidase	3.37×10^{-4}	Y
Acidic conditions	Carbonic anhydrase II	1.63×10^{-4}	N
	Lentil lectin	1.91×10^{-4}	Y
	Myoglobin	2.16×10^{-4}	Y
	Hemoglobin	2.96×10^{-4}	Y
	Trypsinogen	2.99×10^{-4}	Y
	Ribonuclease A	3.09×10^{-4}	Y
	Lysozyme	3.77×10^{-4}	Y

[a] N = protein could not be retained and focused in the channel under the conditions stated in Table 3.1, Y= protein was retained and focused in the channel under the conditions stated in Table 3.1.

voltage-controlled and flow-controlled elution under basic conditions using the hydrogel-based EFGF system.

Figure 3.3 shows the experimental results of voltage-controlled elution of the three remaining proteins under basic conditions. All proteins were first focused and retained in the separation channel for 2 h when 2 kV was applied and the hydrodynamic flow rate was kept at 0.1 μL/min. Using a continuous voltage program shown in Figure 3.3, all three proteins were retained in the channel until the applied voltage was decreased to below 1 kV, at which point the proteins began to elute from the separation channel. Figure 3.4 demonstrates protein separation using a flow-controlled elution method. Starting with the same conditions as used in voltage-controlled elution experiments, the proteins were first focused and retained in the separation channel for 90 min before increasing the hydrodynamic flow-rate. As seen in Figure 3.4, the three model proteins were separated and eluted from the channel using the flow program shown in the inset. The intensity differences of protein peaks in Figures 3.3 and 3.4 were due to different concentrations of proteins in different sample solutions used in the experiments. Compared to the separation performed by voltage-controlled elution, lower resolution of proteins was observed. This was due to increased dispersion as the hydrodynamic flow-rate was raised.

For the three focused proteins, the mobility data (in Table 3.2) matched the elution orders for protein separations shown in Figures 3.3 and 3.4. The analyte with the lowest electrophoretic mobility eluted first and the analyte with the highest mobility

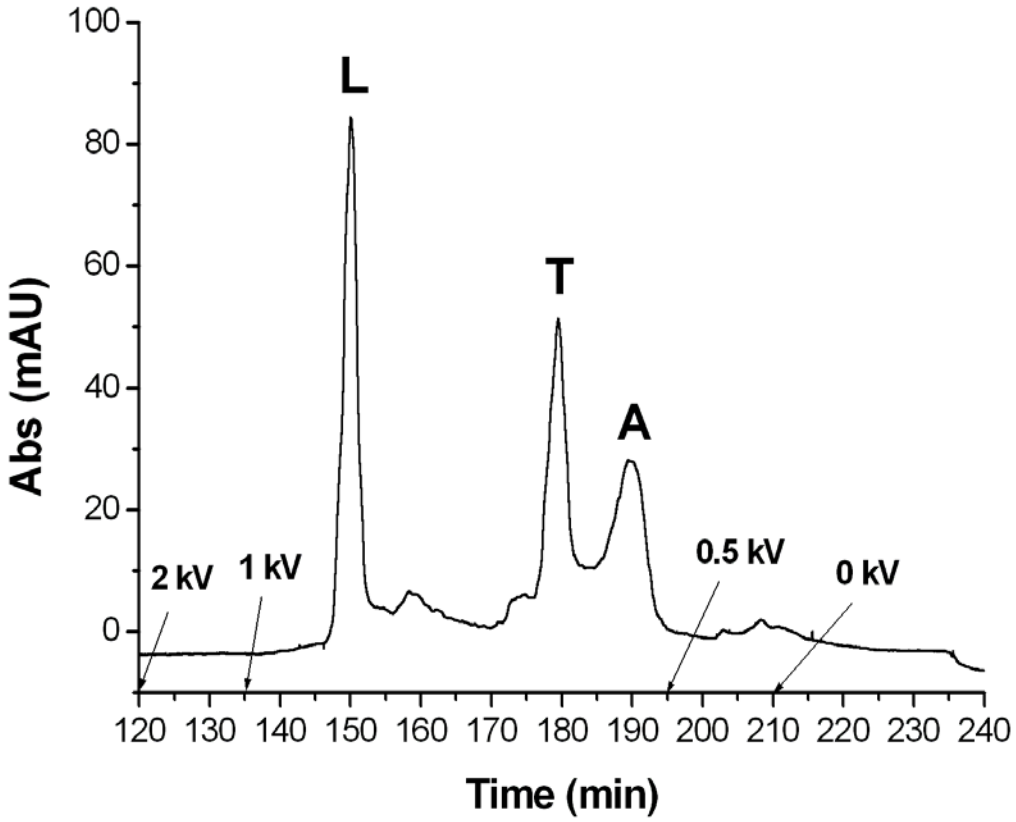

Figure 3.3. Voltage-controlled elution of proteins using an ionically conductive polymeric hydrogel-based EFGF system. After focusing, the initial applied voltage, 2 kV, was linearly decreased to 1 kV in 15 min, further decreased to 0.5 kV in 1 h, and finally dropped to 0 kV in another 15 min. Other conditions are described in Section 3.2.3. A = 0.6 mg/mL amyloglucosidase, T = 0.6 mg/mL trypsin inhibitor, and L = 1.2 mg/mL β-lactoglobulin A.

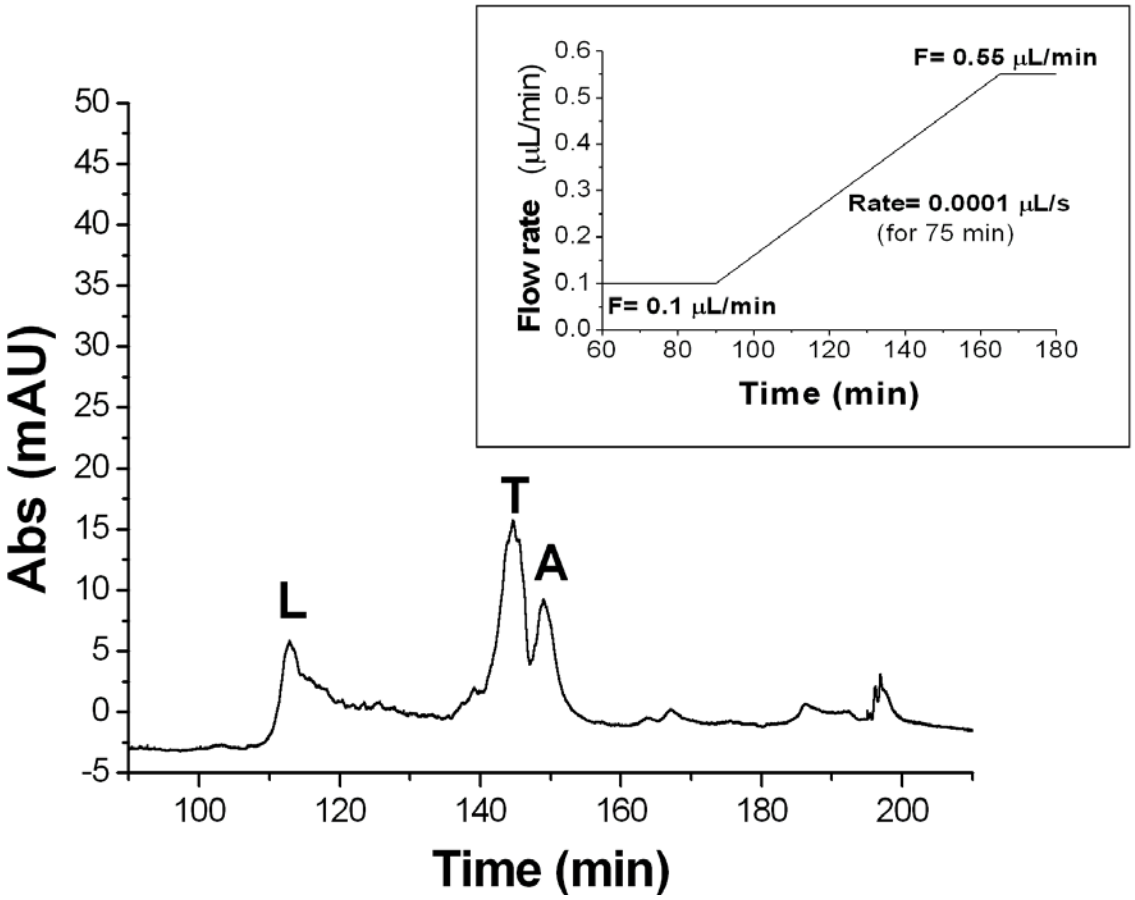

Figure 3.4. Flow-controlled elution of proteins using an ionically conductive polymeric hydrogel-based EFGF system. After focusing, the initial hydrodynamic flow-rate, 0.1 μL/min, was increased for elution (flow program is shown in the inset). Other conditions are described in Section 3.2.3. A = 0.4 mg/mL amyloglucosidase, T = 0.4 mg/mL trypsin inhibitor, and L = 0.2 mg/mL β-lactoglobulin A.

eluted last. Furthermore, β-lactoglobulin A and trypsin inhibitor, with a mobility difference of approximately 3×10^{-5} $cm^2/(V\cdot s)$, were well separated.

3.3.4 Comparison of CE and EFGF

In order to evaluate the performance of EFGF in protein separation, β-lactoglobulin A, trypsin inhibitor, and amyloglucosidase were also used as model proteins for CE experiments using the same buffer conditions. Protein samples were prepared in 10 mM Tris buffer (pH 8.5) and other conditions were described in Section 3.3.2. The sample solutions were injected individually and were then superimposed forcomparison (Figure 3.5).

In Figure 3.5, β-lactoglobulin A and trypsin inhibitor were barely resolved, while amyloglucosidase could be separated from these two proteins. As described in Section 3.3.3, these three proteins could be separated using EFGF (Figure 3.3) and resolution in EFGF between β-lactoglobulin A and trypsin inhibitor was much higher than that in CE. However, trypsin inhibitor and amyloglucosidase could be baseline separated in CE, while only partially separated in EFGF. The resolution in EFGF can be improved by modifying the shape of the polymeric hydrogel and/or the voltage program.

3.3.5 Online Concentration of α_1-Acid Glycoprotein and Simultaneous Removal of Albumin

Online concentration of human α_1-acid glycoprotein, an acute phase protein in plasma, and simultaneous removal of human serum albumin (HSA) were performed to

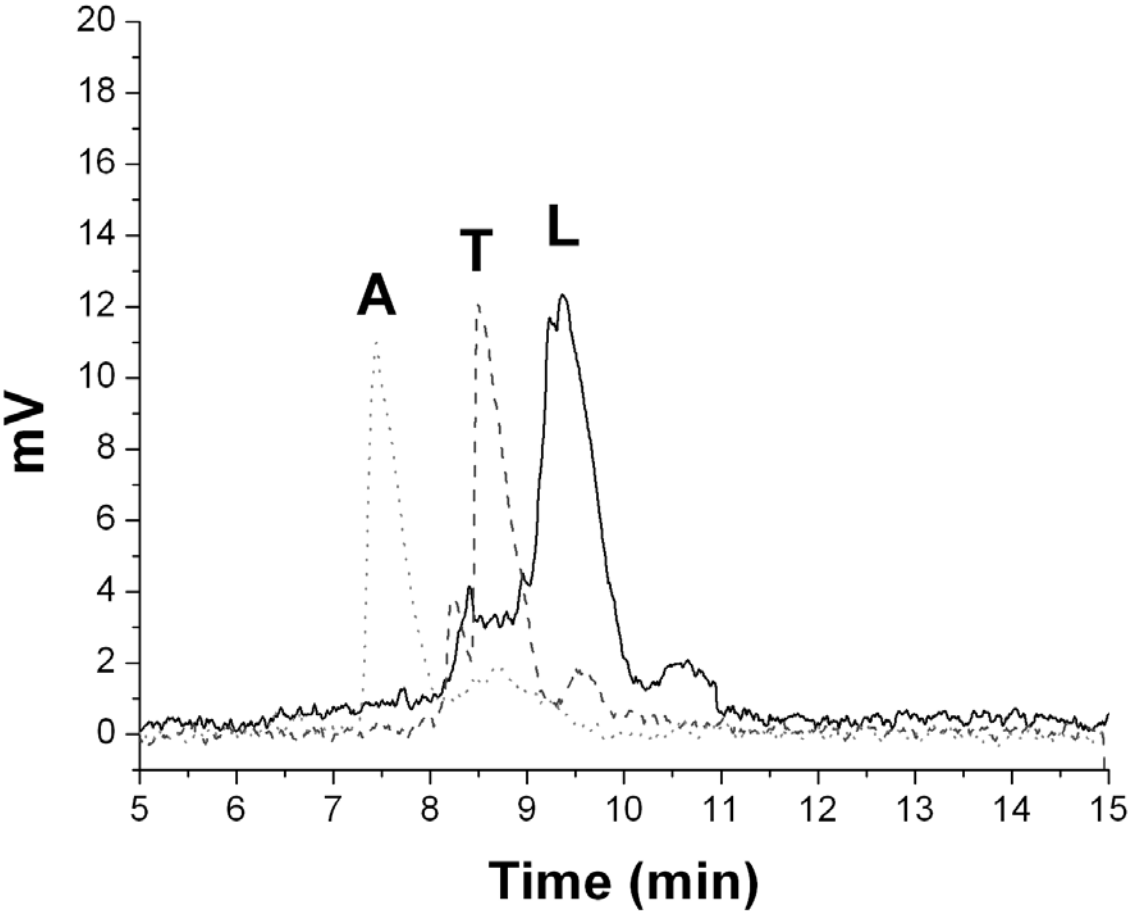

Figure 3.5. Superimposed CE of proteins. Experimental conditions are described in Sections 3.2.3 and 3.3.2. A = 1.0 mg/mL amyloglucosidase, T = 1.0 mg/mL trypsin inhibitor, and L = 1.0 mg/mL β-lactoglobulin A.

demonstrate the potential of using EFGF for more typical protein analysis. AAG, which can be elevated 2- to 5-fold in response to a trauma [4], is found in most body fluids such as plasma, mucus, and gastric fluid. In addition to albumin, AAG is also an important drug-binding plasma protein in adults [5,6]. Serum AAG concentrations have been reported to be in the range of 0.5-1.2 mg/mL in healthy adults between the ages of 20 and 60 [7]. The change in concentration of AAG in plasma under various pathological and physiological conditions may alter the binding of various drugs, which can have a considerable effect on both pharmacodynamics and pharmacokinetics of a drug [8,9]. Several protease inhibitors of human immunodeficiency virus have also been reported to be highly bound to α_1-acid glycoprotein [10,11].

A number of techniques such as SDS-PAGE, HPLC, affinity radioimmunoassay, and immunoelectrophoresis have been used to determine AAG [5]. However, they are either expensive or time-consuming and do not provide the advantages of online concentration and high loading capacity. EFGF has the ability to focus and concentrate charged analytes with large sample loading capacity [3,12]. Isolating AAG from other abundant plasma proteins, such as albumin in human serum and other body fluids, is also important to reduce interferences in studies of drug-binding capacity to AAG in pharmaceutical research. Several methods have been developed to remove albumin, including centrifugal filtration and immunoaffinity methods [13,14]. However, they are either marginally successful or costly in terms of time and money for antibody preparation. In chapter 2, I demonstrated that a fiber-based EFGF device could be used to concentrate ferritin while simultaneously removing albumin from the sample solution [3].

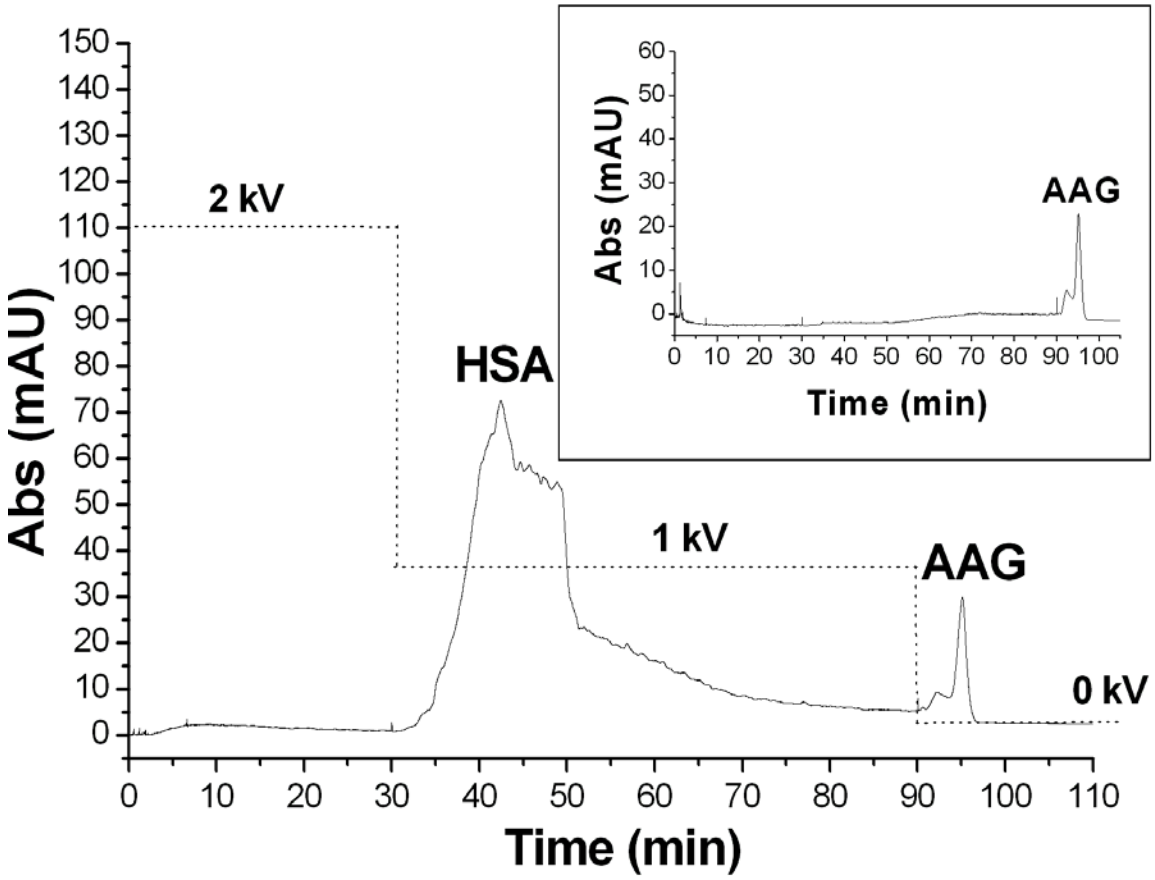

Figure 3.6. Online concentration of human α_1-acid glycoprotein and simultaneous removal of albumin using an ionically conductive polymeric hydrogel-based EFGF system. The dashed lines indicate the voltage program used in the experiments; other conditions are described in Section 3.2.3. The concentrations of HSA and AAG were 2 mg/mL and 0.2 mg/mL, respectively.

In this study, I was able to concentrate α_1-acid glycoprotein while simultaneously removing HSA during five consecutive injections (1-μL sample loop) of a mixture of HSA and AAG using the hydrogel-based EFGF system shown in Figure 3.1. The experiments were carried out under neutral conditions, which is appropriate for proteins in biological samples. Both HSA and AAG were focused in the EFGF separation channel when 2 kV was applied. HSA began to elute from the separation channel as the voltage was dropped to 1 kV, and AAG was concentrated until the voltage was further decreased to 0 kV. The experimental results are shown in Figure 3.6. The complex pattern of HSA was due to incomplete focusing after multiple injections of the protein mixture. The insetindicates that effective removal of albumin and simultaneous online protein concentration are not affected by the presence of large amounts of albumin in the original sample.

3.4 Conclusions

A shaped conductive polymeric hydrogel-based EFGF system can be used to focus and concentrate a target protein with high loading capacity, and protein separation can be achieved using both voltage-controlled and flow-controlled elution methods. The hydrogel-based EFGF system can also be used to remove high abundance proteins such as human serum albumin while simultaneously concentrating a relatively low abundance target protein such as α_1-acid glycoprotein from a mixture.

The limitations of using this open channel EFGF device for protein analysis have been described by Humble et al. [1], which include low peak capacity and relatively large dispersion. Additional efforts to optimize the electric field gradient profile must be made

in order to improve the performance for protein analysis. Adding polymeric micro-particles or incorporating a section of polymeric monolith into the separation channel should reduce band dispersion and lead to improved protein resolution.

3.5 References

[1] Humble, P. H.; Kelly, R. T.; Woolley, A. T.; Tolley, H. D.; Lee, M. L. *Anal. Chem.* **2004**, *76*, 5641-5648.

[2] Clarke, N. J.; Tomlinson, A. J.; Schomburg, G.; Naylor, S. *Anal. Chem*. **1997**, *69*, 2786-2792.

[3] Lin, S.-L.; Tolley, H. D.; Lee, M. L. *Chromatoghraphia* **2005**, *62*, 277-281.

[4] Koj, A. In *Pathophysiology of Plasma Protein Metabolism;* Mariani, G., Ed.; Plenum Press, New York and London, **1984**, pp 221-248.

[5] Israili, Z. H.; Dayton, P. G. *Drug Metab. Rev.* **2001**, *33*, 161-235.

[6] Ganguly, M.; Carnighan, R. H.; Westphal, U. *Biochemistry* **1967**, *6*, 2803-2814.

[7] Johnson, A. M.; Rohlfs, E. M.; Silverman, L. M. In *Tietz Textbook of Clinical Chemistry, 3rd ed.;* Burtis, C. A. and Ashwood, E. R., Eds.; Saunders, Philadelphia, **1999**, pp 477-540.

[8] Belpaire, F. M.; Bogaert, M. G. *Prog. Clin. Biol. Res.* **1989**, *300*, 337-350.

[9] Wilkinson, G. R. *Drug Metab. Rev.* **1983**, *14*, 427-465.

[10] Bilello, J. A.; Bilello, P. A.; Pritchard, M.; Robins, T.; Drusano, G. L. *J. Infect. Dis.* **1995**, *171*, 546-551.

[11] Bilello, J. A.; Bilello, P. A.; Stellrecht, K.; Leonard, J.; Norbeck, D. W.; Kemph, D. J.; Robins, T.; Drusano, G. L. *Antimicrob. Agents Chemother.* **1996**, *40*, 1491-1497.

[12] Wang, Q.; Lin, S.-L.; Warnick, K. F.; Tolley, H. D.; Lee, M. L. *J. Chromatogr. A* **2003**, *985*, 455-462.

[13] Georgiou, H. M.; Rice, G. E.; Baker, M. S. *Proteomics.* **2001**, *1*, 1503-1506.

[14] Bilello, J. A.; Bilello, P. A.; Pritchard, M.; Robins, T.; Drusano, G. L. *Mol. Cell. Proteomics* **2003**, *2*, 262-270.

4 SELECTIVE CONCENTRATION AND SEPARATION OF PROTEINS USING A TANDEM ELECTRIC FIELD GRADIENT FOCUSING SYSTEM✳

4.1 Introduction

Based on the experimental results described in Chapters 2 and 3, two types of EFGF devices were integrated to selectively isolate and concentrate target proteins: (1) a fiber-based EFGF device, which uses a dialysis fiber as a separation channel to generate an electric field gradient by forming an electrolyte concentration gradient along the channel [1,2], and (2) a shaped ionically conductive acrylic polymer with a separation channel along its center axis for generating an electric field gradient based on changing cross-sectional area [3]. In this chapter, an integrated EFGF system with a 3-way switching valve was constructed to demonstrate the utilization of the tandem EFGF system for isolating and concentrating target proteins as well as simultaneous protein concentration and removal of unwanted buffer components.

4.2 Experimental Section

4.2.1 Materials and Sample Preparation

Trypsin inhibitor, an IEF marker protein, was prepared in 10 mM Tris buffer at pH 8.5 for online protein concentration and simultaneous removal of small buffer components. Myoglobin and lysozyme were used as model proteins for selective focusing

---

✳ This chapter is reproduced with permission from *J. Chromatogr. A* **2006**, *in press.*

of proteins under acidic conditions and were prepared in 20 mM acetate buffer at pH 4.3. Poly(vinyl alcohol), PVA, was used to coat fused silica capillaries using procedures published previously to reduce electroosmotic flow [4].

For synthesizing the ionically conductive polymeric hydrogel, the following components were used to prepare a pre-polymer solution: 33.3 wt% 2-hydroxyethyl methacrylate (HEMA), 23.3 wt% methyl methacrylate (MMA), 20 wt% poly(ethylene glycol) acrylate (PEGA, average molecular weight ~375), 16.7 wt% buffer solution, 6.7 wt% ethylene dimethacrylate (EDMA), and 1 wt% 2,2-dimethoxy-2-phenylacetophenone (DMPA) which serves as a photoinitiator. A Nichrom wire with a diameter of 120 μm was used to form a separation channel inside the conductive polymer. All proteins and chemicals mentioned above were purchased from Sigma-Aldrich (St. Louis, MO). Dulbecco's Modified Eagle Medium (DMEM) was purchased from GIBCO BRL Life Technologies (Gaithersburg, MD). The dialysis hollow fiber, a modified cellulose fiber with internal diameter (I.D.) of 200 μm and dry wall thickness of 8 μm, was purchased from Membrana (Wuppertal, Germany). This dialysis fiber had a molecular weight cut-off of approximately 10,000. Untreated fused-silica capillaries, 150 μm I.D. × 360 μm O.D. and 75 μm I.D. × 360 μm O.D., were obtained from Polymicro Technologies (Phoenix, AZ).

4.2.2 Device Fabrication and Instrumentation

The fabrication of the individual fiber-based and hydrogel-based EFGF devices were described in Chapters 2 and 3. The shape of the conductive polymer was designed

to generate a linear electric field gradient for which the field strength increased by a factor of 6 across the whole separation channel. A simple diagram of the setup of the tandem EFGF system is shown in Figure 4.1. A UV lamp (Model 5000, Dymax, Torrington, CT) was used for photoinitiated polymerization.

For the hollow fiber-based EFGF section, a programmable syringe pump (PHD2000, Harvard Apparatus, Holliston, MA) with a 500-μL gas tight syringe (Hamilton, Reno, NV) was used to deliver buffer solution and sample into the separation channel. Another syringe pump (Model 11 Plus, Harvard Apparatus, Holliston, MA) with a 30-mL plastic syringe (Becton Dickinson, Franklin Lake, NJ) was used to deliver buffer solution through the outside tubing around the dialysis fiber to simultaneously remove small buffer components and/or salts.

Sample injections were performed using an injection valve with a 1-μL sample loop from VICI Valco (Houston, TX). High voltage power supplies from Spellman (Model SL 30, Hauppauge, NY) were used to provide the desired voltage applied to the EFGF system. A detection window was made at 2 cm after the end of the separation channel for online detection with a UV-Vis absorption detector from ThermoQuest (Model UV3000, Riviera Beach, FL).

4.2.3 Experimental Conditions

Online protein concentration and simultaneous removal of small buffer components was performed at pH 8.5 (10 mM Tris buffer) with a flow rate of 0.1 μL/min (linear velocity of 1.75×10^{-2} cm/s). Selective isolation and concentration of proteins was

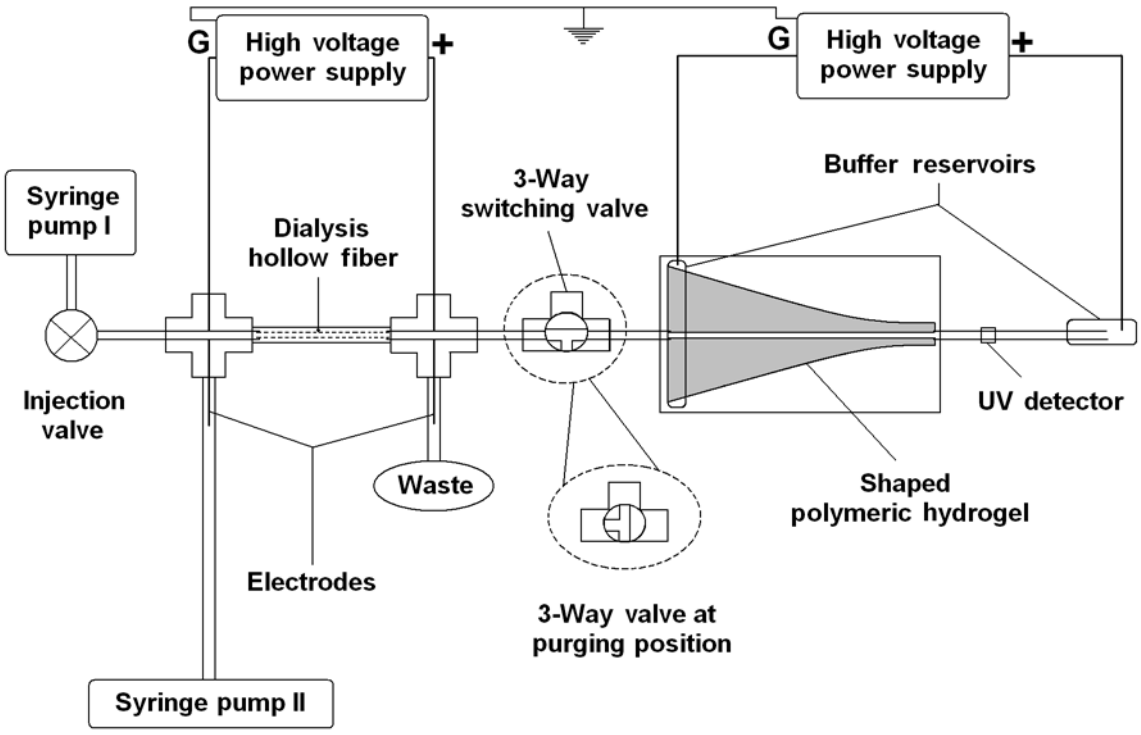

Figure 4.1. Schematic diagram of the tandem EFGF system.

carried out at pH 4.3 (20 mM acetate buffer) with a flow rate of 0.2 μL/min (linear velocity of 3.51×10^{-2} cm/s). The initial applied voltage for focusing was 2 kV for all experiments and the focusing time was varied for different experiments. The voltage programs used in the individual experiments were described in either Section 4.3 or in the figure legends. UV absorption detection was accomplished at 214 nm for all experiments.

4.3 Results and Discussion

4.3.1 Online Protein Concentration and Simultaneous Removal of Small Buffer Components

Proteins of interest are typically present in complex sample matrices, and protein purity is an important issue in protein analysis. Removing unwanted buffer components and concentrating proteins are two major tasks that must be achieved during the purification process. Removal of unwanted buffer components was described in Chapter 2 using a fiber-based EFGF system [2]. A simple integrated EFGF system (similar to the one shown in Figure 4.1), without the 3-way valve and without voltage applied to the fiber section, was utilized to demonstrate the use of more than one EFGF device for online protein concentration and simultaneous removal of unwanted buffer components, such as NaCl, in this chapter.

A solution of trypsin inhibitor (0.5 mg/mL) was prepared in DMEM with 10 mM Tris buffer at pH 8.5 for demonstration. DMEM is a commonly used cell culture medium, which contains more than 30 components including six inorganic salts, eight vitamins, fifteen amino acids, D-glucose, sodium pyruvate, and other substances. Without the fiber attached to the hydrogel-based EFGF device, the complex buffer components generated

local electric field disturbances in the separation channel as 2 kV was applied to the system, which prevented the focusing of a model protein, trypsin inhibitor, in the channel. Figure 4.2 shows the experimental results after removing unwanted small buffer components using the integrated EFGF system. Online concentration of trypsin inhibitor was not affected by the original complex buffer components, and the trypsin inhibitor could be focused and then eluted out of the separation channel by decreasing the applied voltage.

4.3.2 Selective Isolation and Concentration of Proteins

The tandem EFGF system (Figure 4.1) was investigated for selective isolation and concentration of proteins. By carefully controlling the voltages applied to both sections, charged analytes with high mobilities were trapped in the fiber-based section, analytes with medium mobilities in the hydrogel-based section, and analytes with low mobilities not at all. A 3-way switching valve was incorporated in the system to allow operation as a mobility-selective trap, for which analytes with high mobilities could be trapped and purged periodically to reduce local electric field disturbances caused by concentrated charged analytes.

A two-component protein mixture, myoglobin (Mb) and lysozyme (Lyz), containing 0.2 M NaCl was prepared in 20 mM acetate buffer to demonstrate selective concentration and separation of proteins with simultaneous online desalting using this integrated system. A 20 mM acetate buffer at pH 4.3 was used as separation buffer and a 2 mM acetate buffer was used as purging buffer in the fiber-based section to generate a concentration gradient along the channel. The counteracting hydrodynamic flow was set

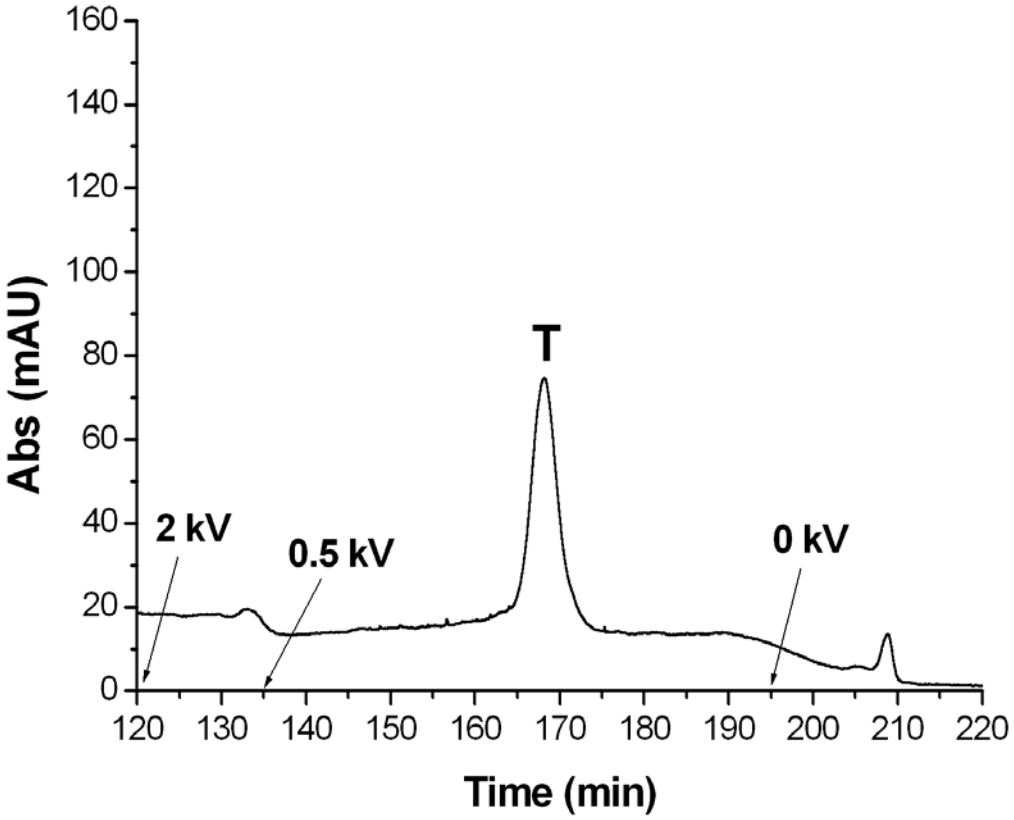

Figure 4.2. Removal of complex buffer components with simultaneous online protein concentration using an integrated EFGF system. After focusing, the initial voltage, 2 kV, was linearly decreased to 0.5 kV in 15 min and then dropped to 0 kV in an additional 1 h. Other conditions are described in Section 4.2.3. T = 0.5 mg/mL trypsin inhibitor.

at 0.2 μL/min for focusing. Lysozyme, a positively charged analyte with high mobility at pH 4.3, was trapped in the fiber-based EFGF section when 300 V was applied to this section. However, these conditions could not retain myoglobin, a charged analyte with lower mobility. Myoglobin could be focused and concentrated in the hydrogel section when 2 kV was applied to the hydrogel section. The bottom trace in Figure 4.3 shows the results of selective concentration and separation of myoglobin and lysozyme. After focusing proteins for 75 min, Mb was first eluted from the system by turning off the voltage applied to the hydrogel section. The hydrodynamic flow was then increased to 2 μL/min at 90 min to elute Lyz. The results also show that the highly concentrated salt (0.2 M NaCl) in this mixture could be removed simultaneously in the fiber-based EFGF section and did not cause local electric field disturbances. The top trace in Figure 4.3 shows the results of selective concentration of myoglobin and lysozyme out of the system. The same focusing conditions were applied to retain both proteins in the system. Mb was eluted by turning off the voltage applied to the hydrogel section at 75 min and the purge was carried out by switching the 3-way valve to the purge position and increasing the hydrodynamic flow to 5 μL/min at 85 min. As seen in the figure, the lysozyme peak disappeared after purge. According to these results, I should be able to selectively concentrate a target analyte and remove most unwanted components including high concentrations of salts in a mixture by carefully controlling the applied voltage and/or the hydrodynamic flow using the tandem EFGF system.

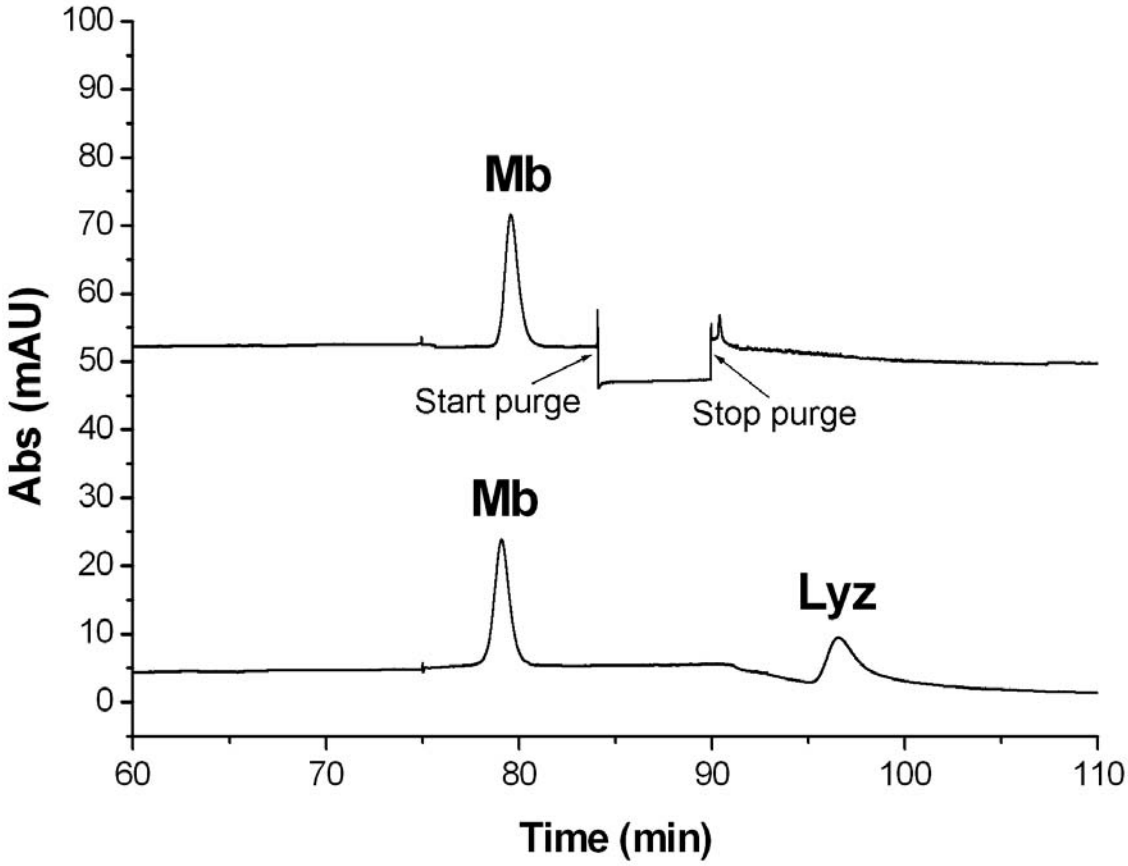

Figure 4.3. Isolation and concentration of proteins with simultaneous desalting using a tandem EFGF system. The bottom trace shows the elution of a mixture of Mb and Lyz in 0.2 M NaCl without purging, and the top trace shows the elution after purging Lyz out of the system. Other conditions are described in Section 4.3.2. Mb = 1 mg/mL myoglobin and Lyz = 1 mg/mL lysozyme.

4.4 Conclusions

Complex buffer components can be removed from a sample matrix using an integrated system containing a dialysis hollow fiber attached to the front of a hydrogel-based EFGF section. In addition, selective concentration and separation of proteins can be achieved by operating the tandem EGFG system as a mobility-selective trap for isolating and concentrating specific analytes of interest from a sample. Tandem EFGF systems such as coupled fiber and hydrogel EFGF devices have the potential to selectively isolate and concentrate target proteins within specific electrophoretic mobility ranges. Mobility measurements of proteins of interest under different conditions are required to design the appropriate EFGF system.

4.5 References

[1] Wang, Q.; Lin, S.-L.; Warnick, K. F.; Tolley, H. D.; Lee, M. L. *J. Chromatogr. A* **2003**, *985*, 455-462.

[2] Lin, S.-L.; Tolley, H. D.; Lee, M. L. *Chromatoghraphia* **2005**, *62*, 277-281.

[3] Humble, P. H.; Kelly, R. T.; Woolley, A. T.; Tolley, H. D.; Lee, M. L. *Anal. Chem.* **2004**, *76*, 5641-5648.

[4] Clarke, N. J.; Tomlinson, A. J.; Schomburg, G.; Naylor, S. *Anal. Chem*. **1997**, *69*, 2786-2792.

5 PROFILING ELUTING PEAKS FROM ELECTRIC FIELD GRADIENT FOCUSING

5.1 Introduction

As described in Chapter 4, EFGF can be used for selective isolation and concentration of charged proteins in a specific range of electrophoretic mobilities using an appropriately designed electric field gradient and counterflow. With continuous sample loading, only the analytes in the mobility range will be focused while all others will be excluded. At the end of the sampling period, the positions and the spreads of the focused peaks will be determined only by the electric field gradient and the counterflow. In addition, the characteristics of the focused peaks will be independent of the sampling time and the amount of sample that has been excluded. The focused analytes are eluted for detection at the end of the sampling period.

Although a focused peak is well defined within the separation channel, the peak profile changes as the peak is moved out of the channel. Theory indicates that the focused peaks will be Gaussian shaped and fully resolved in the channel [1]. However, the eluting peaks detected at or past the end of the channel may not be sharp Gaussian peaks. The change in peak profile must be identified before an appropriate EFGF system can be designed for selectively concentrating and separating target analytes.

Hemoglobin (Hb) is the major protein component of red blood cells. In normal human erythrocytes, more than 90% of total Hb is Hb A, which is made up of two α- and two β-polypeptide chains. Human hemoglobin A_0 (Hb A_0) is a group of glycated hemoglobins, where glycation occurs at sites other than the N-terminal residue of the β-

chain, such as lysine residues. According to experimental results from electrophoretic mobility measurements for Hb A_0 using CE, two partially separated peaks appeared in the electropherogram (Figure 5.1) that indicated Hb A_0 contains two components with close electrophoretic mobilities. Therefore, Hb A_0 is a good candidate for profiling eluting peaks in EFGF.

5.2 Experimental Section

5.2.1 Materials and Sample Preparation

Human hemoglobin A_0 (Hb A_0) was purchased from Sigma-Aldrich (St. Louis, MO), and 1.6 mg/mL Hb A_0 was prepared in 20 mM acetate buffer (pH 4.3) for protein focusing and elution experiments. Fused-silica capillaries used for fabricating the EFGF device were coated with poly(vinyl alcohol), PVA, to reduce electroosmotic flow using procedures published previously [2]. The ionically conductive polymeric hydrogel was constructed using the following components (in weight %) to form a transparent pre-polymer solution: 33.3% 2-hydroxyethyl methacrylate (HEMA), 23.3% methyl methacrylate (MMA), 20% poly (ethylene glycol) acrylate (PEGA, average molecular weight ~375), 16.7% buffer solution (20 mM acetate buffer, pH 4.3), 6.7% ethylene dimethacrylate (EDMA), and 1% 2,2-dimethoxy-2-phenylacetophenone (DMPA) as photoinitiator. A 120-μm Nichrom wire was used to form a separation channel inside the conductive polymer. The chemicals mentioned above were purchased from Sigma-Aldrich (St. Louis, MO). Untreated fused-silica capillaries, 150 μm I.D. × 360 μm O.D. , were obtained from Polymicro Technologies (Phoenix, AZ).

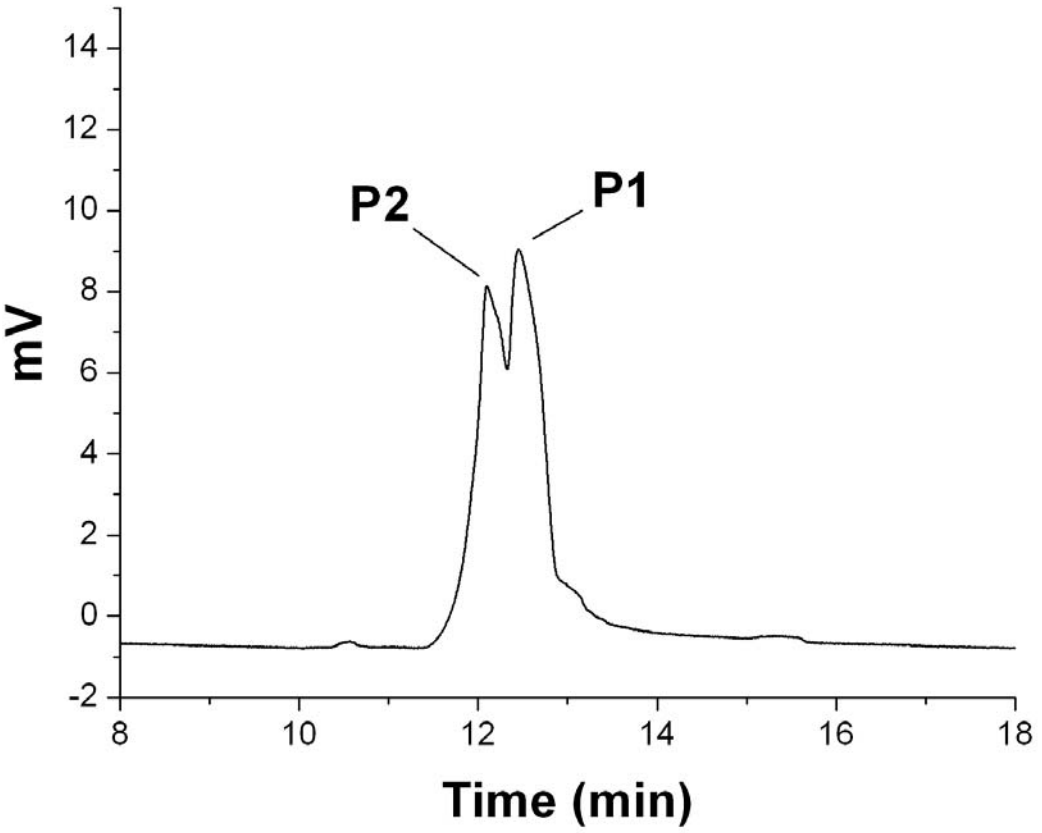

Figure 5.1. CE of Hb A_0 at 30 kV. Experimental conditions are described in Sections 3.2.2 and 3.2.3.

5.2.2 Device Fabrication and Instrumentation

The details for constructing the EFGF device used in this study were described previously [3] and in Figure 1.8. The shape of the changing cross-sectional area, which generated the electric field gradient, was mentioned in Section 3.2.3, and the system setup was shown in the Figure 3.1. A UV lamp (Model 5000, Dymax, Torrington, CT) was used for photoinitiated hydrogel polymerization. A syringe pump (PHD2000, Harvard Apparatus, Holliston, MA) with a 500 μL gas tight syringe (Hamilton, Reno, NV) was used to deliver buffer solution and sample into the separation channel. An injection valve with a 1 μL sample loop from VICI Valco (Houston, TX) was used for sample injection. A high voltage power supply from Spellman (Model SL 30, Hauppauge, NY) was used to provide various voltages for all experiments. A detection window was made 2 cm after the end of the separation channel on a fused silica capillary for online detection with a UV-Vis detector from ThermoQuest (Model UV3000, Riviera Beach, FL).

5.2.3 Experimental Conditions

All experiments were performed at pH 4.3 (20 mM acetate buffer), and the flow rate in the separation channel was set at 0.20 μL/min (a linear velocity of 3.5×10^{-2} cm/s). A voltage of 2 kV was applied initially to focus and retain analytes in the separation channel. The focusing time and the voltage program used in individual experiments are given in the figure legends. A wavelength of 214 nm was used for UV detection in all experiments.

5.3 Profiling the Elution Peak

5.3.1 Basic Theory

It is assumed that the focused band of an analyte in the EFGF separation channel is a Gaussian distribution [1]. The standard deviation of the focused band can be expressed as

$$\sigma = \left(\frac{D_T}{m\mu} \right)^{1/2} \tag{5.1}$$

where D_T is the total dispersion, μ is the electrophoretic mobility of the analyte, and m is the magnitude of the slope of the electric field gradient applied to the channel. Since the focused points (x_0) of various analytes in the channel are usually different at equilibrium, separation occurs along the channel according to analyte electrophoretic mobilities. In this chapter, I investigate how an analyte travels a distance to reach a detection point after the peak has reached its equilibrium position (x_0).

Once in steady state under specific gradient conditions, elution can be achieved by lowering the electric field or increasing the bulk flow velocity [4,5]. The separated analytes then move toward the high-field end of the channel. However, the migration rate is dependent on the remaining electric field gradient. Once the electric field is completely removed, the analytes move with the bulk flow. The peak starts broadening while it moves, and this dispersion can be regarded as a function of the period of time it takes to reach the detection point and possibly the decreasing rate of the electric field gradient. If one assumes that adsorption of the analyte to the channel surface is negligible, then the total dispersion (D_T) can be described as

$$D_T = D_M + \frac{u^2}{2} \cdot D_F \tag{5.2}$$

where D_M is the molecular diffusivity of the analyte, u is the bulk flow velocity, and D_F is the flow dispersion (or Taylor dispersion) [6]. For an open tubular channel, D_F is given by

$$D_F = \frac{r^2}{24 D_M} = \frac{d^2}{96 D_M} \tag{5.3}$$

where r is the radius of the inside channel and d is the inner diameter of the channel. Substituting equation (5.3) into equation (5.2), we obtain

$$D_T = D_M + \frac{u^2 d^2}{192 D_M} \tag{5.4}$$

For studying a single elution profile of an analyte in the separation channel, the following definitions are used in this chapter:

l = length of the separation channel, where the electric field gradient exists

x = analyte position in the channel, where $x = 0$ corresponds to the low field end and $x = l$ corresponds to the high field end

$c(x)$ = concentration of an analyte at point x

$E(x,t) = a + m(x,t)x$ = the electric field intensity at point x and time t

a = the electric field intensity at $x = 0$

u = bulk flow velocity

μ = electrophoretic mobility of the analyte

$-m(x,t) = -\frac{\partial E(x,t)}{\partial x}$ = the electric field gradient at point x and time t

$\upsilon(x,t) = \mu E(x,t) + u = -b_t(x)x + u$ = the total velocity of the analyte at point *x* and time *t*, where we allow the slope, $b_t(x)$, to be a function of time, *t* and the electrophoretic mobility, μ

After reaching the equilibrium state, the analyte is eluted from the channel by decreasing the electric field gradient. Here the time is set to 0 when the slope changes. The total velocity of a particular analyte can be described as

$$\upsilon(x,t) = -b_t(x)x + u \tag{5.5}$$

where $b_t(x) = m(x,t) \cdot \mu$. If we assume that the slope (*b*) is constant with respect to *x* but decreases from α (the original value of the field slope while focusing) at time $t = 0$ linearly to $t = t_1$ at rate β and then is held constant, the slope, b_t, can be expressed as (we suppress *x* since the slope is assumed independent of *x*)

$$b_t = \alpha - \beta t \qquad 0 < t < t_1 \tag{5.6}$$

$$= \alpha - \beta t_1 \qquad t \geq t_1 \tag{5.7}$$

The value of α in equations (5.6) and (5.7) is given by

$$\alpha = b_1 \tag{5.8}$$

where b_1 is the initial field gradient when a peak reaches equilibrium, the time at this point is defined as $t = 0$ and the gradient starts to change. Then the velocity of an analyte at time *t* becomes

$$v(x,t) = u - (\alpha - \beta t)x \qquad 0 < t < t_1 \tag{5.9}$$

Following Giddings [7], the flux equation can be used to determine the concentration at point *x* and at any time *t*, which is given by

$$\frac{\partial c(x,t)}{\partial t} = -\frac{\partial}{\partial x}\big(v(x,t)\cdot c(x,t)\big) + \frac{\partial}{\partial x}\left(D_T \cdot \frac{\partial c(x,t)}{\partial x}\right) \tag{5.10}$$

$$= -\frac{\partial}{\partial x}\big\{\big[\mu E(x) + u\big]\cdot c(x,t)\big\} + D_T \frac{\partial^2 c(x,t)}{\partial x^2} \tag{5.11}$$

Substituting equations (5.2), (5.3), and (5.9) into equation (5.10), we obtain

$$\frac{\partial c(x,t)}{\partial t} = -c(x,t)\big(-\alpha + \beta t\big) + \big(u - \alpha x + \beta x t\big)\frac{\partial c(x,t)}{\partial x} + D_T \cdot \frac{\partial^2 c(x,t)}{\partial x^2} \tag{5.12}$$

5.3.2 Peak Profiling

At equilibrium, the shape of a focused peak in field gradient focusing is assumed to be Gaussian. A proposed solution for equation (5.11) is used to study the shape of the focused peak, and it can be expressed as

$$c(x,t) = \frac{\dfrac{A_t}{\sigma_t\sqrt{2\pi}}\exp\left(-\dfrac{(x-\delta_t)^2}{2\sigma_t^2}\right)}{\displaystyle\int_0^l \frac{\exp\left(-(x-\delta_t)^2 \big/ 2\sigma_t^2\right)}{\sigma_t\sqrt{2\pi}}\,dx} \tag{5.13}$$

where σ_t is the peak spread, δ_t is the center of the focused peak, and A_t is the amount of the analyte between $x = 0$ and $x = l$ at time t. It should be noticed that any portion of the peak reaching point L (the end of channel) leaves the influence of the electric field, and moves with the bulk flow and is not focused in the channel. This decreases A_t. Using this proposed solution for $c(x,t)$ in equation (5.12), we should be able to determine the

quantities of $\frac{\partial c(x,t)}{\partial t}$, $\frac{\partial c(x,t)}{\partial x}$, and $\frac{\partial^2 c(x,t)}{\partial x^2}$ by differentiating equation (5.13) to obtain the following three ordinary differential equations [8]:

$$\frac{1}{A_t}\frac{dA_t}{dt} - \frac{1}{\sigma_t}\frac{d\sigma_t}{dt} = -\frac{1}{\sigma_t^{\,2}}\left(D_T - \sigma_t^{\,2}(\alpha - \beta t)\right) \tag{5.14}$$

$$\frac{d\delta_t}{dt} = u - (\alpha - \beta t)\delta_t \tag{5.15}$$

$$\sigma_t \frac{d\sigma_t}{dt} = D_T - \sigma_t^{\,2}(\alpha - \beta t) \tag{5.16}$$

Equation (5.14) containing A_t represents the change in total analyte due to a portion moving out of the field gradient region. This indicates that the decrease in the amount of analyte at point L results in an asymmetric peak profile.

Once an analyte passes the end of the field gradient (point L), the analyte will be lost to the system and be carried along by bulk flow past the detector, which causes A_t to decrease. The rate of change in A_t depends on the rate analyte passes point L in the channel. If we let A_0 be the amount of analyte at time $t = 0$, the change in A_t is given by

$$\frac{\partial A_t}{\partial t} = \frac{\dfrac{A_t}{\sqrt{2\pi\sigma_t^2}} \cdot \upsilon(l,t) \cdot \exp\left(-\dfrac{(l-\delta_t)^2}{2\sigma_t^2}\right)}{\displaystyle\int_0^l \frac{\exp\left(-(x-\delta_t)^2 \big/ 2\sigma_t^2\right)}{\sigma_t\sqrt{2\pi}}\,dx} \tag{5.17}$$

where

$$\upsilon(l,t) = \frac{\partial \delta_t}{\partial t} + D_T \cdot \frac{\partial c(x,t)}{\partial x}\Big|_{x=l} \tag{5.18}$$

This velocity is independent of A_t in the channel. A_t can be solved by integrating equation (5.17) expressed as

$$A_t = A_0 \cdot \exp\left(-\int_0^t \frac{\upsilon(l,\tau)}{\sqrt{2\pi\sigma_\tau^2}} \exp\left(-\frac{(l-\delta_\tau)^2}{2\sigma_\tau^2} \right) d\tau \right) \Bigg/ \int_0^l \frac{\exp\left(-(x-\delta_t)^2 \Big/ 2\sigma_t^2 \right)}{\sigma_t \sqrt{2\pi}} dx$$

------- (5.19)

The amount of analyte seen at the detector at time T is the sum of the amounts passing the end point L in the channel between time $t = 0$ and $t = T$ and traveling to the detector, (point y) by time T. By integration, the observed amount at the detector at time T (denoted Y_T) is described as

$$Y_T = \int_0^T A_t \cdot \frac{\upsilon(l,t)}{2\pi\sqrt{\sigma_{T-t}^{*2}\sigma_t^2}} \cdot \exp\left(-\frac{(l-\delta_t)^2}{2\sigma_t^2} - \frac{(y-\delta_{T-t}^*)^2}{2\sigma_{T-t}^{*2}} \right) dt \qquad (5.20)$$

The position (δ_{T-t}^*) and the spread (σ_{T-t}^{*2}) represent peak center and spread at time T of a plug passing point L (the end of channel) at time t ($t < T$). These are determined by

$$\delta_{T-t}^* = \int_t^T [u + \mu E(x,t)] dt \qquad (5.21)$$

$$\sigma_{T-t}^{*2} = 2D_T(T-t) \qquad (5.22)$$

We now specialize the results above to the case where we abruptly change the electric field from b_1 to b_2. This is not a linear change but an instantaneous one. Decreasing the potential decreases the slope for the peak as it moves toward the end point

L and then out of the electric field. We can solve equations (5.15) and (5.16) to obtain the position (δ_t) and the spread (σ_t^2) of the peak at time $t > 0$ as

$$\delta_t = x_0 e^{-b_2 t} + x_1\left(1 - e^{-b_2 t}\right) \tag{5.23}$$

where x_o is the peak position at equilibrium before the change in voltage gradient, x_1 is the peak position at equilibrium after the change in voltage gradient, and $b_2 = m_2\mu$ (m_2 = the field gradient after change). Similarly,

$$\sigma_t^2 = \sigma_0^2 e^{-2b_2 t} + \sigma_1^2\left(1 - e^{-2b_2 t}\right) = \sigma_1^2 + \left(\sigma_o^2 - \sigma_1^2\right)\cdot e^{-2b_2 t} \tag{5.24}$$

In addition to the analytical approach, a finite difference solution of the diffusion equation, equation (5.11), was used to simulate a peak profile. This simulated result was then compared to the analytical result using equation (5.20). The time step (Δt) and the spatial step (Δx) were set to be 0.004 s and 0.003 cm, respectively, for simulations. Similar experimental conditions were used in the analytical and simulated solutions. The detailed conditions are described in Section 5.4.1. The initial condition for the analytes was assumed to be a Gaussian concentration profile as given by equation (5.13).

5.4 Results and Discussion

5.4.1 Numerical Calculations

For numerical calculations, the channel diameter (d) was 110 μm, the channel length (l) was 4 cm, and the bulk flow velocity (u) was 0.20 μL/min; 0.035 cm/s (in the separation channel) or 0.019 cm/s (in the capillary; 150 μm I.D.). The electrophoretic mobilities of the two peaks in Hb A_0 were measured by CE to be $\mu_1 = 2.49 \times 10^{-4}$ $cm^2/(V\cdot s)$ for peak 1 (P1) and $\mu_2 = 2.60 \times 10^{-4}$ $cm^2/(V\cdot s)$ for peak 2 (P2). The diffusivity

(D_M) was 6.9 $\times 10^{-7}$ cm^2/s, which was obtained from [9], and the total dispersion (D_T) was determined from

$$D_T = D_M + \frac{u^2 \cdot d^2}{192 D_M} = 1.12 \times 10^{-3} \, cm^2/s \qquad \text{(in the channel)} \tag{5.25}$$

$$\text{or } 6.07 \times 10^{-4} \, cm^2/s \qquad \text{(in the capillary)}$$

The electric field in the separation channel was described as

$$E(x) = a + mx \tag{5.26}$$

At the focused point,

$$u = \mu \cdot E(x) \tag{5.27}$$

Therefore, the focused point (x_0) of an analyte along the channel, under an electric field, $E(x)$, was determined by

$$x_0 = (\frac{u}{\mu} - a) / m \tag{5.28}$$

Based on the device design, the intercept (a = 23.6 V/cm) could be determined using the following equation

$$\frac{E(l)}{E(0)} = \frac{a + ml}{a} = 6 \tag{5.29}$$

The standard deviation of a focused peak was determined by equation (5.1). The position and the standard deviation of each peak in Hb A_0 under different electric field gradients are summarized in Table 5.1.

Table 5.1. Summary of numerical calculations of the two Hb A_0 peaks.

		Applied potential, V (kV)				
		2	1	0.9	0.8	0.5
Maximum slope of field gradient, m (V/cm^2)		62.5	31.25	28.13	25	15.63
Position of focused peak, *x* (cm)	P1	1.88	3.75	4.17	4.69	7.51
	P2	1.78	3.56	3.96	4.45	7.12
Standard deviation of peak, σ (cm)	P1	0.27	0.38	0.40	0.43	0.54
	P2	0.26	0.37	0.39	0.42	0.53

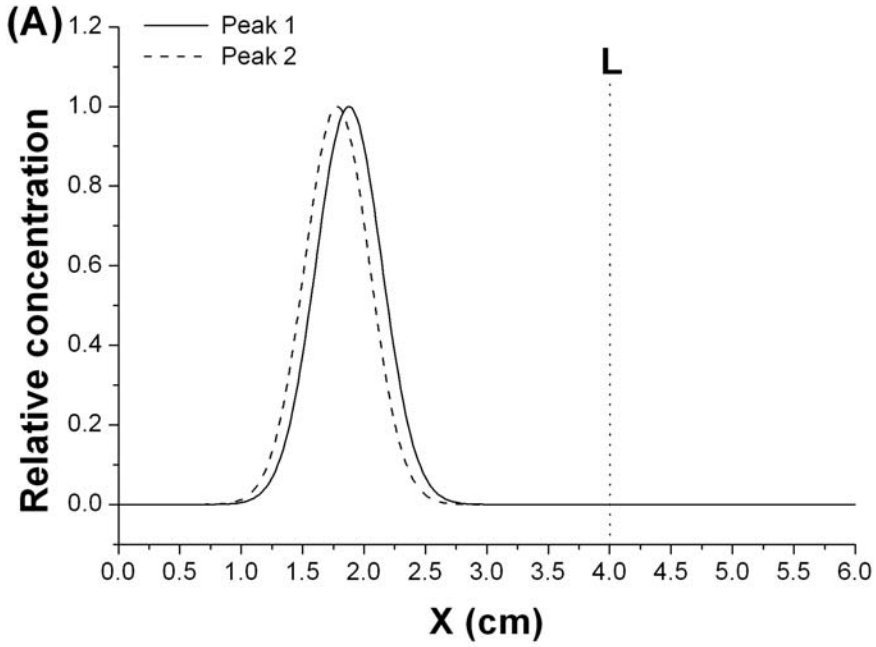
(A)
Peak 1
Peak 2
L
Relative concentration
X (cm)

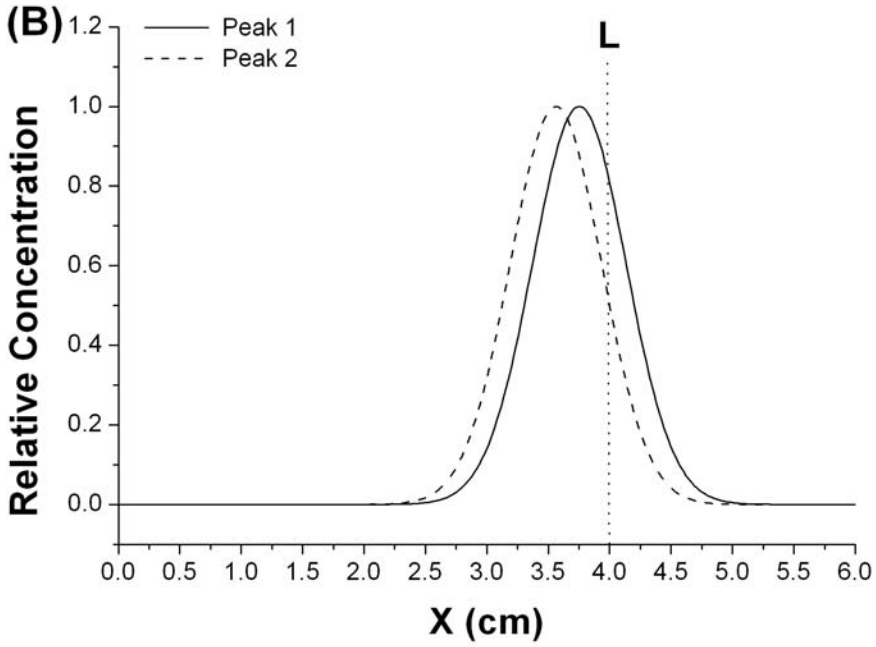
(B)
Peak 1
Peak 2
L
Relative Concentration
X (cm)

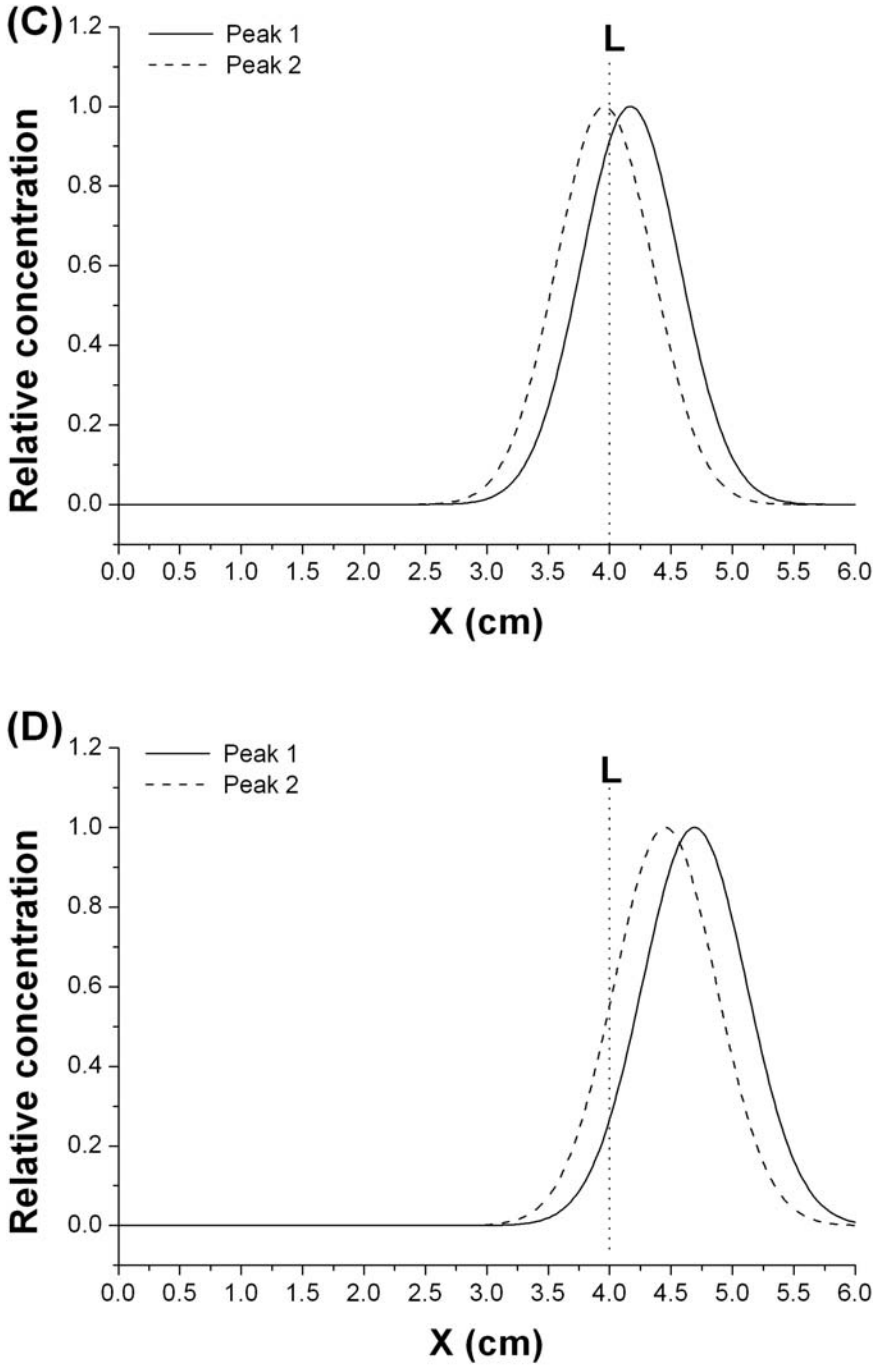

Figure 5.2. Simulated results of the two Hb A_0 peaks along the separation channel (with counterflow). Applied voltage: (A) 2 kV, (B) 1 kV, (C) 0.9 kV, and (D) 0.8 kV. Point L represents the end of the separation channel. Other conditions are described in Section 5.2.3.

In equation (5.13), *c(x)* is proportional to $\exp\left(-\frac{(x-\delta_t)^2}{2\sigma_t^2}\right)$. If this term is defined as the relative concentration (*c*), a plot of *c* vs *x* can be used to trace focused peaks along the separation channel. Figure 5.2 shows the simulated results of the two focused peaks appearing in Hb A_0.

Once a small plug of an analyte passes the end point L, it is driven by the net velocity of the bulk flow and the analyte electrophoretic velocity toward the detection point (2 cm after L). This small plug will take more than 2 min to reach the detection point and be observed. For broad peaks (~2.5 cm wide) shown in Figure 5.2, at least 5 min will be necessary for these peaks to reach the detector to be recorded.

5.4.2 Interpretation of Peak Profiles

Although Figure 5.2 did not well interpret the elution peaks that we observed at the detection point, these results still offered a partial understanding about how focused peaks behave along the EFGF separation channel. In Figure 5.2, the two Hb A_0 peaks were broad and overlapped although they had different focusing points. The broad peaks were due to large dispersion caused by the presence of counterflow. If the dispersion caused by the counterflow is assumed to be 0 ($D_F = 0$), the focused peaks become much narrower and baseline separated. The simulated results of the two focused peaks in Hb A_0 without Taylor dispersion, i.e. $D_T = D_M$, are shown in Figure 5.3.

As described in Section 5.1, Hb A_0 contains two components with close electrophoretic mobilities determined by CE. Using Hb A_0 as model proteins, several different voltage programs were utilized to study the profiles of the eluting peaks from

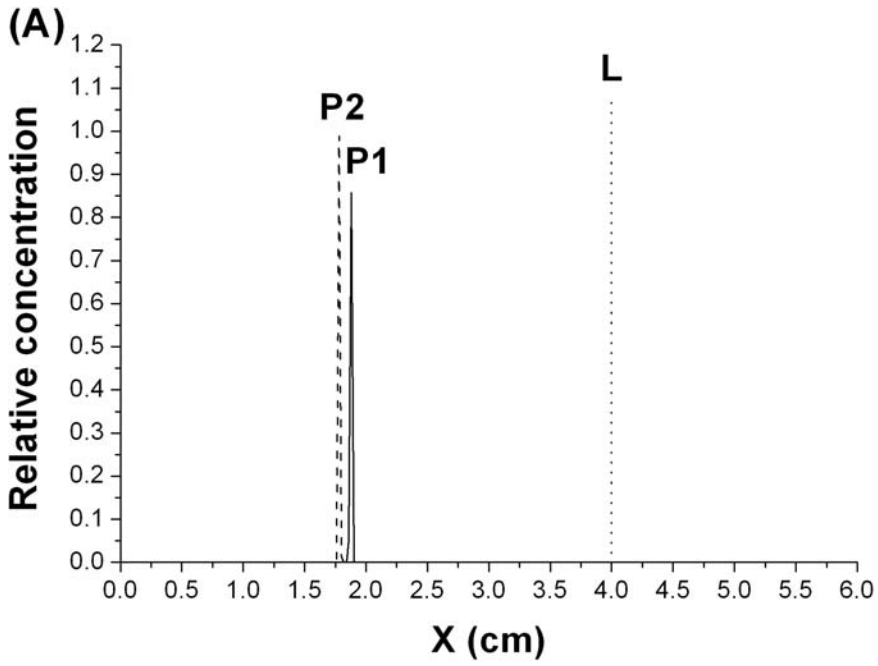
(A)
Relative concentration
X (cm)
P2
P1
L
0.0
0.1
0.2
0.3
0.4
0.5
0.6
0.7
0.8
0.9
1.0
1.1
1.2
0.0 0.5 1.0 1.5 2.0 2.5 3.0 3.5 4.0 4.5 5.0 5.5 6.0

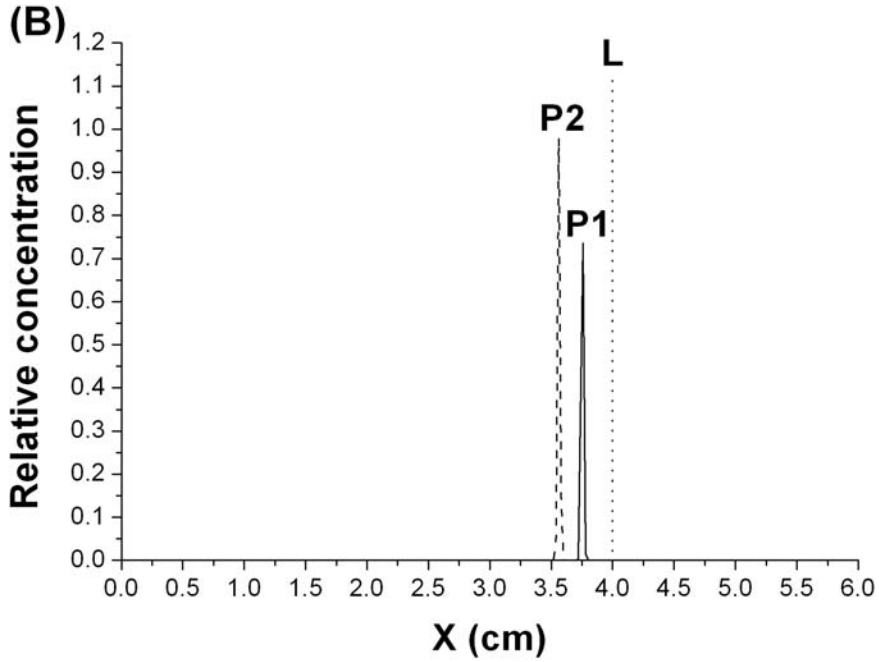
(B)
Relative concentration
X (cm)
P2
P1
L
0.0
0.1
0.2
0.3
0.4
0.5
0.6
0.7
0.8
0.9
1.0
1.1
1.2
0.0 0.5 1.0 1.5 2.0 2.5 3.0 3.5 4.0 4.5 5.0 5.5 6.0

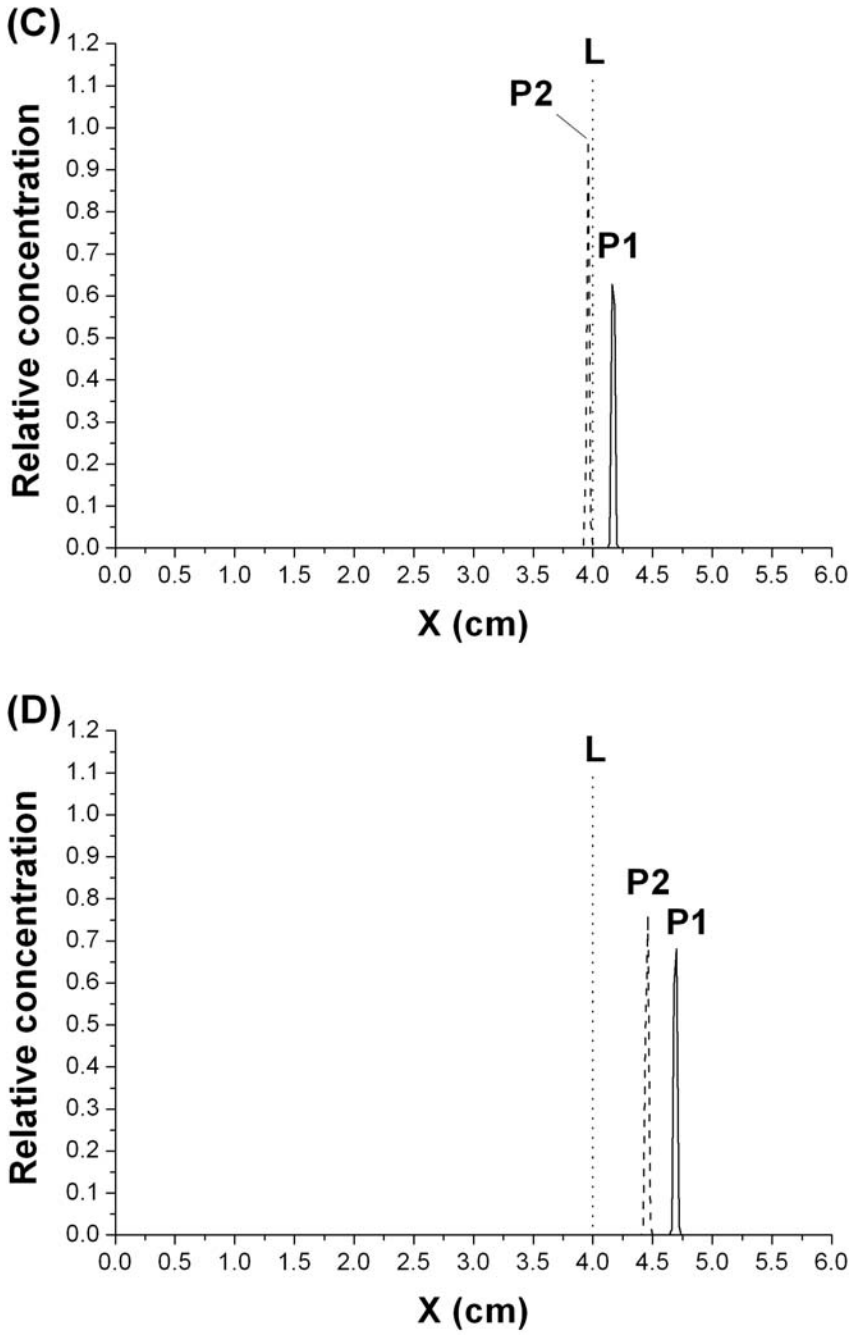

Figure 5.3. Simulated results of the two Hb A_0 peaks along the separation channel (without dispersion from counterflow). Applied voltage: (A) 2 kV, (B) 1 kV, (C) 0.9 kV, and (D) 0.8 kV. Point L represents the end of the separation channel. P1 = peak 1 and P2 = peak 2. Other conditions are described in Section 5.2.3.

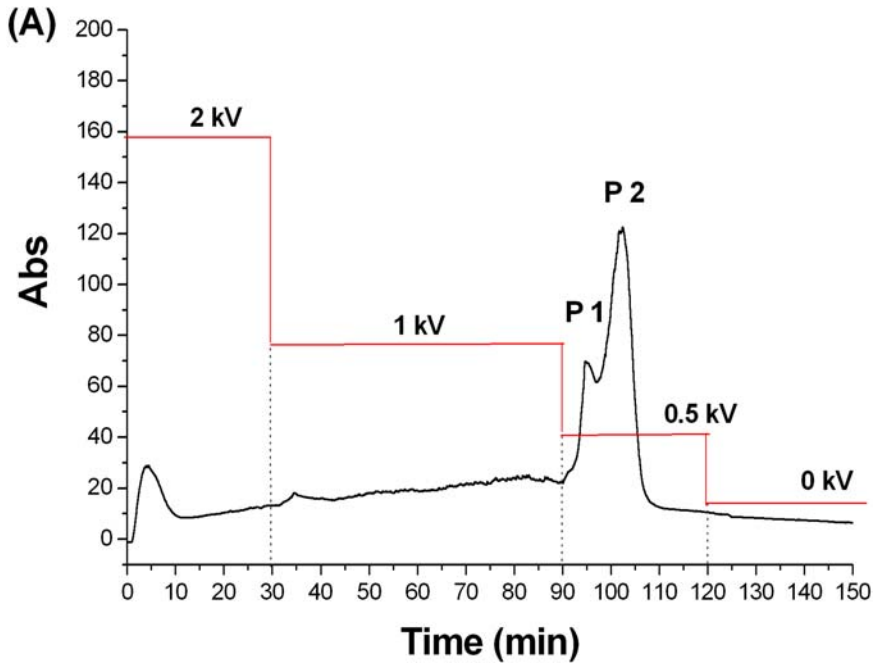
(A)
Abs
Time (min)
2 kV
1 kV
0.5 kV
0 kV
P 1
P 2

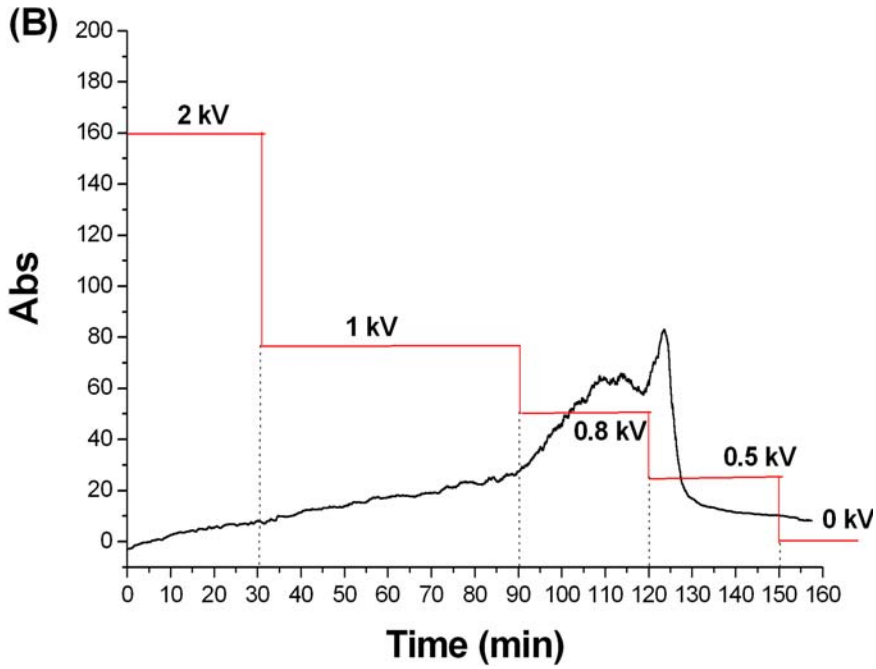
(B)
Abs
Time (min)
2 kV
1 kV
0.8 kV
0.5 kV
0 kV

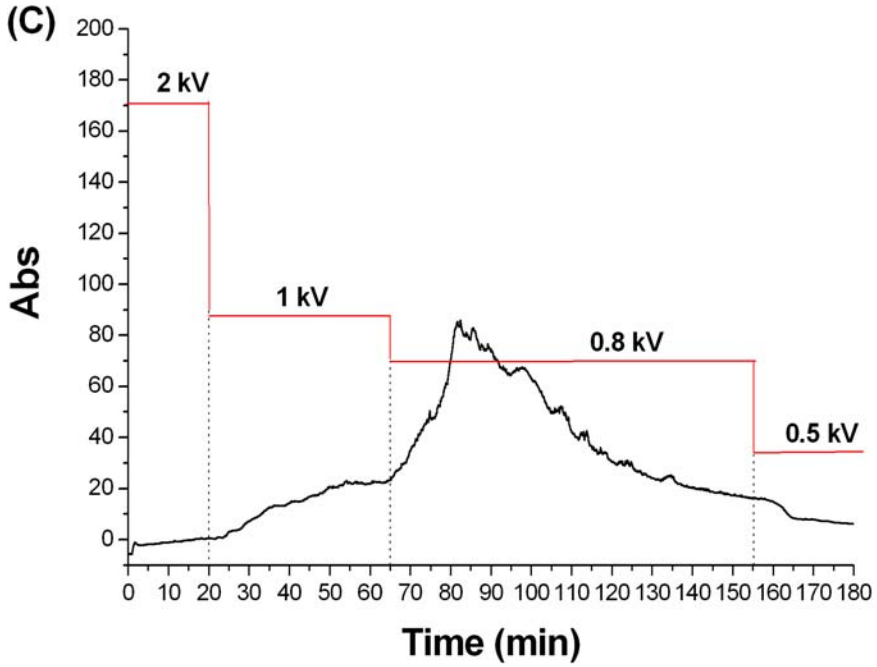

Figure 5.4. EFGF of Hb A_0 using different voltage programs. The individual voltage programs are shown in each figure. Other conditions are described in Section 5.2.3.

EFGF (Figure 5.4). According to Figures 5.2A, the two components would be focused and retained in the separation channel without leaking out of the channel when 2 kV was applied to the system. Although the two peaks were still focused in the channel when the voltage was dropped to 1 kV, part of the peaks would leave the channel and slowly move toward the detection point due to the large peak spread caused by the dispersion from counterflow (Figure 5.2B). This phenomenon can be seen in Figure 5.4. In Figures 5.4A through 5.4C, the baseline absorption gradually increased when the voltage was dropped to 1 kV. If the voltage was suddenly dropped from 1 kV to 0.5 kV, the electrophoretic velocities of the two components were much smaller than the hydrodynamic flow velocity. Therefore, the peaks arrived at the detector much faster and relatively sharp peaks were observed (Figure 5.4A).

The peak profile observed at the detection point may also be simulated using numerical integration of equations (5.11) and (5.20). The plots of Y_T and $c(x,t)$, the observed amount of the analytes or peak intensity at the detector, vs time offer more direct comparison to the experimental results (Figure 5.4) than Figure 5.2. Figure 5.5 shows the superimposed experimental results (Figures 5.4B and 5.4C) and the simulated peak profiles observed at the detection point for comparison. According to the simulations, the observed partially separated peaks in Figure 5.4B were the combination of the two Hb A_0 components at different eluting rates. Analytes moved very slowly as 0.8 kV was applied for elution, gradually increasing the UV absorbance, until the applied voltage was further dropped to 0.5 kV. Both components moved much faster at 0.5 kV, which resulted in a rapid increase in UV absorbance. If the voltage was kept at 0.8 kV for

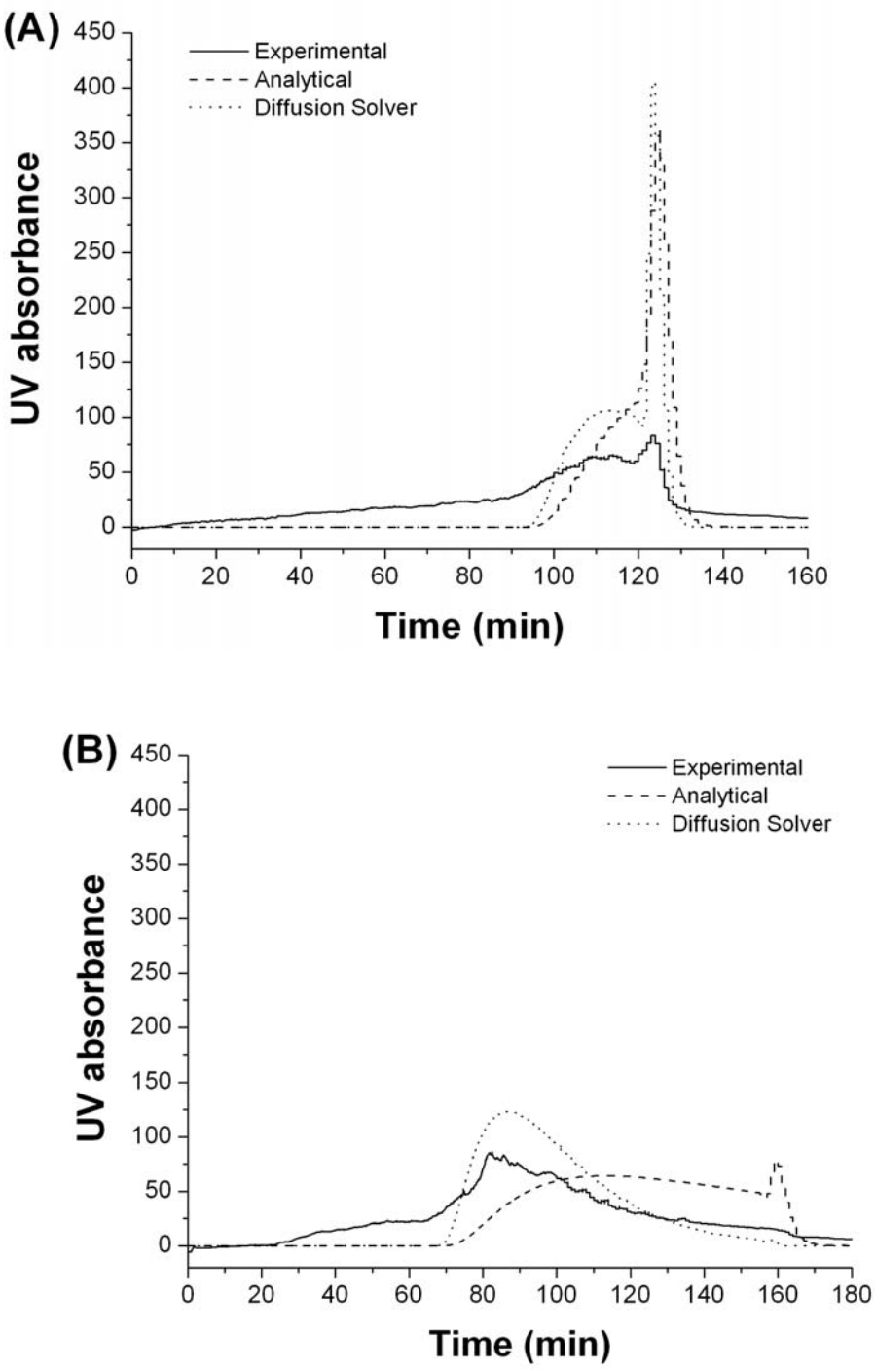

Figure 5.5. Peak profiles of the two Hb A_0 peaks.

90 min for elution, only one broad peak was observed (Figure 5.5B). All analytes passed through the detection point during this time period.

In Figures 5.5 A and 5.5B, the increasing baseline absorption was not observed in the simulated results before the applied voltage was further dropped to 0.8 kV for elution. The disagreement is due to deviation of the actual electric field in the device from equations (5.11) and (5.20) as well as instability in the bulk flow velocity applied to the system.

5.5 Conclusions

Comparing the results shown in Figure 5.2 with those in Figure 5.3, the most important factor that affects the peak widths and the resolution of the eluting peaks is the total dispersion of the analytes. According to equation (5.4), the total dispersion increases dramatically as the bulk flow velocity increases. Based on equation (5.1), the peak spread or the peak width is increased if large total dispersion, due to high bulk flow velocity, appears in the system. In order to have better separation, the bulk flow velocity should be controlled to reduce the total dispersion and obtain narrower peaks. Packing the channel with polymer particles or monolith will also reduce the total dispersion.

Although UV detection is a universal detection method, it does not provide specific molecular information of individual peaks, and the observed peak widths are highly dependent on the moving rate of the analytes toward the detection point. A more distinguishable detection method such as MS may be used to provide more molecular information of the analytes for specification.

To achieve selective focusing of target analytes without losing the analytes in the system, the following considerations should be taken into account. The total dispersion should be reduced to decrease the standard deviation of a focused peak, which reduces the loss of analytes and increases the resolution. The electric field inside the separation channel needs to be well understood in order to design an appropriate electric field gradient for selective focusing of target analytes within a small electrophoretic mobility range.

5.6 References

[1] Tolley, H. D.; Wang, Q.; LeFebre, D. A.; Lee, M. L. *Anal. Chem.* **2002**, *74*, 4456-4463.

[2] Clarke, N. J.; Tomlinson, A. J.; Schomburg, G.; Naylor, S. *Anal. Chem*. **1997**, *69*, 2786-2792.

[3] Humble, P. H.; Kelly, R. T.; Woolley, A. T.; Tolley, H. D.; Lee, M. L. *Anal. Chem.* **2004**, *76*, 5641-5648.

[4] Lin, S.-L.; Tolley, H. D.; Lee, M. L. *Chromatoghraphia* **2005**, *62*, 277-281.

[5] Lin, S.-L.; Y. Li; Tolley, H.D.; Humble, P.H.; Lee, M.L. *J. Chromatogr. A* **2006**, *submitted*.

[6] Taylor, G. *Proc. R. Soc.* (London) **1953**, *219A*, 186-203.

[7] Giddings, J. C. *Unified Separation Science*, John Wiley and Sons, New York, **1990**.

[8] Warnick, K. F.; Francom, S. J.; Humble, P. H.; Kelly, R. T.; Woolley, A. T.; Lee, M. L., Tolley, H. D. *Electrophoresis* **2005**, *26*, 405-414.

[9] Sober, H. A. *CRC Handbook of Biochemistry: Selected Data for Molecular Biology, 2nd ed.*, The Chemical Rubber Co., Cleveland, OH, **1970**.

6 FUTURE DIRECTIONS

6.1 Measurement of Electrophoretic Mobilities of Proteins under Various Conditions

The separation of proteins by electric field gradient focusing is based on the electrophoretic mobilities of analytes under different operating conditions, which include electrolyte ions, pH and ionic strength of the running buffer, buffer additives, etc. Therefore, a thorough investigation of the electrophoretic mobilities of target proteins under various conditions is required to design an appropriate EFGF system for selectively isolating and concentrating target proteins.

Charged proteins are essential to perform EFGF for protein analysis. It is important to know the electrophoretic mobility of a target protein at different pH values, which will help to optimize conditions for separating the target analyte from other unwanted proteins such as albumin. Proteins can be charged at any pH different from their pI values and also contain hydrophobic areas, hydrogen-bonding regions, and biospecific binding sites that may play roles in interacting with the components of buffer solutions, including electrolyte ions and buffer additives [1-3]. These possible interactions vary with buffer pH, electrolyte ions, ionic strength, and buffer additives.

The electrophoretic mobility of a protein is therefore changed with different buffer composition. Since EFGF of proteins has been carried out in a device with relatively large dimensions (i.e., 100 – 200 μm separation channel), the conductivity of the running buffer should be relatively low to avoid high current passing through the channel that increases Joule heating and causes bubble formation. The suitable range of

buffer conductivity used for EFGF must be investigated prior to mobility measurements. A series of buffer solutions need to be prepared by varying the buffer pH, the electrolyte species, ionic strength, and buffer additives within a suitable conductivity range. The electrophoretic mobilities of target proteins should then be measured under these conditions to establish a mobility database for target proteins.

6.2 Improvements for Selective Concentration and Separation of Proteins in a Biological Sample Using Electric Field Gradient Focusing

Previous chapters already demonstrated the potential of utilizing EFGF systems for isolating and concentrating trace proteins in complex buffer solutions. Further efforts should be focused on implementing EFGF (e.g., tandem EFGF system) for selective concentration of target proteins and simultaneous removal of unwanted components, including salts and albumin, from biological samples.

6.2.1 Improvement in resolution on a single EFGF device

The major factor that affects resolution in EFGF is the generation and control of the electric field gradient along the separation channel. The most versatile design to serve this purpose will be the multiple-electrode format [4,5], which uses an array of electrodes to generate and control the electric field gradient along the separation channel. Using this approach, I should be able to change and manipulate the field gradient along the channel at any time during the run. In addition, a nonlinear electric field gradient can be achieved to improve peak capacity in EFGF [6,7]. This approach should be amenable to a microchip format, which will decrease the channel dimensions to reduce the total dispersion appearing in the separation channel [6-8].

A common problem that occurred in both fiber- and hydrogel-based devices, which reduced the performance of EFGF, was protein adsorption on the surface of the separation channel. Using the microchip format, I can either modify the surface [9,10] or use hydrophilic polymers such as PEG-based materials for microchip fabrication to eliminate protein adsorption. Therefore, resolution in EFGF could be improved by eliminating protein adsorption.

6.2.2 Improvements in the tandem EFGF system

Although I demonstrated selective concentration and separation of target proteins using a tandem EFGF system as shown in Figure 4.1, some considerations still need to be taken into account for improving the performance of the tandem system. In the setup shown in Figure 4.1, there were relatively large dead volumes due to the large dimensions of the hollow fiber and the switching valve. In order to reduce the dead volumes and have more uniform channel dimensions, the fiber-based EFGF section and the 3-way valve should be fabricated in a microchip format.

A porous membrane between the purge and the separation channels is required to establish a conductivity gradient. Figure 6.1 shows a simple design for microfabricated EFGF with a conductivity gradient. Using a piece of porous membrane instead of dialysis hollow fiber gives a wider selection of membrane pore sizes, which allows the analysis of small proteins or polypeptides. In order to reduce protein adsorption, PEG-based polymeric materials will be a good choice for making the device due to their protein compatibility.

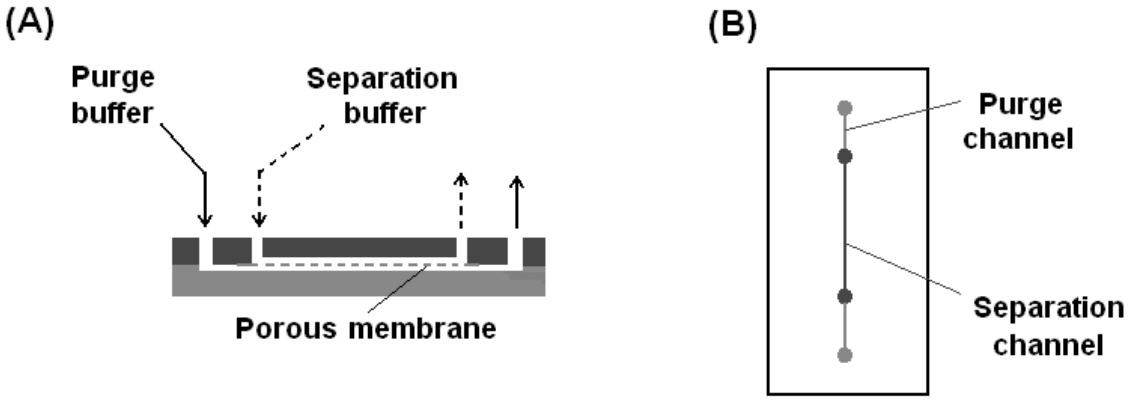

Figure 6.1. Schematic diagram of microfabricated EFGF in a conductivity gradient (membrane-based micro EFGF). (A) Side view. (B) Top view.

In order to effectively reduce the local electric field disturbances caused by concentrating abundant proteins in the first dimension of EFGF, a 3-way switching valve is required to purge abundant proteins out of the system. Poly(dimethylsiloxane) (PDMS) is a frequently used silicone elastomer for fabricating microfluidic devices. PDMS has also been used to make pneumatic microvalves due to its elasticity [11-14]. The schematic diagram of a microfabricated 3-way valve that can be used to control the flow direction and minimize the dead volume occurring in the valve is shown in Figure 6.2. However, PDMS is not protein compatible. Surface modification is required to reduce protein adsorption. Another alternative to surface modification is using BSA solution to flow through the channels to passivate the surface before starting experiments. A simple diagram of the integration of the microfabricated membrane-based EFGF and 3-way valve is shown in Figure 6.3.

The second EFGF in the tandem system is the key element for concentrating a target protein and separating the target from other proteins with similar mobilities. A micro EFGF device with multiple electrodes can vary the electric field gradient at any time during a run to improve resolution, which makes it valuable for the concentration and separation of target proteins. Other EFGF devices may also serve as the second dimension of the tandem system.

The improved tandem EFGF system reduces the channel dimensions and the total dead volumes of the system, which will greatly decrease the time for sample introduction and the total analysis time. In addition, the membrane-based EFGF section (the first dimension of EFGF) can effectively remove unwanted small buffer components,

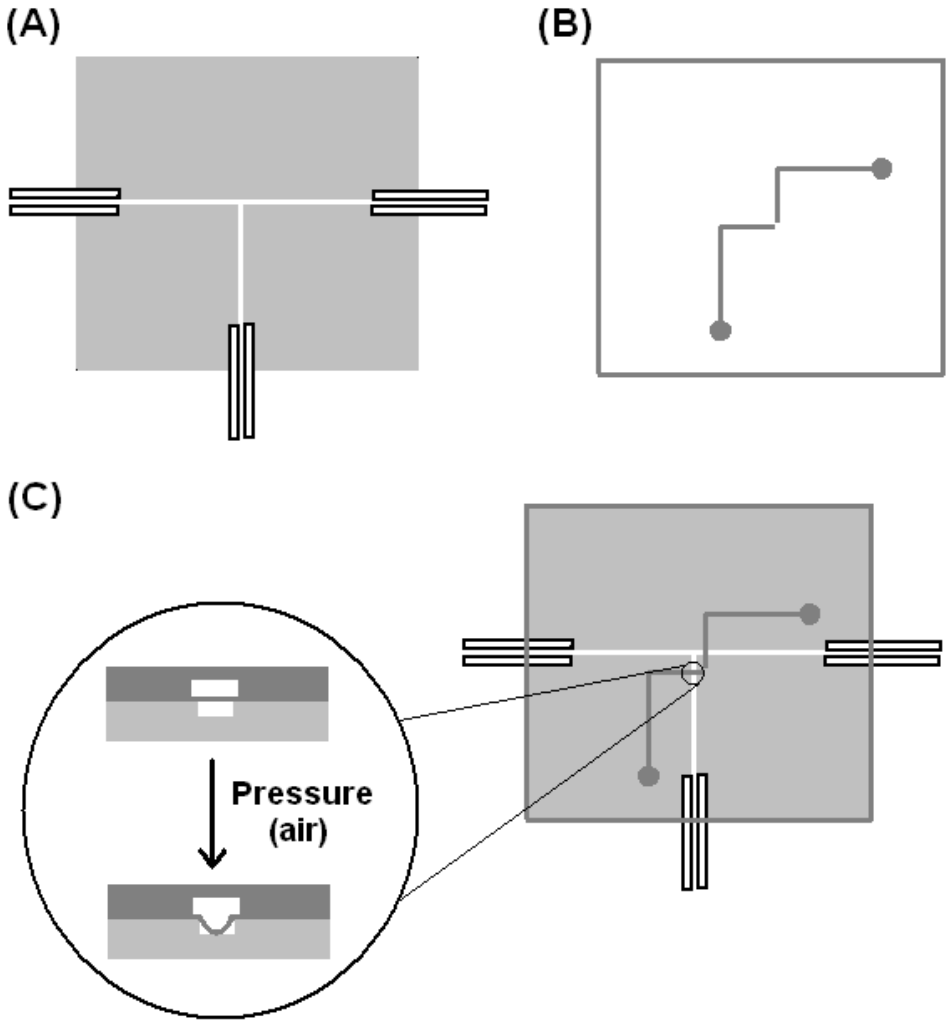

Figure 6.2. Schematic diagram of a microfabricated 3-way valve. (A) The bottom layer contains the flow channels. (B) The top layer contains channels where pressurized air can be introduced to control the valve. (C) Top view of the microfabricated 3-way valve.

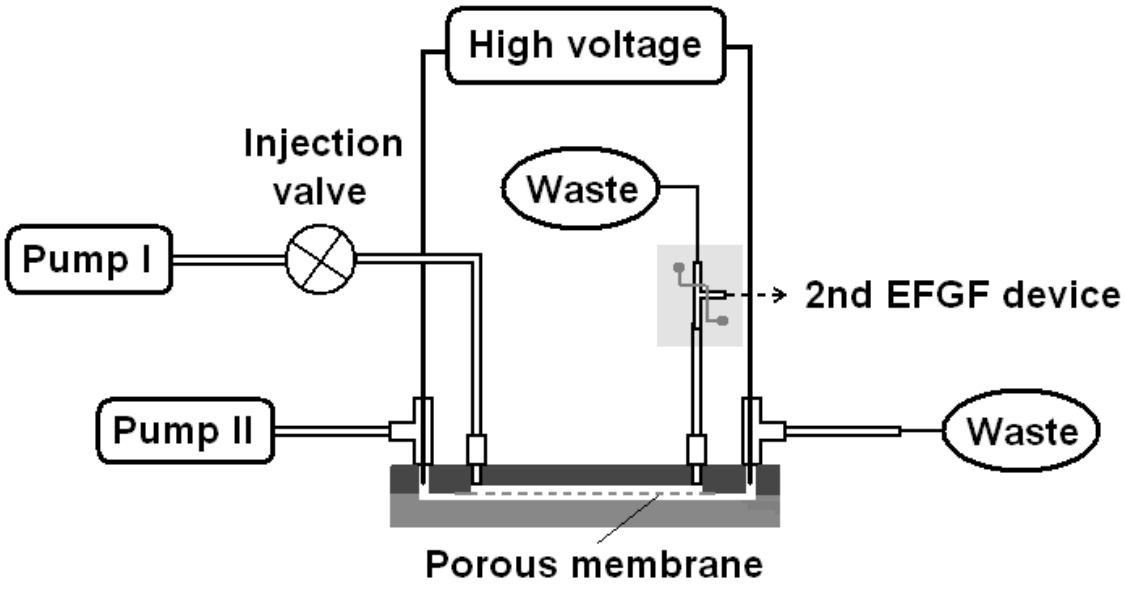

Figure 6.3. Schematic diagram of the integration of the microfabricated membrane-based EFGF and 3-way valve.

including salts, through the porous membrane without producing high current through the whole system to destroy the field gradient and/or increase Joule heating. Control of the 3-way valve needs to be automated to increase reproducibility.

Using the proposed microchip format, the channel dimensions in both sections can be easily controlled to reduce total dispersion in the system, which will lead to narrower peaks and improved resolution in protein analysis. Control of the electric field gradient is an important factor to separate a target analyte from other proteins with similar electrophoretic mobilities. An EFGF device with multiple electrodes, which has the ability to provide a programmable nonlinear field gradient, can increase resolution of proteins by tuning the field gradient to selectively isolate and concentrate target proteins from a complex mixture.

6.3 References

[1] Righetti, P. G. *Capillary Electrophoresis in Analytical Biotechnology*, CRC Press, Inc., Boca Raton, FL, **1996**.

[2] Corradini, D.; Cogliandro, E.; D'Alessandro, L.; Nicoletti, I. *J. Chromatogr. A* **2003**, *1013,* 221-232.

[3] Corradini, D. *J. Chromatogr. B* **1997**, *699,* 221-256.

[4] Huang, Z.; Ivory, C. F. *Anal. Chem.* **1999**, *71,* 1628-1632.

[5] Ivory, C. F. *Sep. Sci. Technol*. **2000**, *35*, 1777-1793.

[6] Wang, Q.; Tolley, H. D.; LeFebre, D. A.; Lee, M. L. *Anal. Bioanal. Chem.* **2002**, *373*, 125-135.

[7] Tolley, H. D.; Wang, Q.; LeFebre, D. A.; Lee, M. L. *Anal. Chem.* **2002**, *74*, 4456-4463.

[8] Taylor, G. *Proc. R. Soc.* (London) **1953**, *219A*, 186-203.

[9] Liu, J.; Pan, T.; Woolley, A. T.; Lee, M. L. *Anal. Chem.* **2004**, *76,* 6948-6955.

[10] Liu, J.; Sun, X.; Lee, M. L. *Anal. Chem.* **2005**, *77,* 6280-6287.

[11] Fu, A. Y.; Chou, H.-P.; Spence, C.; Arnold, F. H.; Quake, S. R. *Anal. Chem.* **2002**, *74,* 2451-2457.

[12] Wang, Y.-C.; Choi, M. H.; Han, J. *Anal. Chem.* **2004**, *76,* 4426-4431.

[13] Cellar, N. A.; Burns, S. T.; Meiners, J.-C.; Chen, H.; Kennedy, R. T. *Anal. Chem.* **2005**, *77,* 7067-7073.

[14] Marcus, J. S.; Anderson, W. F.; Quake, S. R. *Anal. Chem.* **2006**, *78,* 956-958.